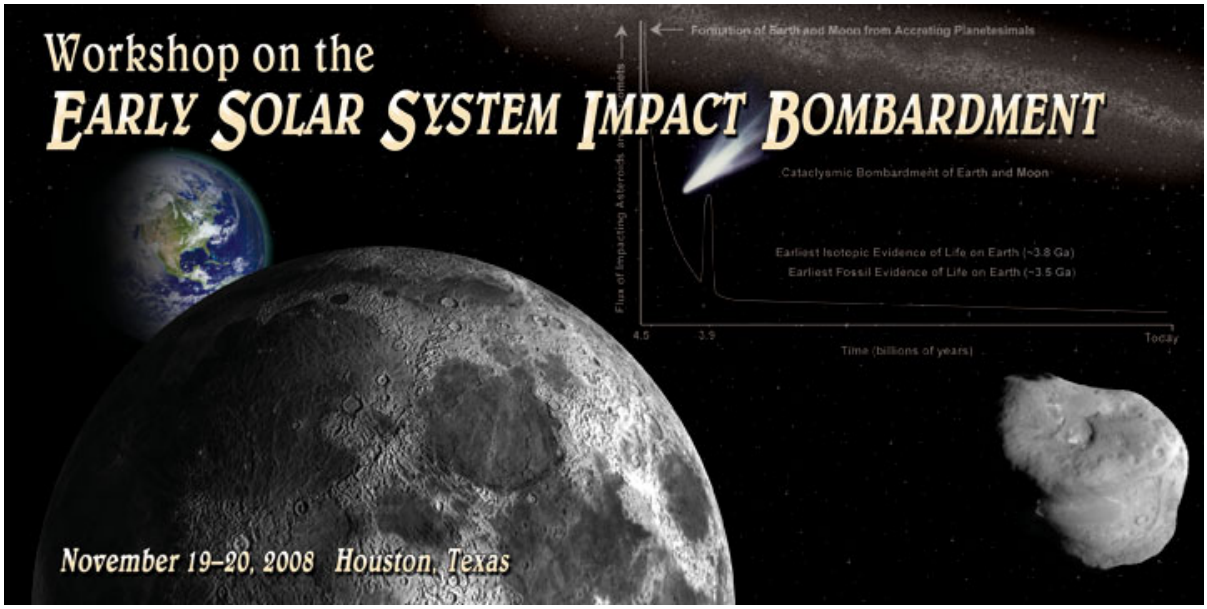

PROGRAM

AND

ABSTRACT VOLUME

LUNAR AND PLANETARY INSTITUTE

LPI Contribution No. 1439

Workshop on the

EARLY SOLAR SYSTEM IMPACT BOMBARDMENT

November 19–20, 2008

Houston, Texas

Sponsored by

Lunar and Planetary Institute
National Aeronautics and Space Administration

Conveners

David A. Kring, *Lunar and Planetary Institute*
William F. Bottke, *Southwest Research Institute*

Scientific Organizing Committee

Donald D. Bogard, *NASA Johnson Space Center*
Barbara A. Cohen, *NASA Marshall Space Flight Center*
Michelle R. Kirchoff, *Lunar and Planetary Institute*
Christian Koeberl, *University of Vienna*
Stephen J. Mojzsis, *University of Colorado*

With special assistance from Gary Lofgren and the Lunar Curatorial Office at the NASA Johnson Space Center

Lunar and Planetary Institute 3600 Bay Area Boulevard Houston TX 77058-1113

LPI Contribution No. 1439

Compiled in 2008 by
LUNAR AND PLANETARY INSTITUTE

Abstracts in this volume may be cited as

Author A. B. (2008) Title of abstract. In *Workshop on the Early Solar System Impact Bombardment,* p. XX. LPI Contribution No. 1439, Lunar and Planetary Institute, Houston.

This volume is distributed by

ORDER DEPARTMENT
Lunar and Planetary Institute
3600 Bay Area Boulevard
Houston TX 77058-1113, USA
Phone: 281-486-2172
Fax: 281-486-2186
E-mail: order@lpi.usra.edu

A limited number of copies are available for the cost of shipping and handling.
Visit the LPI Online Store at https://www.lpi.usra.edu/store/products.cfm

ISSN No. 0161-5297

PREFACE

This volume contains abstracts that have been accepted for presentation at the Workshop on the Early Solar System Impact Bombardment, November 19–20, 2008, Houston, Texas.

Administration and publications support for this meeting were provided by the staff of the Publications and Program Services Department at the Lunar and Planetary Institute.

CONTENTS

PROGRAM

Wednesday, November 19, 2008
CRATER COUNTING
8:30 a.m. Lecture Hall

8:30 a.m. Hartmann W. K. * [INVITED]
Review of Cratering Evidence Regarding Early Solar System Bombardment **[#3032]**

9:00 a.m. Frey H. V. *
Previously Unrecognized Large Impact Basins on Mars and the Moon: Implications for the Late Heavy Bombardment in the Inner Solar System **[#3008]**

9:20 a.m. Chapman C. R. * Merline W. J. Solomon S. C. Head J. W. III Strom R. G.
First MESSENGER Insights Concerning the Early Cratering History of Mercury **[#3014]**

9:40 a.m. Kirchoff M. R. * Schenk P. M.
Bombardment History of the Saturnian Satellites **[#3023]**

10:00 a.m. Johnson T. V. * Castillo-Rogez J. C. Matson D. L. Morbidelli A. Lunine J. I.
Constraints on Outer Solar System Early Chronology **[#3018]**

10:20 a.m. BREAK

Wednesday, November 19, 2008
CHRONOLOGY
10:30 a.m. Lecture Hall

10:30 a.m. Bogard D. D. * [INVITED]
Chronology of Impact Bombardment in the Early Solar System: An Overview **[#3003]**

11:00 a.m. Swindle T. D. * Kring D. A.
Chronological Evidence for the Late Heavy Bombardment in Ordinary Chondrite Meteorites **[#3004]**

11:20 a.m. Norman M. D. *
Lunar Basins and Breccias **[#3009]**

11:40 a.m. Nyquist L. E. * Shih C.-Y.
Chronology and Provenance of Lunar KREEP: A 4.0 or 4.1 Ga Age for Serenitatis? **[#3012]**

12:00 p.m. LUNCH

Wednesday, November 19, 2008
CHRONOLOGY (continued)
1:20 p.m. Lecture Hall

1:20 p.m. Cohen B. A. *
A Review of Lunar Meteorite Impact-Melt Clast Compositions and Ages **[#3031]**

1:40 p.m. Zellner N. E. B. * Delano J. W. Swindle T. D. Whittet D. C. B.
Impacts in the Earth-Moon System as Told by Lunar Impact Glasses **[#3016]**

2:00 p.m. Fernandes V. A. * Garrick-Bethell I. Shuster D. L. Weiss B.
Common 4.2 Ga Impact Age in Samples from Apollo 16 and 17 **[#3028]**

2:20 p.m. Garrick-Bethell I. * Fernandes V. A. Weiss B. P. Shuster D. L. Becker T. A.
4.2 Billion Year Old Ages from Apollo 16, 17, and the Lunar Farside: Age of the South Pole-Aitken Basin? **[#3029]**

2:40 p.m. Walker R. J. * Puchtel I. S. Day J. M. Brandon A. D. James O. B. Loudin L.
Highly Siderophile Elements in the Earth, Moon, and Mars: Update and Implications for Planetary Accretion and Differentiation **[#3011]**

3:00 p.m. BREAK

3:20 p.m. Meyer C. *
Lunar Zircons Don't Record the Lunar Cataclysm

Wednesday, November 19, 2008
DYNAMICS
3:40 p.m. Lecture Hall

3:40 p.m. Levison H. F. * [INVITED]
Review of Dynamic Models Associated with Late Heavy Bombardment

4:10 p.m Bottke W. F. * Levison H. Morbidelli A.
Understanding the Impact Flux on the Moon over the Last 4.6 Gy **[#3005]**

4:30 p.m. Minton D. A. * Malhotra R.
Evidence for Planet Migration in the Main Asteroid Belt: Implications for the Duration of the Late Heavy Bombardment **[#3020]**

4:50 p.m. Schultz P. H. * Crawford D. A.
Impactor Survivors as Additional Sources for the Late Heavy Bombardment **[#3026]**

Wednesday, November 19, 2008
POSTER SESSION
5:10 p.m. Great Room

Minton D. A. Strom R. G. Malhotra R.
Can Impactors from the Main Asteroid Belt Erase a Cometary Cratering Record on the Moon? **[#3022]**

Werner K. Barnstedt J. Kappelmann N. Kley W. Tomczyk H. Wende H. Keller H. U. Mall U. Becker-Roß H. Florek S. Hoffmann H. Mottola S. Kampf D. Staton G.
USMI — Ultraviolet Spectral Mapping Instrument for the German Lunar Exploration Orbiter (LEO) **[#3002]**

Bart G. D. Colaprete A.
LCROSS: Implications for a Lunar Cataclysm **[#3024]**

Briani G. Gounelle M.
Carbonaceous Chondritic Microclasts in Meteorites: Samples of the Late Heavy Bombardment? **[#3013]**

Thursday, November 20, 2008
APOLLO SAMPLES
8:30 a.m. Hess Room

Because the meeting topic has its roots in the Apollo program and is being organized in response to the NRC recommendation to collect new lunar samples that will test models of bombardment, a special session has been created so that participants can examine macroscopic samples and thin sections of lunar impact breccias from the Apollo collection. This session will discuss where and why the samples were collected and what we have learned from them, so that the link between lunar surface operations and scientific outcome is clear. This session is prepared with the generous assistance of Gary Lofgren and the Lunar Curatorial Office at the NASA Johnson Space Center.

10:30 a.m. BREAK

Thursday, November 20, 2008
ENVIRONMENTAL EFFECTS
10:40 a.m. Lecture Hall

10:40 a.m. Kring D. A. * [OVERVIEW]
Environmental Effects of Early Planetary Bombardment

11:10 a.m. Abramov O. * Mojzsis S. J.
Thermal State of the Terrestrial Lithosphere During the Late Heavy Bombardment: Implications for Habitability **[#3019]**

11:30 a.m. Mojzsis S. J. * Abramov O. Harrison T. M. Kring D. A. Levison H. F. Trail D. Watson E. B.
Exploring for Early Bombardments on Earth from Pre-3.83 Ga Thermal Effects Recorded in Hadean Zircons — A Status Report **[#3025]**

11:50 a.m. LUNCH

Thursday, November 20, 2008
ENVIRONMENTAL EFFECTS (continued)
1:20 p.m. Lecture Hall

1:20 p.m. Andrews-Hanna J. C. * Zuber M. T.
The Dichotomy-forming Impact on Mars: Evidence and Implications **[#3015]**

1:40 p.m. Schwenzer S. P. * Kring D. A.
After the Dust Has Settled: Hydrothermally-driven Chemical and Mineralogical Changes in Planetary Crust Following Impact Events **[#3027]**

2:00 p.m. Burt D. M. * Knauth L. P. Wohletz K. H.
The Late Heavy Bombardment: Possible Influence on Mars **[#3030]**

2:20 p.m. Rodriguez J. A. P. * Kargel J.
Construction of a Volatile Rich Martian Upper Crust During the Impact Cataclysm **[#3007]**

2:40 p.m. Kurosawa K. * Ishibashi K. Sekine Y. Sugita S. Kadono T. Ohno S. Ohkouchi N. Ogawa N. O. Matsui T.
Cyanide Production by Chemical Reactions Between Impactor Material and an Ambient Atmosphere After an Oblique Impact **[#3010]**

3:00 p.m. Miura Y. *
Impact Origin of Chlorine-bearing Materials of Salty Sea-Water of Early Earth, Compared with Those on Mars and the Moon **[#3001]**

3:20 p.m. BREAK

Thursday, November 20, 2008
OPEN DISCUSSION
3:40 p.m. Lecture Hall

Moderators:
William F. Bottke and David A. Kring

THERMAL STATE OF THE TERRESTRIAL LITHOSPHERE DURING THE LATE HEAVY BOMBARDMENT: IMPLICATIONS FOR HABITABILITY. O. Abramov and S. J. Mojzsis, Department of Geological Sciences, University of Colorado, 2200 Colorado Ave., Boulder, CO 80309.

Introduction: Hypervelocity impacts of large bolides result in a significant but localized temperature increases in the crust. This process would have been commonplace during the epoch of intense bombardment at ~3.9 Ga [1-3]. This period, commonly termed the Late Heavy Bombardment (LHB), was some 20 to 200 Myr in duration [2,4], and likely resurfaced most of the Earth and may even have vaporized the oceans. Surface habitats for early life would have been doubtlessly destroyed by the LHB. At the same time, however, new subsurface habitats would have been created in the form of impact-induced hydrothermal systems [5], which provided sanctuary to existing life or may even have been the crucible of its origin. The timing of the LHB coincides remarkably well with the earliest isotopic evidence of life on Earth by ~3.83 Ga [e.g., 6]. Furthermore, genetic evidence in the form of 16S ssu rRNA and other molecular phylogenies suggests that all terrestrial life arose from a common ancestral population akin to present-day thermophilic or hyperthermophilic organisms [e.g., 7]. These lines of evidence have been used to suggest that the LHB played an important role in the origin and evolution of life. Conversely, a number of workers have argued that the energy liberated during the bombardment would have precluded the survival of any incipient life [e.g., 8].

The underlying purpose of this study is to assess the habitability of early Earth during the LHB by (i) using new studies of impact cratering records of the Moon and terrestrial planets and size distributions of asteroid populations [e.g., 9]; (ii) taking advantage of a new class of early solar system dynamical models that convincingly reproduce impact rates during the LHB defined by the lunar and meteoritic record [e.g., 10]; (iii) potentially constraining the rate and duration of the LHB by laboratory analysis of terrestrial Hadean zircons [11-13]; and (iv) using numerical modeling to understand the thermal response of the lithosphere to impacts.

Technique summary: The survivability of a nascent biosphere on early Earth during the LHB is assessed by thermal modeling of the lithosphere and monitoring of the surface and near-surface temperatures in what we term the "geophysical habitable zone", or the inhabited crust within a few km of the surface.

A stochastic cratering model is used to populate all or part of the Earth's surface with craters within a probability field of constraints established from both models and observations. The total mass delivered to the Earth during the LHB has been estimated at 1.8×10^{23} g based on dynamical modeling [11], and 2.2×10^{23} g based on the lunar cratering record [14, 15]. For the purposes of this work, we adopted the average value of 2.0×10^{23} g. Impactors that bombarded the Earth and Moon were likely dominated by main belt asteroids [10], and the size/frequency distribution of the asteroid belt is unlikely to have changed significantly since that time [16]. Thus, we used the size/frequency distribution of the asteroid belt, normalized to the total mass of 2.0×10^{23} g. The duration of the LHB in this preliminary analysis is taken to be ~100 Ma, although other values are also investigated.

For each crater in the model, a temperature field is calculated using analytical expressions for shock deposited heat and central uplift [17]. After the crater's thermal field is introduced into a 3-dimensional model representing the Earth's lithosphere, it is allowed to cool by conduction in the subsurface and radiation/convection at the atmosphere interface (Fig. 1). Post-impact crater cooling is modeled using the computer code HEATING, a general-purpose, three-dimensional, finite-difference heat transfer program written and maintained by Oak Ridge National Laboratory.

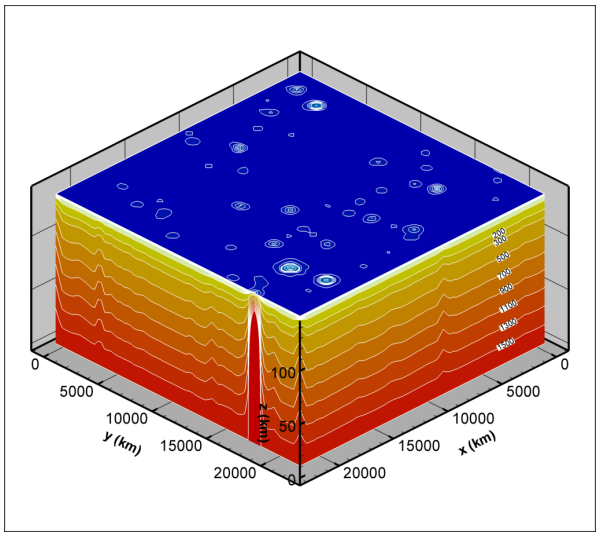

Figure 1. A 3-dimensional model representing the Earth's lithosphere at the end of the 100 Myr LHB. Only impactors larger than 10 km in diameter are included in this model.

Results: Most of the mass (and energy) during LHB was likely delivered by a relatively few very large impactors. Our model predicts ~90 impacts with impactor diameters of 50 km or larger, forming basins ~1,000 km in diameter or greater over the course of a

100 Myr-long bombardment. We find that these impacts would have been temporally separated by over 1 Myr, on average, and would have resurfaced less than 25% of the Earth's surface. Most of the crust was not melted or thermally metamorphosed to a significant degree, with less than 10% experiencing a temperature increase of over 500 °C. Although smaller impactors (1 - 10 km) were as important as gigantic basin formers (100+ km) in terms of sterilizing the surface (Table 1), large craters are nonetheless more biologically significant because they take a far longer time to cool. The LHB scenario in our main model is insufficient to extinguish microbial life (Fig. 2). This model does not explicitly incorporate thermal shock from a global layer of hot ejecta following a large impact [18]; however, the maximum sterilization depth for such a process is only a few hundred meters, and is further reduced or eliminated by the presence of the oceans. The largest impactor in our model (~300 km in diameter) is insufficient to vaporize the oceans [18].

Impactor diameter range	Number of impacts	% of habitable zone sterilized
100+ km	33	15%
10 - 100 km	1500	12%
1 - 10 km	170,000	16%

Table 1. Percentage of habitable zone (~4 km below the surface) exposed to temperatures above 110 ° C (the upper limit for hyperthermophiles) during the LHB.

In addition to our baseline model, we explored the parameter space to evaluate the effects of different LHB durations, mass fluxes, impact velocities, temperature gradients in the crust, and the presence of oceans. In the case of 10 Myr LHB, the mesophile curve in Fig. 2 crosses the themophile curve, indicating that the overall conditions are more favorable for thermophiles. The same effect can be achieved by doubling the impact velocity from 20 to 40 km/s. Either increasing the total mass delivered by a factor of 10, from 2.0×10^{23} g to 2.0×10^{24} g, or doubling the geothermal temperature gradient from 12°C to 24°C results in approximately equal habitable volumes (~6×10^{8} km^3) for mesophiles, thermophiles, and hyperthermophiles towards the end of the LHB. However, it is important to note there is no plausible scenario in which the entire terrestrial habitable zone is fully sterilized.

If oceans are present, heat is lost from the upper boundary up to 10 times faster, and habitable conditions are re-established up to an order of magnitude more rapidly after crater formation. For craters of ~200 km, colonization by thermophiles in the central regions is possible after ~20,000 years [19,20]. This observation further favors the survival of subsurface microbial life throughout the bombardment.

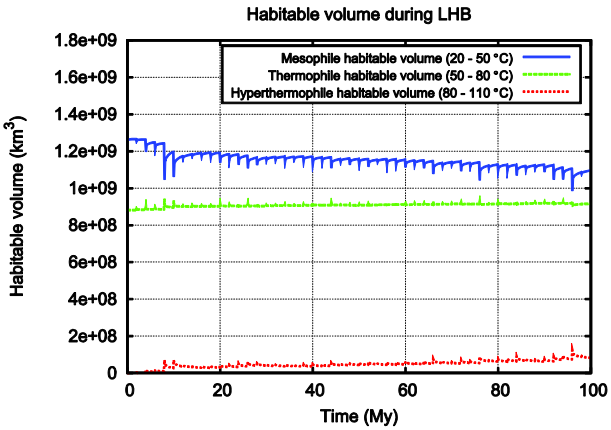

Figure 2. Evolution of habitable volumes during the 100 Myr LHB in the habitable zone within ~4 km of the surface. Only impactors larger than 10 km in diameter are included.

Acknowledgements
This work is funded by the NASA Postdoctoral Program and the NASA Exobiology program. The use of office space and computer resources at the Department of Space Studies of the Southwest Research Institute is gratefully acknowledged.

References: [1] Turner G. et al. (1973) *Proc. Lunar Sci. Conf.*, 4, 1889–1914. [2] Tera F. et al. (1974) *Earth Planet. Sci. Lett.*, 22, 1–21. [3] Cohen B. A. et al. (2000) *Science*, 290, 1754-1756. [4] Ryder G. (1990) *Eos Trans. AGU*, 71(10) 313, 322-323. [5] Zahnle K. J. and Sleep N. H. (1997) in *Comets and the Origin and Evolution of Life*, pp. 175-208, Springer-Verlag, New York. [6] McKeegan K.D. et al. (2007) *Geology*, 35, 591-594. [7] Pace N. R. (1997) *Science*, 276, 734-740. [8] Moorbath S. (2005) *Applied Geochem.*, 20, 819-824. [9] Strom R. G. et al. (2005) Science, 309, 1847-1850. [10] Gomes R. et al. (2005) *Nature*, 435, 466-469. [11] Mojzsis S.J. et al., this meeting. [12] Mojzsis S. J. and Harrison T. M. (2002) *Earth Planet. Sci. Lett*, 202, 563-576. [13] Trail D. et al. (2007) *Geochim. Cosmochim. Acta*, 71(16), 4044-4065. [14] Hartmann W. K. et al. (2000) in *Origin of The Earth and Moon*, pp. 493-451, Univ. Arizona Press, Tucson. [15] Ryder G. et al. (2000) in *Origin of The Earth and Moon*, pp. 475-492, Univ. Arizona Press, Tucson. [16] Bottke W. F. et al. (2005) *Icarus*, 175, 111-140. [17] Abramov, O. and Mojzsis S. J (2008) *LPSC XXXIX*, abstract 1036. [18] Sleep, N.H. and Zahnle K. (1998) JGR, 103, 28,529-28,544. [19] Abramov O. and Kring D. A. (2004) *JGR*, 109, doi:10.1029/2003JE002213. [20] Abramov O. and Kring D. A. (2007) *Met. Planet. Sci.* 42, 93-112.

THE DICHOTOMY-FORMING IMPACT ON MARS: EVIDENCE AND IMPLICATIONS. J. C. Andrews-Hanna[1,2] and M. T. Zuber[1], [1]Dept. of Earth, Atmospheric, and Planetary Sciences, MIT [2]now at the Dept. of Geophysics, Colorado School of Mines, jhanna@mit.edu.

Introduction: The topography and crustal structure of Mars is dominated by the hemispheric crustal dichotomy, dividing the planet between southern highlands and northern lowlands. Recent work revealed evidence that this dichotomy was produced in a giant basin-forming impact, making the northern lowlands of Mars the largest impact basin in the solar system [1-3]. While all of the terrestrial planets likely experienced similar mega-impacts at some stage in their formation, the importance of the dichotomy-forming impact on Mars is heightened by the fact that it post-dated planetary differentiation. We review evidence for the impact basin, and explore the implications for Mars evolution.

Borealis Basin – Evidence for an impact: The primary evidence for an impact origin for the dichotomy lies in the near-perfect elliptical shape of the lowlands, as revealed in a recent analysis of the topography and gravity that removed the superposed Tharsis volcanic rise [1]. The elliptical lowlands shape is strikingly similar to other elliptical impact basins, including Hellas, Utopia, and South Pole-Aitken. The bimodal crustal thickness distribution between the lowlands and highlands is also similar to the bimodal distribution between the Hellas basin floor and surrounding crust. Simulations found that an impacts of 1600-2700 km diameter objects at angles of 30-60° produce basins matching the elliptical lowlands [2]. The impact may also explain the demagnetization of a broad region antipodal to the basin [3].

Borealis Basin – Possible basin-related features: *Arabia Terra: A partial multi-ring structure.* Arabia Terra is the one ancient Noachian province that does not match the characteristics of typical highlands crust [4]. Arabia Terra slopes gently northwards, and is separated from both the lowlands and highlands by distinct breaks in slope [1]. Based on profiles of the Orientale, Hellas, and Argyre basins [1], we propose a topographic definition of a multi-ring structure as an inwards facing slope at ~1.4 radii from the basin center that is separated from the main excavation rim of the basin by a gently sloping to concave upwards bench at intermediate elevation. By this simple observational definition, Arabia Terra is a partial basin ring, though the mechanism responsible for the origin of both Arabia Terra and other multi-ring structures is uncertain.

Highlands ejecta textures. The lowlands forming impact would have buried the primordial highlands crust beneath a thick ejecta blanket [2]. The nearly uniform thickness of the highlands crust suggests either an even distribution of ejecta or viscous relaxation of thickness variations in the hot ejecta blanket. Preservation of the basin rim requires that the ejecta be largely solid upon impacting the surface. Structures in the highlands are likely a result of either textures in the ejecta blanket or subsequent modification processes. In some regions of the highlands, the crust exhibits long wavelength undulations, which do not appear consistent with a volcanic or tectonic origin. This texture may represent the highly relaxed and eroded signature of hummocky or blocky portions of the ejecta blanket.

Impact fractures and fretted terrain. The crust surrounding a crater or basin is intensely fractured at scales ranging from microfractures to large breccia-filled tear faults. Many portions of the dichotomy boundary are characterized by fretted terrain – an intersecting network of valleys with semi-rectilinear plan form [5]. The valleys have been erosionally enlarged, though a clear structural control is evident. Focused groundwater discharge along the dichotomy boundary in the Noachian and Hesperian could have fueled fluvial and glacial erosion, which would naturally concentrate in zones of weakness or high porosity. This fretted terrain may thus represent erosionally enlarged impact-induced faults around Borealis.

Implications for Mars evolution: *Early crustal structure.* The ancient highlands basement is the only crust on Mars dating back to planetary differentiation. The crustal thickness [6] histogram of the highlands

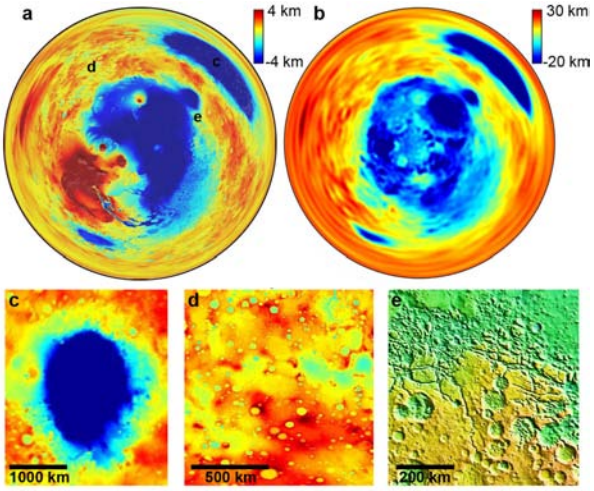

Figure 1. Polar plots of the Borealis basin in the topography (a) and modeled isostatic roots, representing the pre-Tharsis crust (b), show a clear similarity with the Hellas basin (c). Hummocky textures in the highlands (d) may represent ejecta. Fretted terrain (e) may reveal eroded basin fractures.

(excluding Arabia Terra and regions of volcanic/impact modification [1]) is sharply peaked at a thickness of 65 km and a full width at half max of 7 km. This suggests that the pre-dichotomy crust exhibited a nearly uniform thickness, with implications for the mechanism of primary crustal formation.

Timing of the impact. If the crust of Mars was near the solidus temperature after differentiation [7] (likely within ~20 Myr of solar system formation [8]), this would require substantial cooling prior to the dichotomy-forming impact in order to maintain the abrupt dichotomy boundary against relaxation. For a 50 km thick crust, the thermal diffusion timescale is ~65 Myr, suggesting that the impact likely occurred one to several hundred Myr after accretion.

Climate and atmosphere. Mars is thought to have acquired its volatiles through accretion of carbonaceous asteroids (accounting for less than 1% of the mass of the planet) in the first 20 Myr of solar system formation [9]. Formation of the atmosphere then resulted from outgassing during differentiation and late-stage accretion of volatile-rich projectiles. The Borealis impact clearly occurred after the main phase of crustal formation and outgassing. Large impacts are thought to strip the atmosphere above the plane tangent to the impact basin [10], suggesting removal of a minimum of 40% of the primordial atmosphere by the dichotomy-forming impact. Above a critical energy, complete atmospheric ejection by the shock wave and expanding silicate vapor plume is possible [11]. The estimated energy of the impact [2] exceeds that required for total atmospheric removal by a factor of 10.

An impact more than 100 Myr after accretion would have been long after Jupiter had cleared the asteroid belt of large bodies [12], suggesting a water poor projectile from the vicinity of Mars. Alternatively, a carbonaceous projectile would likely have been differentiated and may have lost much of its initial volatile inventory before impact. In either case, the impact would have resulted in a net loss of water. Mars may have had a thicker outgassed CO_2–H_2O atmosphere that was lost during this late-stage mega-impact. Subsequent atmospheric replenishment by degassing of the impact-generated local magma ocean, volcanic outgassing at Tharsis, and accretion of a late-stage veneer of volatile-rich projectiles would have partially restored the atmosphere, allowing a short-lived clement climate before loss to solar wind and small impact erosion led to the present cold and arid conditions.

Surface composition. The dichotomy-forming projectile represents the largest post-differentiation contribution of meteoritic material to Mars. Estimated projectile sizes [2] correspond to a global equivalent layer (GEL) of 14-71 km of meteoritic material, dwarfing the combined contribution from the Hellas, Utopia, Argyre, and Isidis impacts (~0.6-6 km GEL).

The highlands is likely blanketed in ejecta from the lowlands-forming impact up to several 10's of km in thickness [2,3], composed of a mixture of excavated crust, mantle, and projectile material. The lowlands crust likely differentiated from the local impact-generated magma ocean, and was later covered in a thin veneer of volcanic and sedimentary material. These two provinces roughly correlate with the spectral surface types 1 and 2, with the more mafic surface type associated with the highlands (possibly consistent with a physical mixture of crust and mantle ejecta). However, the lowlands and highlands are of different provenance regardless of the mechanism of dichotomy formation, and existing observations do not disambiguate impact and endogenic mechanisms. It has been suggested that the characteristic red color of Mars may due to oxidized meteoritic Fe in the dust [13]. The vast majority of post-differentiation meteoritic iron would have been delivered to Mars in the Borealis impact.

Analyses of isotopic ratios in the martian meteorites suggest that the martian interior includes two compositionally distinct mantle reservoirs [8]. This result is surprising in light of evidence for likely plume-sourced volcanism, and theoretical arguments for whole-mantle convection on early Mars [14]. A distinct mantle reservoir could have been produced by the Borealis impact, in the form of a local magma ocean composed of a mixture of martian and foreign projectile material. The roughly even division of known martian meteorites between the two compositional groups is consistent with the similar sizes of the highlands and lowlands.

Summary: The dichotomy-forming impact on Mars affected all aspects of Mars' evolution, particularly given its timing after planetary differentiation. While there is much uncertainty regarding the effects of the impact, this much is clear: the fundamental nature of Mars and the course of its evolution were changed dramatically by this single event.

References: [1] J. C. Andrews-Hanna, et al. (2008) *Nature* 453, 1212-1215. [2] M. M. Marinova, et al. (2008) *Nature* 453, 1216-1219. [3] F. Nimmo, et al. (2008) *Nature* 453, 1220-1223. [4] M. T. Zuber, et al. (2000) *Science* 287, 1788-1793. [5] M. H. Carr and G. D. Clow (1981) *Icarus* 48, 91-117. [6] G. A. Neumann, et al. (2008) *LPSC* XXXIX abstract 1391. [7] L. T. Elkins-Tanton, et al. (2005) *JGR* 110 (E12), E12S01, doi:10.1029/2005JE002480. [8] A. N. Halliday, et al. (2001) *Space Sci. Rev.* 96, 197-230. [9] J. I. Lunine, et al. (2003) *Icarus* 165, 1-8. [10] H. J. Melosh and A. M. Vickery (1989) *Nature* 338, 487-489. [11] T. J. Ahrens (1993) *Annu. Rev. Earth Planet. Sci.* 21, 525-555. [12] A. Morbidelli, et al. (2000) *Meteorit. Planet. Sci.* 35, 1309-1320. [13] A. S. Yen (2001) *LPSC* XXXII Abstract 1766. [14] S. Zhong and M. T. Zuber (2001) *EPSL* 189, 75-84.

LCROSS: IMPLICATIONS FOR A LUNAR CATACLYSM. G. D. Bart[1], A. Colaprete[2], [1]*Dept. of Physics, Univ. of Idaho, Moscow, ID (USA), (gwen@barnesos.net)*, [2]*NASA Ames Research Center, M/S 245-3, Moffett Field, CA 94035.*

Introduction: The evolution of the early solar system was dominated by impacts. The rate at which these impacts occurred over the first billion years of solar system history is not yet entirely understood. One possibility is that the number of impacts simply tapered off slowly with time. However, evidence from both returned Apollo samples [1], and from found lunar meteorite samples [2] indicate that there was also a brief but intense period of bombardment about 3.9 billion years ago. Several unknowns remain regarding this lunar cataclysm. For instance, what was the source of the impactors? Were they asteroids or comets? What perturbed their orbits to produce this cataclysm? In this abstract we first introduce the LCROSS mission, and then discuss some ways that the LCROSS data may be able to help answer some questions about the lunar cataclysm.

LCROSS:

Lunar CRater Observation and Sensing Satellite (LCROSS), will be launched on the same rocket as the Lunar Reconnaissance Orbiter (LRO) later this year (http://lcross.arc .nasa.gov). The primary LCROSS objective is to confirm the presence or absence of water ice in a permanently shadowed region on the Moon. Other related objectives include identifying the form and state of hydrogen observed at the lunar poles; quantifying (if present) the amount of water in the lunar regolith, with respect to hydrogen concentrations; and characterizing the lunar regolith within a permanently shadowed crater on the Moon. The presence of the water ice is hypothesized [3, 4] and supported by data from the Lunar Prospector neutron spectrometer showing hydrogen in permanently shadowed regions at the poles [5].

The LCROSS spacecraft will set the rocket's Centaur Earth departure upper stage (EDUS) on an impact trajectory with the Moon. Once the trajectory is set, the spacecraft will release the EDUS, which will then impact the Moon in a permanently shadowed region characterized by high concentrations of hydrogen according to the Lunar Prospector neutron spectrometers. Following four minutes behind the EDUS, LCROSS will fly through the impact plume, using its 9 instruments to examine the impact ejecta. The LCROSS payload includes 5 cameras (1 visible, 2 Near IR, 2 Mid IR), three spectrometers (1 visible, 2 NIR) and one photometer.

Although the primary LCROSS objective is to look for water, its instruments will be taking data about the entire impact plume. It will be excavating to a depth of about 10 m, identifying subsurface composition at the pole.

Impact Site Candidates: Four regions are currently candidates for the LCROSS impact: Shoemaker crater (88.1°S, 44.9°E, 50.9 km diameter), Shackleton crater (89.9°S, 0.0°E, 19 km diameter), Faustini crater (87.3°S, 77.0°E, 39 km diameter), and Cabaeus (85°S, 35°E). These regions are labeled in Fig. 1.

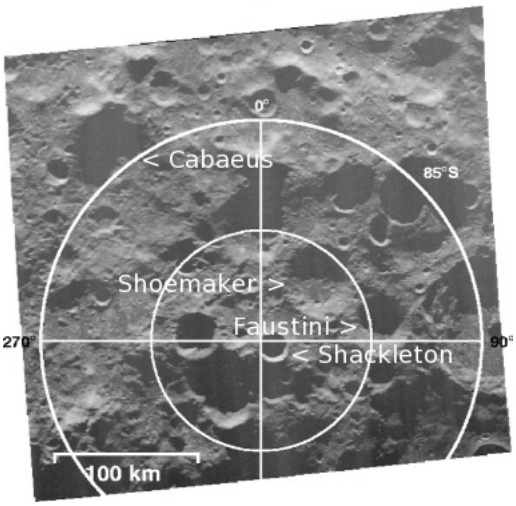

Figure 1: Illustration of the location of possible candidate impact locations for LCROSS, superimposed on a radar backscatter map of the lunar south pole from [6].

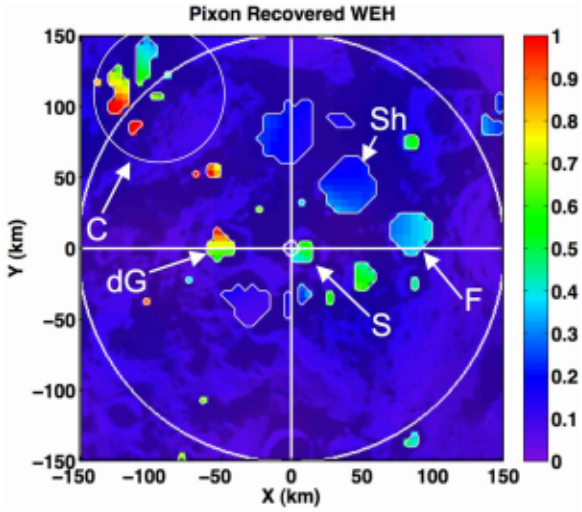

Figure 2: Water-equivalent hydrogen (WEH) in wt% corresponding to the epithermal count rates. Large circle denotes 85S. *C* = Cabaeus, *Sh* = Shoemaker, *dG* = de Gerlache, *S* = Shackleton, *F* = Faustini. From [7].

Target Selection Criteria:

In order to meet its primary science objectives, LCROSS has several required criteria for target selection. One criteria is that the site must be observable from ground based observatories. There are a variety of ground-based and orbital observations planned that will observe the dust and water plumes caused by the LCROSS impacts. The impacts are currently planned to occur with most favorable viewing geometry from Hawaii and North and South America.

Another criteria is that the ejecta plume be illuminated by sunlight. Since the LCROSS instruments primarily measure reflected light, instrument sensitivity will be greatest when the maximum amount of ejecta is exposed to sunlight.

Target properties are also important. Slopes should not exceed 10 degrees; lower slopes are preferred. Surface roughness must also be considered; a smoother surface is preferred. Low slopes and low surface roughness will will provide the best ejecta plume for detecting water.

The final criteria is that the location have an observed concentration of increased hydrogen, which could indicate the presence of water (Fig. 2).

Impact Site Characterization:

In order to meet these criteria we first must characterize the potential impact sites. Characterizing the terrain within the crater is difficult because the target impact site must be permanently shadowed. Because of lack of high resolution visible imaging at the poles, we would like to use high resolution ground based radar data [8]. Because the radar illuminated the Moon from the Earth, some of the observations were made in the permanently shadowed regions. Using this data we would like to characterize, if possible, the crater age, slope steepness, crater density, boulder density, and regolith depth.

Once the observable target parameters are established, we can conduct comparison studies of similar craters elsewhere on the Moon. We can obtain high resolution images of such craters and study their interior topographic profiles to better constrain the LCROSS impact site. Furthermore, once the tools and analysis methods are established, we will be ready to quickly assess new data provided by the instruments on LRO, which will begin taking data 2-3 months prior to the LCROSS impact.

Implications for the Lunar Cataclysm:

There are two main ways that LCROSS can contribute to understanding the lunar cataclysm. One is by simply carrying out its primary objective: detecting water (or the lack thereof.) One of the questions regarding the lunar cataclysm is the source of the impactors. It has been proposed that as the orbits of the giant planets migrated in the early solar system, disruptive resonances arose that should scatter small, icy, outer solar system bodies and send them into the inner solar system.

If LCROSS finds water, it may support such a model. There are several sources for water trapped in permanently shadowed regions of the Moon [4]: one is delivery of water by water rich meteorites (comets). Recent studies [9] used hydrocode models to simulate lunar water retention from cometary impacts. They show that 2% of the impactor mass will be retained at impact velocities of 15 km/s. The discovery of water on the Moon would support the model of a cometary-impact-dominated lunar cataclysm.

In addition to detecting water, the LCROSS instruments will determine the composition of the impact site, providing a data point for validation of orbital compositional data [10, 11, 12], assisting in determination of the variability of the lunar crustal composition.

Conclusion:

Characterizing potential impact sites will be critical to providing the best scientific return from the LCROSS mission. Understanding the target as well as possible will both optimize the quality of data return and improve the analysis of the data.

The detection of water by LCROSS would support the model of a lunar cataclysm dominated by cometary impacts. Furthermore, LCROSS will determine the composition of the lunar crust at the impact location.

References:

[1] Turner G. and Cadogan P.H. (1975) in Lunar and Planetary Science Conference, vol. 6 of *Lunar and Planetary Science Conference*, 1509–1538.

[2] Cohen B.A., Swindle T.D., and Kring D.A. (2000) *Science*, *290* 1754–1756.

[3] Watson K., Murray B.C., and Brown H. (1961) *J Geophys Res*, *66* 3033–3045.

[4] Arnold J.R. (1979) *J Geophys Res*, *84* 5659–5668.

[5] Feldman W.C., Maurice S., Binder A.B., Barraclough B.L., et al. (1998) *Science*, *281* 1496–1500.

[6] Margot J.L., Campbell D.B., Jurgens R.F., and Slade M.A. (1999) *Science*, *284* 1658–1660.

[7] Elphic R.C., Eke V.R., Teodoro L.F.A., Lawrence D.J., et al. (2007) *Geophys Res Lett*, *34* L13,204.

[8] Campbell B.A. and Campbell D.B. (2006) *Icarus*, *180* 1–7.

[9] Ong L., Asphaug E., Nimmo F., Korycansky D., et al. (2007) in Lunar Planet. Sci. Conf. 38th, abstract #1433.

[10] Jolliff B.L. and Gillis J.J. (2005) *Met and Planet Sci*, *40* 5330.

[11] Gillis J.J. (2004) *Geochim Cosmochim Acta*, *68* 3791–3805.

[12] Lawrence D. (2003) in Lunar Planet. Sci. Conf., 1679.

Chronology of Impact Bombardment in the Early Solar System: An Overview

Donald D. Bogard, ARES, code KR, NASA-JSC, Houston TX, 77058. donald.d.bogard@nasa.gov

Most bodies without atmospheres in the solar system have heavily cratered surfaces, which give testimony to the importance of impacts as a geological process. Determining the chronology of this impact bombardment addresses whether the impact rate has been constant or variable over solar system history, and also may give insight to the origin of the impactors. To determine the absolute age of a given impact crater or cratered surface requires that radiometric age information be obtained on rock samples ejected by that crater or representative of that cratered surface. Lunar rocks returned to Earth constitute the largest data base for deciphering the chronology of solar system bombardment, although some meteorite data also contribute. Data on ages of specific lunar surfaces are combined with the numbers of craters of various diameters on that surface to define a linked impact cratering rate for the Moon over the past ~3.5 Gyr. This linked "impact-chronometer" for the Moon, adjusted for relative solar system position, has been applied to other planets and satellites to estimate the ages of their cratered surfaces. Although this process of determining surface ages is thought to work reasonably well for surfaces younger than ~3.5 Gyr, additional problems arise when the process is applied to older lunar surfaces. The impact rate prior to ~3.5 Gyr ago was apparently much higher, and the linked "impact-chronometer" breaks down. Old lunar surfaces begin to saturate with craters, and the surface ages become uncertain. From early analyses of lunar-returned samples, it became apparent that various radiometric ages (i.e., Ar-Ar, Rb-Sr, U-Pb) of most highland rocks had been impact reset after the Moon's formation, but prior to ~3.5 Gyr ago. This resetting was postulated to have been produced by an increased flux of impacting objects long after the Moon formed [1]. Another explanation offered was that the early age resetting was not the result of a spike in the bombardment rate, but rather of a long declining bombardment after the Moon's formation, in which radiometric ages were reset over an extended time period [2].

Four experimental approaches have been employed to determine the radiometric chronology of the early impact period, often referred to as an impact cataclysm or the late heavy bombardment (LHB). These approaches are: 1) determine the radiometric ages of individual lunar highland rocks, and examine the data statistically for the impact rate versus time; 2) age date lunar rock clasts and melts identified with a specific large crater or basin and presumably reset in age when ejected; 3) determine the ages of small impact melt samples in lunar meteorite breccias, and examine the data statistically for the impact rate versus time; 4) statistically characterize impact age resetting in meteorite samples. Many of these are Ar-Ar ages, which is the most sensitive to resetting. Dating many lunar highland rocks (approach #1) has given a range in ages mostly between 3.7 and 4.1 Gyr. Many fewer rocks give ages outside this range, and this was the initial observation that indicated impact resetting on the Moon was restricted to a relatively narrow time period. Meteorite impact melts (method #3) has yielded a much wider range of radiometric ages, ranging from <1 Gyr to ~4 Gyr, with perhaps an age concentration at ~3-4 Gyr [3]. Although few of these impact melts give ages >4 Gyr, the existence of many ages <3.5 Gyr indicates that many of these glasses were formed by impacts not associated with the LHB. Age determinations of tiny impact spheres in the lunar regolith also show a wide range, with most ages <1 Gyr [4]. The preponderance of young regolith ages may reflect a recent enhance flux of smaller impactors or a bias in the production and survivability of glass spheres in the regolith. Overall, there seems to be a correlation of smaller scale impact melts showing younger ages, reflective of formation in smaller events.

Radiometric dating of highland rocks thought to have been ejected by a specific lunar basin gives a somewhat narrower range of ages compared to highland rock ages as a whole. Based on samples of Apollo 15 and 17 impact melts, the Imbrium and Serenitatis basin ages appear to be relatively well determined at 3.85 ±0.02 Gyr and 3.89 ±0.01 Gyr, respectively [5]. The large abundance of ~3.85-3.9 Gyr ages among highland rocks occurs because the Apollo 14, 15 and 17 missions targeted ejecta from these basins. However, even among rocks identified with one of

these two basins, some ages fall below and above these defined basin ages (see summary in [6]), suggesting incomplete age resetting by the basin events or resetting by later impacts. Because Imbrium and Serenitatis are the 3rd and 7th youngest of the ~42 large, recognized basins [7], formation of the last large lunar basin (Oriental) probably occurred ~3.7-3.8 Gyr ago. This is somewhat earlier than the apparent ~3.5 Gyr inflection in the age-crater density curve, and the younger reset ages of eucrites (discussed below).

Although Apollo 16 was supposed to have targeted rocks ejected by the Nectaris basin, ages of Apollo 16 rocks vary over a wide range and the formation age of Nectaris remains uncertain. The observation that Ap-16 rocks with higher K concentrations give Ar-Ar ages ~0.2 Gyr younger, on average, than rocks with smaller K concentrations [8] suggests that high-K ejecta from Imbrium may have contributed to these ages. Further, Ar-Ar ages of several Ap-16 impact melts gave an age distribution similar to Imbrium impact melts rocks, with a concentration of ages at ~3.86, but a total age spread of 3.75-4.19 [9].

Among meteorites, the eucrites are thought to derive from the large asteroid Vesta, and the common occurrence of breccias among eucrites attest to an active impact history. Essentially all brecciated eucrites show Ar-Ar ages of 3.4-4.0 Gyr, with very few ages lying outside this range [6 & unpublished data]. Presumably these ages were reset during the LHB; and they are suggestive of about three to five large impact events. Among ordinary chondrites, several also show reset Ar-Ar ages in the period of ~3.5-4.0 and also may reflect resetting in the LHB [6, 10, 11]. Because meteorite parent bodies are smaller than the Moon, impacts produced less heating and less resetting of radiometric ages, and affect the Ar-Ar chronometer more than other radiometric chronometers that are harder to reset. Reset ages among eucrites and chondrites in the approximate period 3.5-4.0 Gyr ago argues that the LHB affected not only the Moon-Earth system, but also the whole inner solar system.

An important parameter in defining the nature and time span of the LHB is the total range in lunar basin ages. Accepting the determined ages of Imbrium and Serenitatis means that nearly one-fifth of the recognized lunar basins formed after 3.9 Gyr ago. If the age of Nectaris is ~3.91 Gyr, as assumed by Ryder (2002), then at least one-third of the large basins formed long after the Moon formed. The origin and late arrival of so many large bodies constitutes a type of cataclysm and requires explanation. If the largest lunar basin, SPA, formed at 4.0 Gyr, as speculated by Ryder [12], then the LHB would have been entirely contained within a period of 200 Myr. However, the age of Nectaris may be considerably older than 3.91 Gyr, and the age of the oldest basin, SPA, is totally unconstrained. Thus, it may have been the case that large impacts struck the Moon over a period of many hundreds of Myr, and possibly dating back to lunar formation. This scenario might resemble the declining impact flux proposed by Hartmann [2], and it could be a challenge to explain the origin of these impacting bodies over such a long time period. Determination of the formation ages of Nectaris and SPA is important to resolve this question. A related question is when did the LHB end, shortly after formation of Imbrium ~3.85 Gyr ago or ~3.5 Gyr ago as suggested by the inflection in the lunar age-flux curve and meteorite data? Could smaller impacting objects have persisted after the large, basin-forming objects ceased? Another related question is whether the rarity, but not absence, of lunar rock ages >4.1 Gyr is due to LHB resetting, or continuous resetting over 4.4-4.1 Gyr, or even a much lower impact flux in this time span? If this earliest epoch was also a time of intense bombardment, why do some lunar rocks and meteorites still give radiometric ages in this period? Many questions about the chronology of impacts in the early Solar System are as yet unanswered.

References. [1] Tera et al., 1974, Earth Planet Sci. Lett. 22, 1; [2] W. Hartmann, 2003, Meteor. Planet. Sci. 38, 579; [3] B. Cohen, 2008, LPSC 39th, #2532; [4] Levine et al, 2005, Geophys. Res. Lett. 32, L15201; [5] Dalrymple and Ryder, 1993; J. Geophys. Res. 98, 13085; 1996, J. Geophys. Res. 101, 26069; [6] Bogard, 1995, Meteoritics 30, 244; **[7]** Petro and Pieters, 2004, J. Geophys. Res. 109, E06004; [8] P. Warren, 2003, LPSC 34th, #2149; [9] Norman et al., 2006, Geochim. Cosmochim. Acta 70, 6032; [10] Grier et al., 2004, MaPS 39, 1475; [11] Swindle et al., 2008, submitted MaPS ; [12] G. Ryder 2002, J. Geophys. Res. 107, 1.

UNDERSTANDING THE IMPACT FLUX ON THE MOON OVER THE LAST 4.6 GY. W. F. Bottke[1], H. Levison[1], & A. Morbidelli[2]. [1]Southwest Research Institute, 1050 Walnut St, Suite 400, Boulder, CO 80302, USA (bottke@boulder.swri.edu). [2]Obs. de la Côte d'Azur, B.P. 4229, 06034 Nice Cedex 4, France

Introduction. Asteroids and comets have been bombarding the terrestrial planets since they formed almost 4.6 Ga. The impact flux over Solar System history, however, has seen considerable variation and is directly tied to the events that drove the planets to their current orbital configuration. We find it useful to divide the impact history of the terrestrial planet region into several stages: (i) the post-planet formation era (4.6-4.0 Ga), the late heavy bombardment (LHB) era (4.0-3.8 Ga), the post-LHB era (3.8 Ga-3.2 Ga) and (iv) the current era (3.2 Ga-Today).

Stage 1. The post-planet formation era (4.6-4.0 Ga). The earliest bombardment history of the Moon is a record of events that took place after the Moon-forming event and the solidification of the lunar crust (i.e., ~100 My after CAI formation). Little is known about the impact flux that occurred during this time. Using insights from planet formation models [e.g., 1], we can postulate different impact scenarios for this era: (a) A large swarm of planetesimals survived planet formation and proceeded to steadily pummel the terrestrial planets and Moon for 500-600 My; the heavily-cratered lunar highlands were presumably produced by these putative impactors. (b) Few planetesimals survived accretion. If so, the impact flux would have been dominated by refugees from the asteroid belt and "primordial" comet disk regions. If few of these objects escaped, or their size-distributions were very different from those currently observed, the impact flux for 500-600 My may have been limited (e.g., [2]).

Note that some crater-age chronologies assume scenario (a) is valid [3]. Using numerical simulations, we find that the post-accretion planetesimal population decays too rapidly to explain the formation of large lunar basins like Imbrium, Orientale, Serenitatis, and Crisium [4] (**Fig. 1**). These results, when combined with evidence of limited impacts during this epoch from terrestrial zircons [5], implies that the terrestrial impact flux during this stage was surprisingly low.

Stage 2. The LHB era (4.0-3.8 Ga). Recent numerical modeling work of the primordial evolution of the Solar System supports the view that the LHB is an impact spike [6, 7]. According to [6], the giant planets initially had orbits that were circular and much closer to each other ($5 < a < 15$ AU). In particular, the ratio of orbital periods of Saturn and Jupiter was smaller than 2, while it is almost 2.5 at present. This crowded region was surrounded by a massive disk of

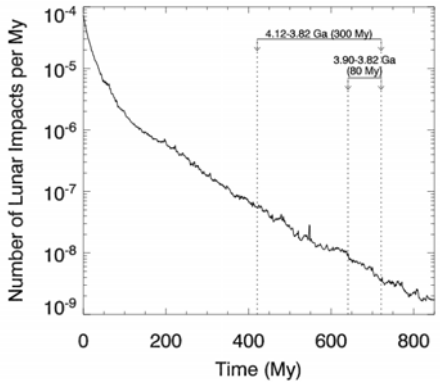

Fig. 1. The number of lunar impacts per My produced by a post-planet formation population (PPP). Lunar constraints indicate 2 and 4 D > 60 km basin-forming impactors struck between 3.90-3.82 Ga and 4.12-3.82 Ga, respectively. For the PPP to produce these impactors, it would need to have at least 1-10 Earth masses of material, exceeding Solar Nebula estimates

planetesimals of about 35 Earth masses; this was the forerunner of the current Kuiper belt and scattered disk. Dynamical interactions of the planets with this disk caused a slow increase of the orbital separation of planets. After 500-600 My, the ratio of orbital periods of Saturn and Jupiter became exactly equal to 2. This orbital resonance excited the eccentricities of these two planets which, in turn, destabilized the planetary system as a whole. The planetary orbits became chaotic and started to approach each other, which produced a short phase of encounters. Consequently, Uranus and Neptune were scattered outward into the disk, which destabilized it and abruptly increased the migration rates of the planets.

During this fast migration phase, the eccentricities and inclinations of the planets decreased via dynamical friction exerted by the planetesimals, allowing the planetary system to stabilize on their current orbits. At the same time, a huge flux of planetesimals reached the orbits or the terrestrial planets, from both the asteroid belt and the original trans-Neptunian disk [7]. Simulations show that $\propto 10^{22}$g of planetesimals hit the Moon during a ~100-200 My interval. This "terminal cataclysm" is consistent with the magnitude and duration of the LHB inferred from lunar craters [4, 7].

This model is consistent with additional lunar crater studies that argued that (i) asteroids dominated the LHB, (ii) asteroids were ejected from the asteroid belt by a size-independent process (presumably a resonance sweeping due to the migration of Jupiter and Saturn) and (iii) the total asteroid mass was insufficient to cause such a migration [8]. Moreover, the wave-like

shape of the main belt size distribution at this time [9] matches the shape of the crater size distribution found on the lunar highlands.

Stage 3. The Post-LHB Era (3.8-3.2 Ga). Crater counts of Apollo-sampled terrains indicate that the lunar impact flux declined by a factor of ~5 between 3.8-3.2 Ga [e.g., 2, 3]. The source of this very gradual decline over 500-600 My is unknown, but we hypothesize it was produced by small body populations placed onto marginally unstable orbits during Stage 2 [10].

In Stage 2, resonances are forced to move into new locations by Jovian planet migration; this causes some to sweep across the asteroid belt and drive off ~90% of the indigenous population [7]. Some refugees, however, are placed onto orbits that are unstable over very long time periods (hundreds of My on average). At the same time, comets and asteroids forced out of their source locations can become trapped inside or near the periphery of the asteroid belt. This implies that a large population of comet-like bodies may have been captured at the time of the LHB in the outer main belt [10].

As those asteroids and comets placed onto long-term unstable orbits dynamically escape via planetary perturbations into the terrestrial planet region, they bombard the Moon and other planets. Accordingly, the lunar cratering record from the late Imbrium period constrains events from Stage 2. Comparable craters records on other bodies (e.g., Mercury, Mars) add to this picture.

Stage 4. The Current Era (3.8 Ga-Today). The lunar impact flux over the last 3 Gy has been relatively constant except for occasional changes possibly related to asteroid breakup events [3]. Most impactors on the terrestrial planets in Stage 4 are now thought to have been asteroids that were driven out of the main belt through a combination of collisions, non-gravitational (Yarkovsky) thermal drift forces, and resonances (e.g., [11, 12]). The asteroids reaching the planet-crossing region are the end-products of a collisional cascade process, such that the shape of the size distribution is near equilibrium [9]. This explains why the NEO size distribution is a near reflection of the main belt's wavy-shaped size distribution (**Fig. 2**; see also [13]).

Asteroids provide more than 90% of the near-Earth object (NEO) and Mars-crossing asteroid populations located at $a < 7.4$ AU [12]. The rest come from Jupiter-family comets, who likely account for less than 10% of the remaining population. The contribution from Long-period and Halley-type comets to the lunar impact flux

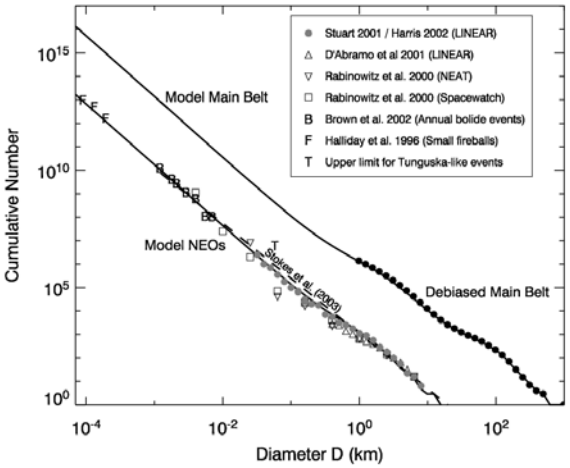

Fig. 2. The present-day main belt and NEA populations based on our model runs (solid lines). The shape of the NEA population is a reflection of the main belt, where Yarkovsky thermal drag causes $D < 40$ km asteroids to drift into resonances that in turn deliver them to the NEA population.

is only likely to be 4-5% of the total crater rate (which may increase by a factor of ~3 during putative comet showers).

Short-term deviations in this population may be caused by stochastic break up events. For example, the formation of the Baptistina asteroid family 160 My ago in the inner main belt [14] may have increased the NEO flux by a factor of 2-3 or so for ~100 My. We consider it likely that other major asteroid breakup events over the past 3 Gy (e.g., Flora [15]) have similarly influenced the lunar impact flux.

References: [1] O'Brien et al. (2006) *Icarus* **184**, 39; [2] Hartmann, W.K. et al. (2000) *Origin of Earth & Moon* (U. Arizona Press), 493. [3] Neukum, G. & Ivanov, B.A. (1994) *Hazards from Comets & Asteroids* (U. Arizona. Press), 359; [4] Bottke et al. (2007) *Icarus* **190**, 203. [5] Trail, D. et al. (2006) *LPSC* **37**, 2139. [6] Tsiganis, K. et al. (2005) *Nature* **435**, 459. [7] Gomes, R. et al. (2005) *Nature* **435**, 466. [8] Strom, R. et al. (2005) *Science* **309**, 1847. [9] Bottke, W.F. et al. (2005) *Icarus* **179**, 63; [10] Levison et al. (2008) *Nature*, submitted. [11] Bottke, W.F. et al. (2006) *Ann Rev. Earth Planet. Sci.*, in press; [12] Bottke et al. (2002), *Icarus* **156**, 399. [13] Brown, P. et al. (2002) *Nature* 420, 294; [14] Bottke et al. (2007) *Nature* **449**, 48. [15] Nesvorny, D. et al. (2002) *Icarus* **157**, 155.

Carbonaceous Chondritic Microclasts in Meteorites: Samples of the Late Heavy Bombardment? G. Briani[1,2] and M. Gounelle[1], [1]Laboratoire d'Étude de la Matière Extraterrestre, Muséum National d'Histoire Naturelle, 57 rue Cuvier, CP52, 75005 Paris, France, [2]Dipartimento di Astronomia e Scienza dello Spazio, Università di Firenze, largo E. Fermi 2, 50125, Firenze, Italy (briani@mnhn.fr).

Introduction: Xenoliths in meteorites are fragments not genetically related with the host meteorite. They can be of different types and sizes [1-14]. A problem concerning xenoliths is that in most cases the identification of their origin, i.e. of their parent bodies, is very difficult. Carbonaceous chondrite-like inclusions represent the majority of xenoliths [15]. We contend that all or part of these xenoliths sample the Late Heavy Bombardment (LHB) [16].

The Nice model [17-19] suggests that the LHB was triggered when Jupiter and Saturn crossed the 1:2 mean motion resonance, about 700 My after the planets formation. This caused the depletion and migration of icy bodies in the Kuiper Belt (beyond ~15 AU) and of asteroids in the main belt (between ~2 and 3.5 AU). In this context objects composed by more fragile and/or unconsolidated material, such as chondritic asteroids and cometary bodies, are the most affected by collisions [20], i.e. the best candidates for the production of fragments.

The goal of our work is to look for carbonaceous chondritic microclasts (CCMs) in as many meteorites groups as possible. The characteristics we expect from a population of LHB fragments are: (1) their presence in different meteorites; (2) mineralogical and structural properties similar to those of primordial, chemically unprocessed material; (3) difficulties to classify them with respect to meteorites, micrometeorites and IDPs and (4) the presence of some "unusual" xenolith, possibly cometary. The basic idea of this work is to realize a general "survey" of CCMs in meteorites. Instead of characterize some particular inclusion in a meteorite, we want to search for fragments that can reveal, by their common properties, their common origin in a single event.

Experimental procedures: To extend the research of CCMs to meteorites groups other than howardites, we have chosen breccias or gas-rich meteorites, as they clearly show a history of exposure to space and collisions. Analyses of the prepared polished sections by means of an optical microscope are the starting point for the selection of potential xenoliths. Subsequent back-scattered electron images taken by a scanning electron microscope allow a better identification of CCMs, e.g. with respect to the meteorite matrix or impact melt inclusions. We utilize a JEOL JSM 840-A scanning electron microscope, also equipped with an EDAX Genesis X-rays detector to perform energy dispersion spectroscopy of CCMs. Quantitative analyses for the mineralogical composition of CCMs are realized with a CAMECA SX-100 electron microprobe at the University of Paris VI. A 10 nA focalized beam, accelerated by a 15 kV potential difference, is used for punctual analyses of CCMs oxides and metals. For carbonates, a 4 nA defocalized beam, with a 15 kV accelerating voltage, is used.

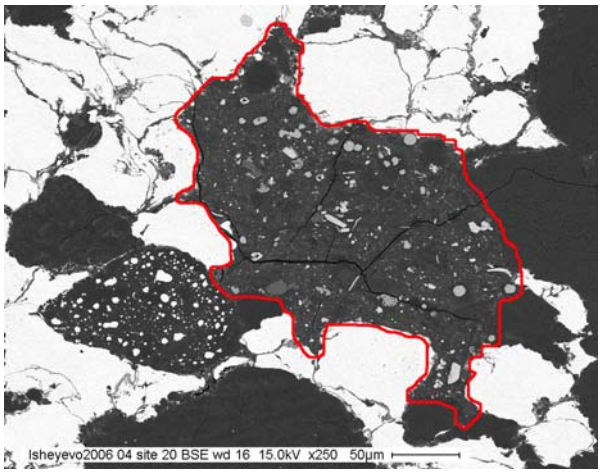

Figure 1. A CCM in the Isheyevo CB chondrite, surrounded by metal grains and silicates. Many magnetite inclusions are present. Lower-left is also visible an impact-melt inclusion.

Results: Up to now, we have identified CCMs in the CB carbonaceous chondrite Isheyevo and in the H5 ordinary chondrite Leighton. Good candidates to be CCMs have been found in the ordinary chondrites Krymka (LL3.2), Mezo-Madaras (L3.7) and Sharps (H3.4). Further analyses and comparisons with precedent works are being performed to establish if they are really xenoliths. No evidence of CCMs has been found in Weston (H4), Bremervorde (H/L3.9), Adzhi-Bogdo (LL3-6) and the aubrite Pesyanoe, despite the fact that they are all breccias.

All new CCMs range in size between 50 and 750 µm (Fig. 1 and 2). In both Isheyevo and Leighton their structure is dominated by a fine-grained matrix composed by sub-µm-sized phases, mainly phyllosilicates with variable amount of sulfides and magnetite. In an Mg-Fe-Si+Al ternary diagram, analyses of matrix plot in the region of CM2 serpentine and CR2 phyllosilicates for Leighton CCMs, while they are more shifted toward the Fe pole for Isheyevo (Fig. 3). A common feature of matrix analyses is the high values of S (between 2 and 15 %wt), due to the presence of either tochilinite or sub-µm-sized sulfides. Anhydrous sili-

cates like olivine and pyroxene are present either as isolated crystals in the matrix or as micro-chondrules. Olivine is mainly Mg-rich, its composition ranging between Fo_{98}-Fa_2 and Fo_{84}-Fa_{16}. In general the same is true for pyroxene, for which enstatite is the principal phase, but in same cases it has been found also Ca-rich pyroxene (En_{13}-Wo_{80}). Magnetite is very abundant in some of the CCMs, and absent in others. When present, it is in the form of either aggregates of a few crystals or of small framboidal clusters. Carbonates are quite rare (of the order of one in some xenoliths) in the Isheyevo CCMs, while they are very abundant in three CCMs in the Leighton ordinary chondrite. In both cases, they are mainly Ca- and Mg-rich carbonates. Sulfides are mostly troilite, with some rare grains of pentlandite. Metals are present as small, µm-sized grains coupled with sulfides.

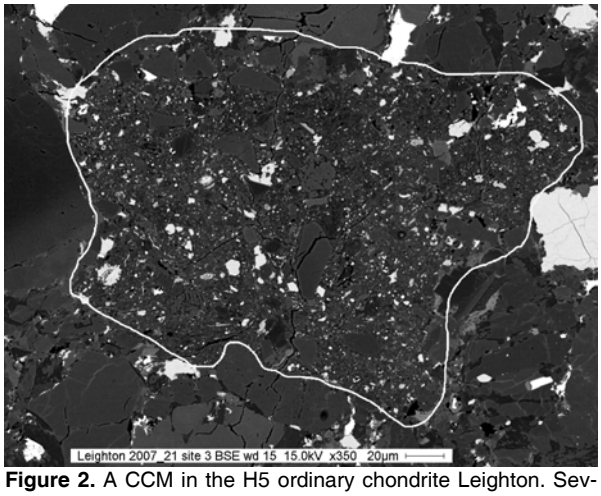

Figure 2. A CCM in the H5 ordinary chondrite Leighton. Several silicates and metal inclusions are visible.

It has to be noticed that one CCM in Isheyevo has an unusual aspect. It is very dark, with a very fine-grained matrix, composed by sub-µm-sized grains of phyllosilicates, magnetite and sulfides. It does not resemble to any previously known CI- or CM-like xenolith, but it might have some of the properties indicates for cometary material [21].

Conclusions: We propose that CCMs, present in meteorites as xenoliths, are fragments produced by collisions during the LHB. Our preliminary results on the mineralogy of new CCMs indicate that they are made by C2-like material. Further analyses are in progress in order to obtain a more precise classification of micro-xenoliths in meteorites. But the fact that CCMs are composed by chemically unprocessed material is one of the characteristic we expect from a population of fragments coming from collisions of primordial bodies. Discovering and analyzing other xenoliths is necessary to establish if they are really widespread in meteorites, as supposed by the hypothesis that they originate from the LHB event. In addition, new "unusual" CCMs, as the one found in Isheyevo, might reveal new insights on possibly cometary samples.

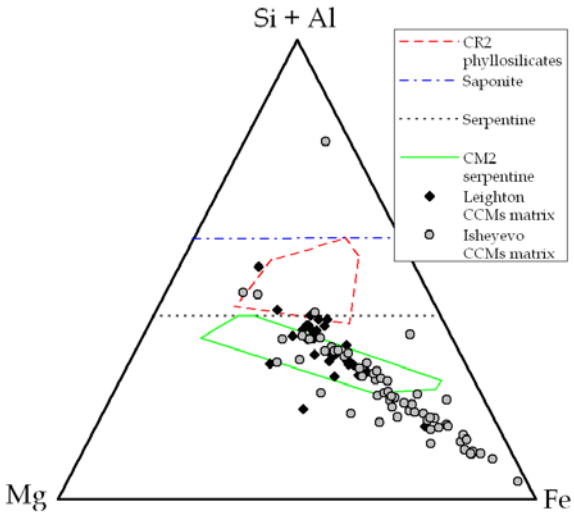

Figure 3. Ternary diagram for matrix of CCMs in the H5 ordinary chondrite Leighton and in the CB chondrite Isheyevo.

References: [1] Whal W. (1952) *GCA, 2*, 91-177. [2] Wilkening L. L. (1976) *LPSC, 7*, 3549. [3] Leitch C. A. & Grossman L. (1977) *Meteoritics, 12*, 125-139. [4] Wilkening L. L. (1977) In *Comets, Asteroids, Meteorites*, 389-395. [5] Neal C. W. & Lipschutz M. E. (1981) *GCA, 45*, 2091-2107. [6] Brearly A. J. & Printz M. (1992) *GCA, 56*, 1371-1386. [7] Noguchi T. et al. (2003) *GCA Supplements, 67*, 341. [8] Nakashima D. et al. (2003) *EPSL, 212*, 321-336. [9] Ikeda Y. et al. (2003) *Antarct. Meteorite Res., 16*, 105-127. [10] Gounelle M. et al. (2003) *GCA, 67*, 507-527. [11] Semenenko V. P. (2005) *GCA, 69*, 2165-2182. [12] Rubin A. E. et al. (2005) *GCA, 69*, 3419-3430. [13] Bischoff A. et al. (2006) In *Meteorites and the Early Solar System II*, U. of A. Press, 679-712. [14] Zolensky M. E. (2006) *MAPS, 31*, 518-537. [15] Meibom A. & Clark B. E. (1999) *MAPS, 34*, 7-24. [16] Gounelle M. et al. (2005) *GCA, 69*, 3431-3443. [17] Tsiganis K. et al. (2005) *Nature, 435*, 459-461. [18] Morbidelli A. et al. (2005) *Nature, 435*, 462-465. [19] Gomes R. et al. (2005) *Nature, 435*, 466-469. [20] Levison H. F. et al. (2008), American Astronomical Society, DDA meeting #39, #12.05. [21] Campins H. & Swindle T. D. (1998) *MAPS, 33*, 1201-1211.

THE LATE HEAVY BOMBARDMENT: POSSIBLE INFLUENCE ON MARS. D. M. Burt[1], L. P. Knauth[2], and K. H. Wohletz[3] [1]School of Earth and Space Exploration, Arizona State University, Box 871404, Tempe, AZ 85287-1404, dmburt@asu.edu, [2]same, knauth@asu.edu, [3]Los Alamos National Laboratory, Los Alamos, NM 87545, wohletz@lanl.gov.

Introduction: From orbit, Mars appears to be as heavily cratered as Earth's moon. The cratering record is best exposed on the ancient Southern Highlands; in the Northern Plains it is largely covered by a thin veneer of younger sediment and lavas. The martian cratering is widely assumed to date from the same episode of bombardment that cratered the Moon (the so-called Lunar Cataclysm). On the basis of radiometric dating of returned lunar impact melts, this episode has tentatively been assigned to the interval 4.0-3.8 Ga. The Late Heavy Bombardment (LHB) on Mars and other terrestrial planets, if it occurred, probably spanned the same geologically short time interval.

Somewhat surprisingly, given the wide discussion of the LHB for the Moon and Mercury, current and past geological literature on Mars tends to ignore this apparent spike in cratering, and rather implicitly assumes that the bombardment of Mars was continuous from its formation at about 4.5 Ga until about 3.8 Ga, an interval called the Noachian. In light of the LHB, the Noachian interval of Mars may actually have been rather short, with the record of the first half-billion years having been largely destroyed or buried (as on Earth).

The excellent preservation of the martian cratering record from 3.8 Ga on probably implies that Mars has been dry and cold since then. Other than continued cratering at a much reduced rate, the major geological process appears to have been extremely slow erosion and deposition by the wind. Important local contributions were made by basaltic volcanism, landslides and debris flows, ground ice (leading to terrain softening), glaciers (including rock glaciers), catastrophic flooding in outflow channels, and extremely minor chemical and physical weathering. Still, the ancient craters are all there. The major reason for their preservation is probably the LHB itself.

Compared to Earth, Mars is small and much farther from the Sun. Whatever its nature beforehand, the catastrophic cratering of the LHB, in addition to completely resurfacing the planet, should have resulted in catastrophic loss of hydrosphere and atmosphere to space. How then to explain the widespread evidence of ancient drainage networks, crater lakes, buried clay horizons, and surface sulfates (including acid sulfates)? These features are widely cited as evidence that Noachian Mars was warm as well as wet, and furthermore was literally bathed in sulfuric acid, supposedly (acid fog model) owing to atmospheric enrichment in volcanogenic sulfur dioxide (SO_2) to provide the greenhouse warming that carbon dioxide (CO_2) couldn't.

Inasmuch as these "warm, wet, acid" geological features coincide in time and space with the craters of the LHB, a simpler hypothesis might be that they are directly related. That is, the LHB itself can probably account for most of them, and especially their transient nature, although local volcanism, especially in the Tharsis region, was occurring at the same time.

Geological Changes. Before the onset of the LHB (i.e., prior to 4.0 Ga), Mars probably had more of an atmosphere and hydrosphere than at present; it also appears to have had a magnetic field (but none since). Given its distance from the Sun, and apparent inability to retain a thick atmosphere, most surface water was probably present as ice, nevertheless. Freezing of surface water would concentrate soluble salts in dense brines beneath the ice; salts would crystallize if temperatures were cold enough or enough ice sublimed. In other words, brine freezing (probably with ice sublimation) provides a possible alternative to direct brine evaporation for crystallizing salts [1].

Following each major impact, or at the height of the LHB (when many smaller impacts followed in close succession), enough steam should have been generated to create a temporary greenhouse, and condensation of and alteration by this steam could explain contemporaneous water-related features - clays, drainage networks, and lakes. If the impact target was rich in iron sulfides or various sulfate salts, the steam condensate could have been acid (i.e., acid rain). However, such acidity would have been ephemeral, given that Mars consists of basic silicates (silica or SiO_2 combined with MgO, FeO, CaO, and some Al_2O_3). That is, the liquid acid would have reacted with (neutralized itself against) basaltic rock, unless flash freezing or evaporation preserved it in the form of crystalline ferric acid sulfates, such as those found by the two rovers. Another way to create this mine dump mineralogy [2] would be for the impact to scatter shattered iron sulfides, which could later oxidize during damp diagenesis (the Roger Burns method). Neutral salts could similarly result from impact scattering of salty target materials or flash evaporation of brines. The important point is that acid surface waters are not required to make sulfate salts ("evaporites"), because

salty impact deposits could have derived their salts via impact reworking of salts of various origins from various target areas [1]. The acid sulfates could be direct impact condensates or sulfide oxidation products.

By the tail end of the LHB (that is, by the time of the near-surface geological interval investigated by the two rovers Spirit in Gusev Crater, and Opportunity at Meridiani Planum), most of the martian hydrosphere and atmosphere had presumably already been lost to space (via impact erosion), and Mars would have been cold and dry. In part, impacts rework older impact deposits. Impact-generated steam would probably condense as snow or ice, at least far from the impact site. Lack of exposure to liquid water presumably accounts for the excellent preservation of features (including metastable acid sulfates), lack of salt recrystallization, and minimal erosion at these two surface sites.

Impact Surge Deposits and Spherules. Although it is smaller and colder and its surface is far older, Mars does have two important features in common with Earth - the presence of an atmosphere and of abundant subsurface volatiles (mainly water on Earth, mainly ice on Mars). These features mean that the LHB on Mars should have been distinct from the LHB on dry, atmosphereless bodies such as the Moon and Mercury. The young martian rampart craters, believed to form via impacts into an icy substrate, reflect this distinctness. On Earth, cross-bedded fine-grained sediments, locally containing various types of small spherules (glassy condensates and accretionary lapilli), are known to be deposited via explosions that vary from nuclear to volcanic to impact-derived. These explosion-deposited sediments (so-called surge or base surge deposits) can greatly resemble sediments deposited by flowing water or wind, a fact that has led to multiple misattributions [3]. In places, small radial scours caused by vortices, or bomb sags caused by the landing of ballistic ejecta, can help identify such sediments. In this regard, a bomb sag has tentatively been identified in the cross-bedded surge beds at Home Plate, Gusev Crater and a deep scour is present at the top of a large cross bed in the Burns Cliff exposure, Endurance Crater, Meridiani Planum.

Surge deposits can vary from wet to dry, depending on the initial steam content. Spherical accretionary lapilli typically form in rather wet deposits, via condensation of sticky steam on particles in a turbulent, dilute density cloud. Accretionary lapilli, unlike sedimentary concretions, tend to be strictly size and shape limited and unclumped; they also can contain high temperature minerals. Millimetric spherules of unspecified composition occur in a distinctive horizon beneath Home Plate in Gusev Crater; somewhat larger (up to about 5mm) and more abundant spherules occur in cross-beds in various near-surface horizons along the Opportunity Rover traverse in Meridiani Planum. The most common (at least 50%) phase in these lapilli is the crystalline, specular, high temperature form of hematite (so-called gray hematite, with detected enrichment in Ni); their blue-gray color led to the spherules initially being called “blueberries”. Other than some doublets and a linear triplet, the spherules tend to be unclumped and uniform in size (within a given horizon); they show no evidence of concentration by flowing or mixing groundwaters. Wind erosion has left them exposed as a lag deposit uniformly exposed over an area hundreds of km across.

Steam Alteration. A common phase in basaltic surge deposits (phreatomagmatic types, wherein steam explosions result from explosive mixing of magma and water) is yellow-orange palagonite, or hydrated and oxidized volcanic glass. Palagonite is believed to be extremely common all across Mars, and may partly be responsible for its distinctive color. Rather than forming by volcanism, palagonite could have originated by hydration and oxidation of basaltic impact melts in steamy impact surge clouds.

Terrestrial impact cratering, in the presence of water or ice, commonly results in silica alteration and deposition by hot springs. Given the low atmospheric pressure on Mars, acid fumarolic or steam alteration should be more common than hot springs. Such alteration, followed by impact scattering, could account for the silica-rich fragmental horizon recently identified beneath Home Plate, Gusev Crater. This horizon occurs above the one containing the spherules.

Conclusion: Impact surges seem to require either a volatile-rich target or an existing atmosphere or both, as on Mars. By the tail end of the LHB, when the impact surge deposits (our interpretation [4]) and spherules at Meridiani Planum and Home Plate (Gusev Crater) formed, Mars was already dry and cold. Surface waters are not indicated at that time (i.e., by available evidence either at Meridiani or Gusev), although they probably were ephemerally present earlier in martian history (especially during the most intense period of bombardment). Mars is indeed an impact-dominated planet, and many of its most interesting features apparently date from and probably were caused by the LHB.

References: [1] Knauth, L.P. and Burt, D.M. (2002) *Icarus 158*, 267. [2] Burt D.M et al. (2006) *Eos, 87*, 549. [3] Burt D.M. et al. (2008) *JVGR* (in press). [4] Knauth L.P. et al. (2005) *Nature, 438*, 1123.

FIRST *MESSENGER* INSIGHTS CONCERNING THE EARLY CRATERING HISTORY OF MERCURY.
C. R. Chapman[1], W. J. Merline[1], S. C. Solomon[2], J. W. Head, III[3], and R. G. Strom[4]. [1]Southwest Research Institute, Suite 300, 1050 Walnut St., Boulder CO 80302, cchapman@boulder.swri.edu; [2]Dept. of Terrestrial Magnetism, Carnegie Institution of Washington, Washington DC 20015; [3]Dept. of Geological Sciences, Brown Univ., Providence RI 02912; [4]Lunar and Planetary Lab., Univ. of Arizona, Tucson AZ 85721.

Introduction: Mercury has long been recognized as a key planet for understanding the early bombardment history of the Solar System, but until early this year the only spacecraft views of its cratered landscape were Mariner 10's vidicon images of 45% of the planet's surface (much of it seen at high solar illumination angles) obtained in the 1970s. Beginning with its first flyby of Mercury in January 2008, the MESSENGER spacecraft will continue through its orbital mission (commencing in March 2011) to image the whole planet from a variety of perspectives. It will also obtain laser altimetry and other important geophysical measurements that will dramatically increase our understanding of the impact history in the inner Solar System and of Mercury's planetary response to the bombardment.

Basins on Mercury: Even from Mariner 10 images, numerous impact basins were identified, although researchers differed on whether or not Mercury is more densely covered with basins than is the Moon [1, 2, 3]. The dramatic Caloris basin, the eastern half of which was revealed by Mariner 10, is one of the largest and youngest multiring impact basins in the Solar System. The entirety of Caloris dominates the new sector of Mercury imaged by MESSENGER during the first flyby (Fig. 1), and Caloris is now measured to have a diameter of about 1,550 km, or more than 200 km larger than estimated from Mariner 10. This makes Caloris roughly the size Borealis (a stratigraphically old basin near the north pole), which previously had been regarded as Mercury's largest basin.

Additional basins, or evidence of possible basins, are seen in the new MESSENGER images. A particularly interesting example is the double-ring (peak-ring) basin, Raditladi. (Raditladi is about 260 km in diameter, somewhat bigger than a somewhat arbitrary dividing line between large craters and small basins, 250 km.) Raditladi appears to be unusually fresh, with a very small density of superposed small craters; it is possible that it formed within the last billion years [4].

As MESSENGER makes its next two flybys of Mercury and eventually enters orbit, high-quality imaging of the entire surface will provide a basis for a more thorough photogeologic assessment of the planet's basins. However, in recent years, other kinds of data sets have been used to assess basin populations on other terrestrial bodies. MGS MOLA topography and gravity data for Mars have revealed many large circular structures, especially in the northern lowlands, which are likely basins [5]. Frey [6] has used the Unified Lunar Control Network (based largely on photogrammetric measurements of Clementine images) to nearly double the number of potential lunar basins assessed by Wilhelms [7]. MESSENGER's Mercury Laser Altimeter should enable a similar advance in recognition of Mercury's basins from precise topography.

Mercury's Bombardment History: Mercury's "Population 1" crater size distribution has been attributed to the same population of impacting bodies responsible for the Late Heavy Bombardment (LHB) on the Moon [8]. ("Population 2" refers to more recent, generally smaller craters not relevant to early bombardment.) Besides the basins, Population 1 includes craters 10 – 250 km diameter in Mercury's more heavily cratered regions. Although crater size-frequency distributions for the more heavily cratered terrains on the Moon and Mars are similar to Mercury's Population 1, there are significant differences among all three bodies [8]. The relative depletion of craters smaller than 40 km diameter on Mars compared with the Moon is reasonably attributed to the wide variety of geological processes that have been, and continue to be, active on Mars. The depletion in numbers of craters smaller than 40 km is even greater on Mercury, which lacks an atmosphere and many of the processes active on Mars. This depletion has generally been ascribed to more pervasive erasure by formation of the so-called intercrater plains, which are stratigraphically timed as having formed during the LHB [9].

There has been debate about the nature of intercrater plains. If they are primarily formed by basin ejecta, like the Cayley plains on the Moon, then why would they be so much more pervasive on Mercury compared with the Moon? Possibly they represent pervasive early volcanism.

As the youngest large basin, Caloris provides insight to issues of plains formation. The formation of at least some of the so-called smooth plains on Mercury has been as controversial as the formation of intercrater plains. Smooth plains are common on the periphery of Caloris in Mariner 10 images. Many researchers considered these plains to be of volcanic origin, although no explicitly volcanic features could be iden-

tified, while others considered the plains to have been formed by Caloris ejecta, like the lunar Cayley plains [10]. Now MESSENGER has found unequivocal evidence that at least some of the plains in the newly imaged region of Mercury are volcanic in nature [11, 12]. Yet many other circum-Caloris plains may be related to basin ejecta. Since these basin-related smooth plains may simply be the most recent, pristine examples of what we classify as intercrater plains when they are much older, final resolution of the relative contributions of volcanism and ejecta emplacement to plains formation will profoundly affect our understanding of Mercury's early bombardment history.

It has been suggested [13] that a cataclysmic bombardment of Mars could have deposited sufficient heat to have affected the thermal evolution of the planet's upper mantle and generated widespread surface volcanism. Due to gravitational focusing by the Sun, comets and asteroids dislodged during a Solar-System-wide LHB, as proposed by the Nice model [14], might have pummeled Mercury with especially energetic impacts, perhaps contributing to a volcanic production of abundant intercrater plains.

Recently it has been suggested [15, 16, 17] that the global dichotomy of Mars was caused by an extremely large impact in that planet's northern hemisphere. Perhaps that happened near in time to the hypothesized giant-impact formation of the Moon and a hypothetical impact that may have stripped away much of proto-Mercury's once-more-massive crust and upper mantle [18]. But these events all surely preceded the LHB, while planetary embryos were still around. Events in this very early epoch may have created geochemical and geophysical attributes of Mercury that can be studied by MESSENGER, but the geological record on the planet's surface likely is restricted to the later phases of the LHB around 3.9 Ga and more recently.

Puzzles remain, however, about the several-million- year period following formation of the last lunar basin, Orientale, when the impact rate was still much higher than it is now, though declining. Meteoritic evidence suggests asteroids were still colliding more often than they are now [19] and post-Caloris impacts may be better preserved on Mercury than they are on other planets if Mercury's global contraction terminated volcanic resurfacing. So comparisons of Hesperian Mars, post-Orientale Moon, and post-Caloris Mercury may help decipher the declining bombardment at and after the end of the LHB epoch in the Solar System.

A lingering complication is the possibility that the intense phase of Mercury's impact history extends to more recent times than for other terrestrial planets because of a hypothetical population of Mercury-specific impactors, called vulcanoids [20]. This would potentially obscure our interpretation of Mercurian cratering as being due solely to the same population of asteroids and comets that have impacted the other terrestrial planets, both during and after the LHB. While Earth-based searches for vulcanoids have constrained the current population to being rather small bodies if they exist at all, vulcanoids could have been largely depleted by now but remained well beyond the end of the LHB [21]. MESSENGER has already taken a few of a planned campaign of images of the outer portions of the would-be vulcanoid belt, which may eventually be able to establish stricter limits on the significance of this putative population of small bodies.

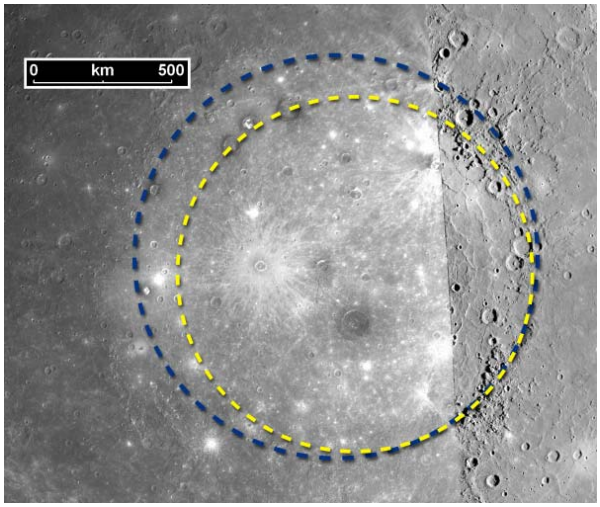

Fig. 1. The Caloris basin (Mariner 10 image on the right, MESSENGER image on the left) and early and recent diameter estimates.

References: [1] Frey H. and Lowry B. L. (1979) *Proc. LPSC 10th*, 2669-2687. [2] Pike R. J. (1988) in "Mercury" [U. Ariz. Press] 165-273. [3] Strom R. G. and Sprague A. L. (2003) "Exploring Mercury" [Springer-Praxis], 216 pp. [4] Strom R. G. et al. (2008) *Science 320, Issue 5885*. [5] Edgar L. A. and Frey H. V. (2008) *GRL.*, doi: 10.1029/2007GL031466. [6] Frey H. V. (2008) *LPS XXXIX*, Abstract #1344. [7] Wilhelms D. E. (1987) "The Geologic History of the Moon," USGS *Prof. Paper* #1348. [8] Strom et al. (2005) *Science, 309*, 1847-1850. [9] Spudis P. D. and Guest J. E. (1988) in "Mercury" [U. Ariz. Press] 118-164. [10] Head J. W. et al. (2007) *Space Sci. Revs., 131*, 41-84. [11] Head J. W. et al. (2008) *Science 320, Issue 5885*. [12] Murchie S. L. et al. (2008) *Science 320, Issue 5885*. [13] Solomon S. C. and Head J. W. (2007) *LPS XXXVII*, Abstract #1636. [14] Gomes R. et al. (2005) *Nature, 435*, 466-469. [15] Andrews-Hanna J. C. et al. (2008) *Nature, 453*, 1212-1215. [16] Marinova M. M. et al. (2008) *Nature, 453*, 1216-1219. [17] Nimmo F. et al. (2008) *Nature, 453*, 1220-1223. [18] Wetherill G. W. (1988) in "Mercury" [U. Ariz. Press] 670-691. [19] Chapman C. R. et al. (2007) *Icarus, 189*, 233-245. [20] Leake M. A. et al. (1987) *Icarus, 71*, 350-375. [21] Vokrouhlický D. et al. (2000) *Icarus, 148*, 147-152.

A REVIEW OF LUNAR METEORITE IMPACT-MELT CLAST COMPOSITIONS AND AGES. Barbara A. Cohen, Marshall Space Flight Center, Huntsville AL 35812 (Barbara.A.Cohen@nasa.gov).

Introduction: One of the important outstanding goals of lunar science is understanding the bombardment history of the Moon and calibrating the impact flux curve for extrapolation to the Earth and other terrestrial planets. Obtaining a sample from a carefully-characterized interior melt sheet or ring massif is a reliable way to tell a single crater's age. A different but complementary approach is to use extensive laboratory characterization (microscopic, geochemical, isotopic) of float samples to understand the integrated impact history of a region. Both approaches have their merits and limitations. In essence, the latter is the approach we have used to understand the impact history of the Feldspathic Highland Terrain (FHT) as told by lunar feldspathic meteorites.

Feldspathic lunar meteorites: The feldspathic lunar meteorites are regolith and fragmental breccias with high Al_2O_3 / low Th content relative to the KREEPy, mafic impact-melt rocks of the Apollo collection. The stochastic nature of lunar meteorite launch events implies that these meteorites are more representative of the feldspathic lunar highlands than the Apollo and Luna samples [e.g., 1-3]. More than 100 impact melt clasts from 12 feldspathic lunar meteorites (MAC 88105, QUE 93069, DaG 262, DaG 400, NWA 482, Dhofar 025, Dhofar 303, Dhofar 910, Dhofar 911, Kalahari 008) and two possible nearside lunar meteorites (Calcalong Creek and SaU 169) have been studied [4-10]. Impact-melt clasts within the meteorites in the meteorites have usually been identified without regard for their composition, using textural criteria with the petrographic and scanning-electron microscopes. The identified clasts are generally microporphyritic or quench-textured and fully crystalline, having textures similar to well-known rocks of impact origin that establish their origins as impact-melt samples.

Clast Compositions: Figure 1 shows that the majority of impact-melt clasts in the studied meteorites are similar in composition to the bulk feldspathic meteorite field rather than the typical mafic, KREEPy impact melts of the Apollo collection, which came from the Procellarum KREEP Terrain (PKT). The impacts in which they were produced either predate the PKT or were sited in the feldspathic highlands where KREEPy material is rare. By extension, breccias that do not contain KREEPy clasts either formed far from the PKT or were lithified and closed to new input prior to formation for the PKT. Impact-melt clasts within each meteorite tend to cluster around the bulk composition, indicating that they are locally derived. However, the textural variety and the range in Mg# (Fig. 1c) suggest that the clasts originated in more than one impact event. The range of clast com-

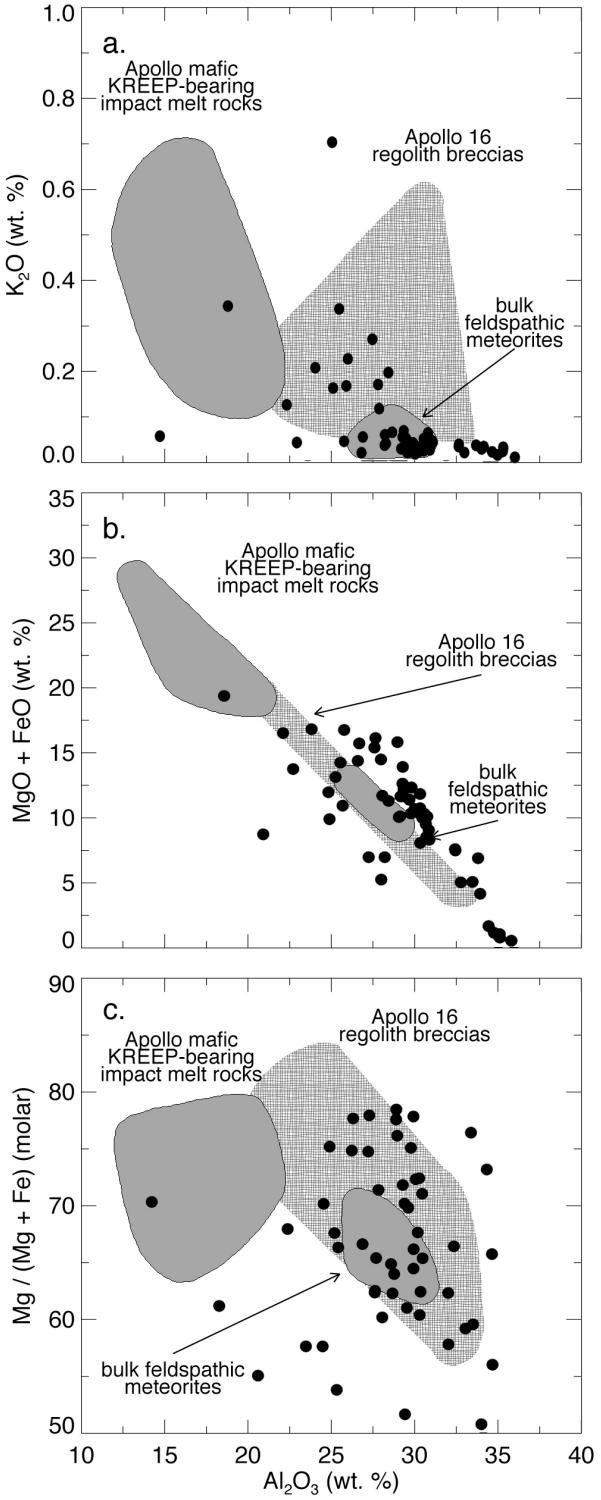

Fig. 1: Impact-melt clast compositions in lunar meteorites [4-10].

positions within each meteorite is similar to the compositional range displayed by Apollo 16 regolith breccias, which is the result of mixing of feldspathic lithologies with the more mafic lithologies of the PKT. Though trace elements on dated impact-melt clasts have not yet been obtained, Fig. 1 implies that the mafic component in the meteorite breccias is not the same as in the A16 breccias, and is more likely to be gabbroic or basaltic.

Clast Ages: Figure 2 shows that impact-melt clast ages range from ~4.0 Ga to younger than 2.0 Ga, with a statistical peak around 3.5 Ga. It appears that impact-melt rocks created in post-basin bombardment dominate the very surface of the lunar regolith and are readily incorporated into regolith breccias until the breccia lithification event. No samples are >1.1 σ older than 4.0 Ga, the older limit of the predominant age range among Apollo impact melt rocks. This older age limit is consistent with a resurfacing event in the FHT at that time, such as a global lunar cataclysm. Alternatively, older impact melt rocks may have been gardened back into the regolith column, becoming volumetrically rare. Either way, the impact rate after 4.0 Ga is probably low enough that the impact-melt clasts now at the surface effectively sample the impact flux since 4.0 Ga.

Conclusions: Impact-melt clasts in lunar meteorites show that surface breccias provide a relatively representative sample of the upper lunar surface in the area where they formed. The impact-melt ages within them therefore record of the impact history of that region between the time of the last major resurfacing (or gardening) event and the time of breccia closure, perhaps with a statistically small number of older samples entrained in the upper regolith. Because the samples come from the uppermost surface, we can correlate composition of the clasts with lunar terrains from remote sensing data [11-12] to conclude that the age distribution of clasts in the feldspathic meteorites reflects the impact history of the FHT from ~4 Ga to the closure age of the meteorites.

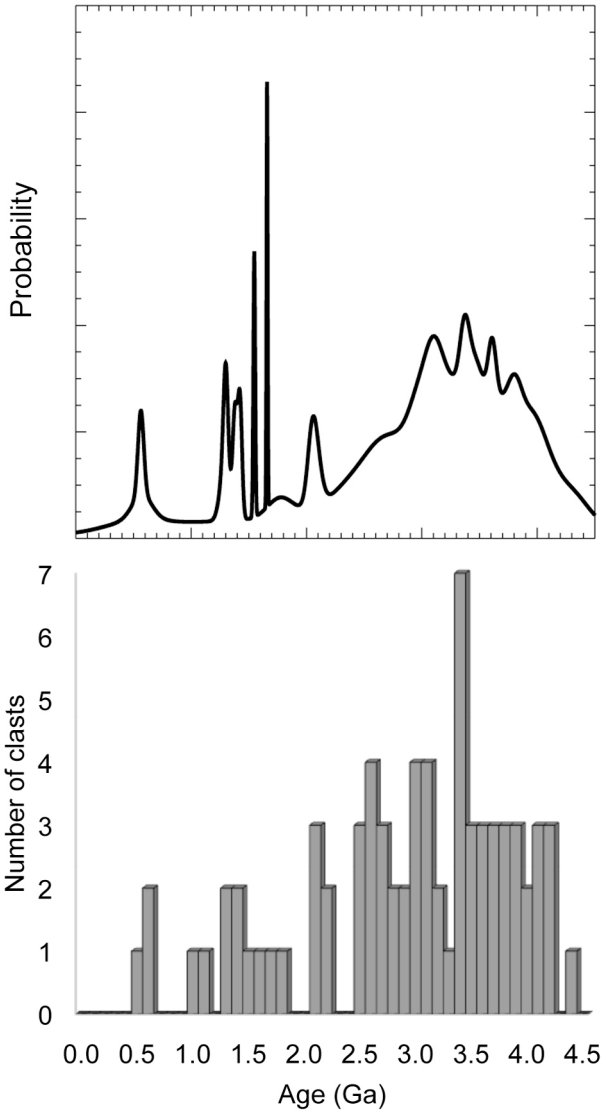

Fig. 2: Impact-melt clast ages in lunar meteorites [4-10].

References: [1] Taylor, G. J. (1991) Impact melts in the MAC88105 lunar meteorite: Inferences for the lunar magma ocean hypothesis and the diversity of basaltic impact melts. GCA 55(11): 3031-3036. [2] Warren and Kallemeyn (1991) The MacAlpine Hills lunar meteorite and implications of the lunar meteorites collectively for the composition and origin of the Moon. GCA 55:3123–3138.3. [3] Korotev (2005) Lunar geochemistry as told by lunar meteorites. Chemie der Erde 65: 297–346. [4] Cohen, B. A., T. D. Swindle, et al. (2000) Support for the lunar cataclysm hypothesis from lunar meteorite impact melt ages. Science 290(5497): 1754-1756. [5] Fernandes et al. (2000) Laser argon-40-argon-39 age studies of Dar al Gani 262 meteorite. MAPS 35(6): 1355-1364. [6] Cohen et al. (2002). ^{40}Ar-^{39}Ar ages from impact melt clasts in lunar meteorites Dhofar 025 and Dhofar 026. LPSC 33, #1252. [7] Daubar et al. (2002) Northwest Africa 482: A crystalline impact-melt breccia from the lunar highlands. MAPS 37(12): 1797-1813. [8] Fernandes et al. (2004). Ar-Ar studies of Dhofar clast-rich feldspathic highland meteorites: 025, 026, 280, 303. LPSC 35, #1514. [9] Cohen et al. (2005) Geochemistry and ^{40}Ar-^{39}Ar geochronology of impact-melt clasts in lunar meteorites Dar al Gani 262 and Calcalong Creek. LPSC 36, #1481. [10] Cohen (2008) Lunar Meteorite Impact Melt Clasts and Lessons Learned for Lunar Surface Sampling. LPSC 39, #2532. [11] Zellner et al. (2002) Impact glasses from the Apollo 14 landing site and implications for regional geology. JGR E107: 12-1. [12] Gnos et al. (2004) Pinpointing the source of a lunar meteorite: Implications for the evolution of the Moon. Science 305: 657–659.

ORBITAL EVOLUTION OF THE MOON AND THE LUNAR CATACLYSM. Matija Ćuk, Harvard University, Department of Earth and Planetary Sciences, 20 Oxford St, Cambridge, MA 02138; cuk@eps.harvard.edu

Introduction: The concept of Lunar Cataclysm (and sometimes synonymous Late Heavy Bombardment) originated from the the study of lunar samples collected by Apollo missions [1]. Despite many new lines of evidence, the best data we have on the LC/LHB is still that from Earth's Moon [2]. There has even been skepticism if the LC/LHB even happened outside the Earth-Moon system [3]. In any case, the question of there being a connection between the Moon's complex orbital evolution and the Cataclysm is legitimate given that the timescales involved are similar. Also it is interesting to see what consequences for the lunar orbit would result from different scenarios of LC/LHB.

Multiple Moons of Earth: In principle, the Moon-forming impact could have resulted in multiple satellites [4], in which case their subsequent orbital evolution would have been rather complex. A lunar-only cataclysm all but requires some sort of late instability in a terrestrial multiple-moon system. Canup et al. [5] studied evolution of such systems using both analytical and numerical methods, and found that smaller satellites always get trapped in eccentricity-type mean-motion resonances. Orbital evolution in these resonances invariably leads to extremely high eccentricities and relatively rapid instability. Therefore [5] concluded that a terrestrial multiple-moon system could have lasted for less than million years, with the clear implication that they were not the cause of the Cataclysm.

Our own more recent research mostly confirms results of [5]. We integrated a full three-dimensional system with solar perturbations, and found that the moons often tend to become trapped in inclination-type, rather than eccentricity-type mean-motion resonances (this applies to the 1:3 resonance, among others). Despite this difference, the system always encounter instability rather fast, after the smaller moon attains first large inclination and then also large eccentricity.

While the results so far on the stability of such systems are quite discouraging, there are reasons to assume that there might be some aspects of the problem that have been overlooked. In particular, the curious configuration of Pluto's three-satellite system contradicts our present models of multiple-moon doom [6,7], so the long-lived other moons of Earth cannot be completely dismissed until we better understand Pluto's system.

Lunar Trojans: Few years ago my collaborators and myself [8] suggested that lunar Trojans could be very long-lived, escaping only when the Moon reaches the distance of 38 Earth radii, which is plausibly synchronous with the LC/LHB. However, our initial numerical simulations failed to take into account variations of Earth's orbital eccentricity (crucial for the strength of resonances involving the Sun) as well as the Trojan's own gravity, which is also crucial for the outcome of resonance crossings. Our final conclusion is that a Trojan massive enough to cause the LC/LHB could not have survived the evolution all the way to 38 Earth radii, but would have likely escaped when Moon was at about 27 Earth radii, which likely happened within the first 100 Myr of the system's history.

Planet V and the Lunar Orbit: One of the recent theories of the LC/LHB involves a quasi-stable fifth terrestrial planet between Mars and the asteroid belt [9]. After destabilizing the asteroid belt for 100-200 Myr, this 'Planet V' meets its end similar to an NEA, with solar or planetary collision and ejection all being possible. During its final scattering phase, Planet V should have had close encounters with the Earth-Moon system. Using a simple Monte-Carlo approach where many sets of such encounters are integrated with a Burisch-Stoer integrator we conclude that a Mars-sized Planet V would have likely excited lunar eccentricity beyond values compatible with the present state. On the other hand, a lunar-sized Planet V can be reconciled with the present lunar orbit. Interestingly, inclination is relatively more resistant to such encounters, requiring at least a Mars-sized interloper to account for the present value of 5.5 degrees. Therefore Planet V is unlikely to be the source of the Moon's inclination, but a similar encounter in the early Solar System is still a possibility (as first suggested by [10]). Interestingly, despite large mass involved in the 'Nice model' of the LC/LHB [11], Earth-Moon system is relatively unaffected, as rogue TNOs spend very little time among inner planets, as they are all times dynamically coupled to Jupiter (unlike what is expected of Planet V).

References: [1] Tera F. et al. (1974) *E&PSL 22,* 1–21. [2] Chapman, C. R. et al. (2007) *Icarus 189*, 233-245. [3] Ryder G. (1990) *EOS 71*, 313-323. [4] Kokubo E. et al. (2000) *Icarus 148*, 419-436. [5] Canup R. M. et al. (1999) *AJ 117*, 603-620. [6] Ward W. R. & Canup R. M. (2006) *Science 313*, 1107-1109. [7] Lithwick Y. & Wu Y. (2008) arXiv 0802.2951. [8] Cuk M. et al. (2006) *DDA XXXVII*, 13.01. [9] Chambers J. E. (2007) *Icarus 189*, 386-400. [10] Atobe K. et al. (2004) *DDA XXXV*, 7.02. [11] Gomes R. et al. (2005) *Nature 435*, 466-469.

COMMON 4.2 GA IMPACT AGE IN SAMPLES FROM APOLLO 16 AND 17. V.A. Fernandes[1], I. Garrick-Bethell[2], D.L. Shuster[1]and B. Weiss[2], [1]Berkeley Geochronology Center, Berkeley, CA 94709, USA (veraafernandes@yahoo.com), [2]Dep. of Earth, Atm. and Planet. Sci., MIT, 77 Massachusetts Av., Cambridge, MA 02139, USA

Introduction: The history of impactors to the Earth–Moon system both before and after the putative ~3.9 Ga heavy bombardment, is not well known. Early craters that would record this history on Earth have been erased either due to erosion or plate tectonics, while the limited number of sites visited and samples collected during the Apollo and Luna missions, and analytical challenges associated with dating impact events in general, have made the early lunar impact history difficult to estimate.

Both the lunar cataclysm theory and the continuous decline in impact events [1-5] prior to ~3.9 Ga are not well constrained and thus there is a need of additional geochronometry to better define this early period. Samples that exist in the Apollo and Luna collections potentially record this history (not only impactites but also other rocks, e.g. highlands rocks and basalts that have been affected by impact(s))-, as well as impact melts in meteorites, and in the future, samples that will be collected from more and diverse lunar sites. Here we present recently acquired $^{40}Ar/^{39}Ar$ data for age determination and thermocronology for samples from Apollo 16 and 17: 60025, 63503, 78155, 78235 and 78236.

Method and Samples: ^{40}Ar-^{39}Ar laser step-heating experiments were carried out on a total of 16 different samples from Apollo 16 (60025 and soil 63503) and Apollo 17 (78155, 78235 and 78236) (Table 1). The sample weight varied from 0.32 to 1.24 mg; In several cases the $^{40}Ar/^{39}Ar$ analyses were replicated using multilple aliquots. To minimize Ar blanks and improve temperature control, the samples were placed inside small platinum packages and heated using a diode laser and pyrometer feedback control. Ar diffusion kinetics were quantified using the ^{39}Ar and ^{37}Ar data and packet temperatures. Up to 32 heating steps were performed for each aliquot.

60025 has been described as a moderately shocked, cataclastic ferroan anorthosite [6-10]. A crystallisation age of 4.44±0.02 Ga as been determined by [11].

Soil 63503 is composed of different size clasts ranging from single mineral phases (plagioclase, pyroxene, olivine, ilmenite) to recrystallised rock (e.g. metabasalt and metanorite). At least four of the soils checked thus far by SEM do not show evidence of agglutonitic material and/or troilite. However, the clasts in these four soils show evidence of anaeling and recrystallisation. Previous Ar-Ar ages range is 1.38-4.27 Ga [12&13].

78155 is a thermally anhealed polymict breccia of anorthositic norite composition[14], previous $^{40}Ar/^{39}Ar$ data suggested an impact age of 4.22±0.04 Ga [2]

78235/78236 is a heavily shocked plutonic norite of cumulate origin with a glass coating and glass veins [15&16]. Chronology for this sample suggests a crystalisation of 4.43 ± 0.05 Ga [17] and to have been disturbed more than once (i.e. ~4.2 Ga and ~2.6 Ga, [17]).

^{40}Ar-^{39}Ar Results: The ^{40}Ar-^{39}Ar release data obtained for the 16 Apollo samples are divided into 3 main groups for ease of presentation in this abstract, data summary (error is 2σ):

63503,9, 78155,1 and 79235,139: The argon release of these samples is straightforward and shows a plateau over 90 to 95% of the ^{39}Ar-release Fig.1. The initial, low temperature steps suggest a small contribution from excess argon and are not considered for age calculation. The ages obtained are 4.210±0.180 Ga (63503,9), 4.195±0.074 Ga (averaged over 4 aliquots of 78155) and 4.188±0.074 Ga (78235, 139),.

60025, 63503,14, 63503,16, 63503,17, 63503,20 and 63503,21: The age spectra of these samples suggest that the Ar release shows two shock related phenomena, loss and implantation of argon. Further more, more than one shock event is observed from the argon release Fig.2. The initial ~50% of ^{39}Ar release are dominated by trapped $^{40}Ar/^{36}Ar$ (0.54 to 1.46) and having large apparent ages. These ages start as high as 6.0 Ga and are followed by a decrease to ages of ~3.91 Ga to ~ 4.2 Ga at intermediate temperatures. At intermediate to high temperature steps, the release forms a plateau, compriside only of radiogenic ^{40}Ar, with a constant Ca/K, a ^{39}Ar release between 23 and 53%. Two samples show evidence for only one resetting event at 4.054±0.072Ga (63503,17) and 4.251±0.046 Ga (63503,20). Samples suggesting two distinct events at intermediate (i) and high (h) temperatures. For example, sample 63503,21 high temperature age is 4.237±0.040 Ga and intermdiate temperature is 4.040±0.034 Ga (Table 1). The high-temperature plateau age (17% ^{39}Ar release) of 4.453±0.05 Ga for 63503,14 suggests this to be a preserved crystallization of the primary rock and the 4.191±0.034 Ga age over 36% of the ^{39}Ar release at intermediate indicates an impact event.

63503,1, 63503,4, 63503,11, 63503,13, 63503,15: The samples in this group, show that ~30-40% of the argon release at low temperature was disturbed by an event (i.e. impact) Fig.3. There are three impact ages suggested based on initial ^{39}Ar release, 3.345±0.084 Ga (63503,1 and 63503,15), 3.695±0.096 Ga (63503,4) and 3.866±0.098 Ga (63503,13). At intermediate to high temperature steps a well defined plateau over ~60-70% of the ^{39}Ar release and corresponding to ages of 4.188±0.074 Ga (63503, 4), 4.296±0.176 Ga (63503,13), 4.237±0.078 Ga (63503,11) and 4.211±0.045 Ga (63503,15). Sample 63503,1 shows at intermediate and high temperature steps (~51% ^{39}Ar-release) an age of 3.874±0.030 Ga, and the maximum ap-

parent age observed for the last heating step of 4.549±0.054 Ga suggests a minimum crystallisation age for this sample.

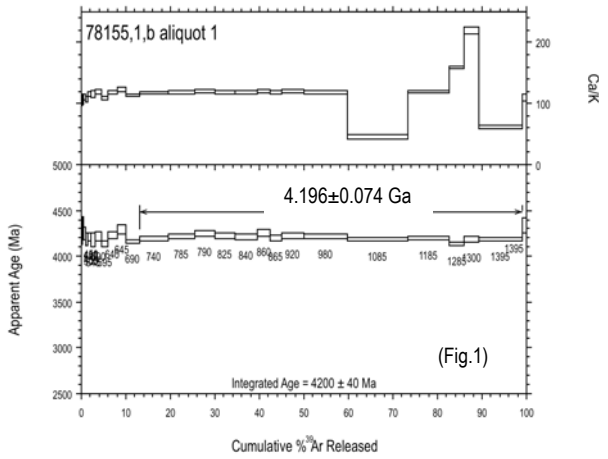

Figure 1 Apparent age vs.%^{39}Ar release for thermally anhealed polymict breccia 78155 showing an almost perfect plateau

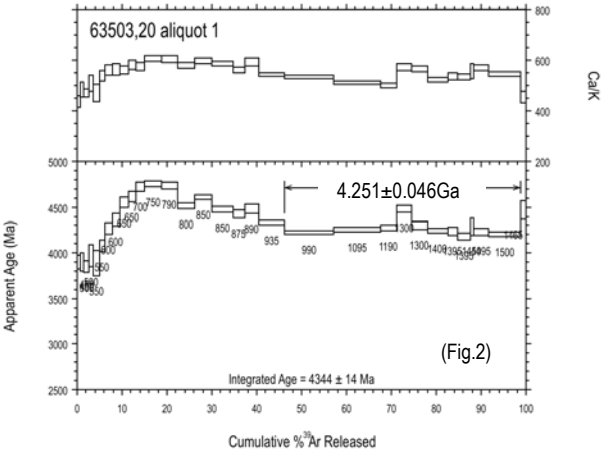

Figure 2 Apparent age vs.%^{39}Ar release for thermally anhealed regolith 63503,20. Initial ~46% of ^{39}Ar release shows the influence of excess/implanted Ar.

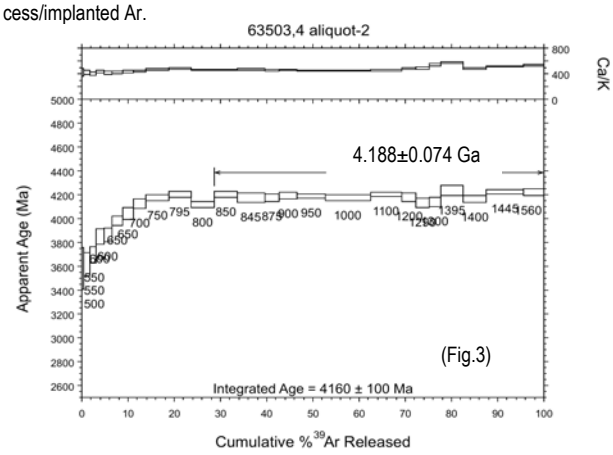

Figure 3 Apparent age vs.%^{39}Ar release for thermally anhealed regolith 63503,4 showing a partial re-setting event at ~3.7 Ga.

Conclusions: If we assume, based on petrologic information, that the ^{40}Ar/^{39}Ar ages represent the ages of impact events, the Apollo 16 and 17 samples show a similar signature for an impact event(s) at ~4.2 Ga. A similar age for breccia 67955 was recently reported by [18], and SIMS U-Pb analyses on several Apollo 14 and 17 zircons also suggest similar shock ages [19]. Thus, it is suitable to say that a significant impact event(s) occurred at ~4.2 Ga to affect not only the K-Ar system in plagioclases and pyroxenes, but also the U-Pb of zircons. The petrology and argon release of Apollo 16 and 17 samples also suggest other more recent impact events (~ 3.3 Ga, ~3.7 Ga and ~3.9 Ga). The maximum apparent age observed for the last heating step release of 4.549±0.054 Ga is within error the same as the Moon's formation age reported by [20] making this one of the oldest lunar rocks (e.g. [21]) thus far analysed……

Table1: Summary ^{40}Ar-^{39}Ar ages obtained for Apollo 16 and 17 fragments

	Early event (Ga)	Later event (Ga)	Max. age (Ga)	Sample wt (mg)
60025,1	4.260± 0.076	3.911±0.014	-	0.42
63503,4	4.188± 0.074	3.695± 0.096		1.18
63503,9	4.210±0.180	-	-	0.50
63503,11	4.237±0.078	3.306±0.194	-	0.53
63503,13	4.296±0.176	3.866±0.098	-	0.53
63503,14	4.191±0.034	-	4.453±0.050€	0.55
63503,15	4.211±0.136	3.345±0.092	-	0.50
63503,16	-	3.995±0.068	4.424±0.110$	0.65
63503,17	4.054±0.072	-	-	0.65
63503,20	4.251±0.046	-	-	0.82
63503,21	4.237±0.040	-	-	-
78155 (x4)	4.195±0.074	-	-	0.39-0.85
78235,139,1	4.188±0.074	-	-	0.64
78235,139,2	4.157±0.074	-	-	1.24
78236,18,2	4.228±0.030	3726±0.106	-	-
63503,1	3.874± 0.030	3.345± 0.084	4.549±0.054£	0.86
63503,3	3.904± 0.072	3.387± 0.162	-	0.81

€A plateau comprised of 17% ^{39}Ar release at high temperature.
$A plateau comprised of 24% ^{39}Ar release at high temperature
£Maximum apparent age comprised of the last step at high-temperature, and likely minimum crystallisation of primary rock.

Acknowledgements: Use of online ads-NASA and Lunar Compendium.
References: [1] Tera F. et al. (1974) *EPSL 22*, 1-21. [2] Turner G. and Cadogan P. H. (1975) *PLSC 6*, 1509-1538. [3] Ryder G. (2002) *JGR 107*, 5022, 10.1029/2001JE001583. [4] Hartmann (2003) *MAPS 38*, 579-593. [5] Chapman C.R. et al. (2007) *Icarus 189*, 233-245. [6] Hodges and Kushiro (1974) PLPSC 5th, 505-520. [7] Walker et al. (1973) EPSL 20, 325-336. [8] Dixon and Papike (1975) PLPSC. 6th, 263-291. [9] Ryder (1982) GCA 46, 1591-1601., [10] James et al. (1991)LPSC 22nd, 635-636. [11] Carlson &Lugmair (1988) EPSL 90, 119-130. [12] Mauer et al. (1978) GCA 42, 1687-1720. [13] Shaeffer&Husain (1973) GCA supp. 4, vol. 2, 1847-1863. [14] Bickle (1977) PLPSC 8th, 2007-2027. [15] Jackson et al. (1975) GSA Bull. 86, 433-442. [16] Nyquist et al (1981) PLPSC 12th, 67-97. [17] Nyquist et al (1981) PLPSC 12th, 67-97. [18] Norman et al (2007)LPSC 38th, abst.#1991. [19] Nemchin and Pidgeon (2007) LPSC 39th , abst.#1558. [20] Touboul et al (2007) Nature 450, 1206-1209. [21] Jessberger et al (1974) Nature 248, 199-202.

PREVIOUSLY UNRECOGNIZED LARGE IMPACT BASINS ON MARS AND THE MOON: IMPLICATIONS FOR THE LATE HEAVY BOMBARDMENT IN THE INNER SOLAR SYSTEM H. V. Frey, Geodynamics Branch, Goddard Space Flight Center, Greenbelt, MD 20771, Herbert.V.Frey@nasa.gov,

Summary: Crater retention ages of the Martian highlands and lowlands, and of the interior of South Pole-Aitken basin on the Moon, suggest the cumulative number of basins on Mars is about 12 times, and on the Moon about 2 times, greater than previously thought (at least). Crater retention ages for large impact basins on Mars suggest most formed in a relatively short time, perhaps in less than 200 million years. This supports a spike-like Late Heavy Bombardment which may have been common throughout the inner solar system.

Introduction: The discovery of previously unrecognized craters and large basins on Mars [1-3] and the Moon [4-6] has significantly changed ideas about the early history of Mars [3] and is likely to do the same for the Moon. At the very least it is clear that early cratering was far greater than previously thought, which has implications for using the Moon as a standard for estimating absolute surface ages from crater counts. Despite the large increase in the inferred number of impact craters now detectable on Mars using MOLA data [3] and more recently crustal thickness data [7,8], and on the Moon [6] using Clementine-derived gridded topographic data [9], it is likely crater retention ages will still be minimum estimates of the actual crater density on these surfaces. Despite this, important implications concerning both the Late Heavy Bombardment and the early crustal evolution of the planets of the inner solar system, including the Earth, derive from these new insights into the greater than previously thought cratering of Mars and the Moon.

Early Cratering at Mars and the Moon: Both the highlands and lowlands of Mars have extensive, previously unrecognized, populations of likely impact basins revealed by MOLA data and crustal thickness model data derived from MOLA topography and gravity data. As shown in table 1, the N(300) CRA for the highlands and lowlands have increased from earlier estimates based only on visible basins by factors ~12 and ~80 respectively, such that both regions now appear to have a similar N(300) CRA of about 3.18 [8]. The greater increase in crater density seen in the lowlands supports the idea that most of the previously unrecognized basins on Mars are probably buried.

Table 1. Change in N(300) Crater Retention Ages for the Highlands and Lowlands of Mars based on Basins found in MOLA Topography and Crustal Thickness (CT) Data (from Edgar and Frey [6])

	Vis	Vis+Topo	Vis+Topo+CT
Highlands	0.27	1.98	3.18
Lowlands	0.04	0.87	3.19

On the Moon, which has fewer ways to bury large basins, the increase in the cumulative number of basins > 300 km in diameter is at least a factor of 2: we found 92 [6] using ULCN topography compared with the 45 listed by Wilhelms [10] based on photogeologic mapping. This is similar to the increase found for basins > 100 km diameter superimposed on the large South Pole-Aitken basin, where the N(100) CRA for visible basins was found to be 12 and that for the total population (visible plus previously unrecognized) was 21, a factor 1.8 higher. These are likely minimum CRAs because there may be even more previously unrecognized basins (PUBs) which better topographic and crustal thickness data will reveal. At present, we can say with some confidence that the early cratering on the Moon was likely a (cumulative) factor of 2 greater than thought, and on Mars likely a (cumulative) factor of 12 higher than thought (based on the highlands CRAs.

Ages of Large Impact Basins on Mars: Crater retention ages for the 20 largest impact basins on Mars (D> 1000 km) based on superimposed large visible or buried basins [6] and even more deeply buried impacts revealed in crustal thickness data [8] suggest that most of the basins formed in a relatively short period of time [11]. As shown in Figure 1, N(300) CRAs for 65% of the large basins lie between 2.5 and 5.0 [3], and 50% of the population have CRAs between 2.5 and 4.0. Conversion to the Hartmann-Neukum model chronology [12] suggests an absolute age of 4.10 to 4.25 BYA for all but the three youngest (Hellas, Argyre and Isidis), with most falling within an even narrower interval of 4.12-4.14 BYA [11].

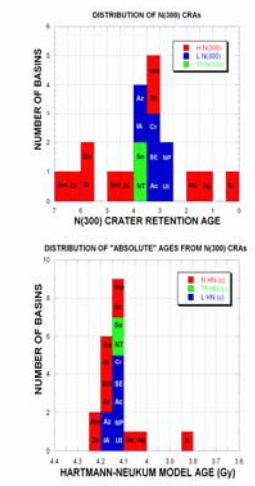

Figure 1. Distribution of N(300) Crater Retention Ages (CRAs) (upper left) and model absolute ages (lower left) for the 20 largest impact basins on Mars. Absolute age bin 50 MY. Highland basins (red) have a broader range of ages than lowland basins (blue). If CRAs are equivalent to formation ages, > 50% may have formed in a relatively short time between 4.1 and 4.2 BYA.

The sharp peak in likely formation ages for the largest impact basins on Mars has several important implications. It suggests the possibility of a cataclysmic Late Heavy Bombardment (LHB) on Mars. The short time is consistent the NICE model [13,14] and a "terminal lunar cataclysm" [15,16]. The absolute ages, however, are wrong: the lunar cataclysm occurred between 4.0 and 3.8 BYA. The Martian ages are model ages based a number of assumptions [12] and could be off by several hundred million years. If the peak shown in Figure 2 is part of an inner solar system event, it

may be that the Martian chronology can be corrected by pinning this peak to the ~3.9 BYA cataclysm on the Moon.

The Martian global magnetic field apparently died during the peak in impact basin formation, and likely abruptly [17,18]. This would have left the Martian atmosphere (what remained or recovered from the effects of these very large impacts) unprotected from the solar wind. Combined with the likely environmental insult due to the formation of impacts up to 10 times larger than Chixulub, the time immediately during and after the Late Heavy Bombardment on Mars was not very hospitable.

The apparent lack of large basins earlier than those shown, if real, suggests the impacts may have been very tightly confined in time, permitting a ~400 MY period before 4 BYA during which planet-sterilizing impacts did not occur. This may support the idea of a "cool early Earth" [19] during which Earth (and Mars?) may have been more habitable than during the 4.0-3.8 BYA LHB interval.

Late Heavy Bombardment on the Moon and Mars: Open Questions. Topography reveals a significant number of large lunar basins > 300 km diameter that were not previously recognized [6]. Lack of previous recognition does NOT mean these newly-found basins are all older than those previously known: it may be poor lighting geometry contributed to lack of previous discovery. Large diameter crater retention ages for these are being determined, and absolute ages could be estimated through ties with basins of known age. It is important to know if the lunar basins are tightly confined in time as it appears the Martian basins may have been. This has bearing on the exact nature of the Late Heavy bombardment on the Moon and elsewhere.

The size distribution of lunar basins as currently known from photogeologic mapping and topography (see Figure 2) suggest a significant gap between the 2600 km wide SPA and the next largest basin, Imbrium, at ~ 1160 km. There are currently no known 1500, 1800 or 2200 km diameter basins. It is interesting to speculate whether this suggests SPA is of a different population than the other lunar basins, which tend to follow a -2 power law trend in a cumulative frequency diagram. Alternatively, it may be that better topography or crustal thickness data will reveal some subtle expression of basins in this size range that have not yet been recognized. We are currently looking at existing crustal thickness data [20,21] for such possibilities. We have not yet identified any obvious candidates in this size range but have found smaller features not previously identified. Improved topography from LOLA [22] and especially the better gravity field anticipated from GRAIL [24] should provide even better limits on the actual number and size of large lunar basins.

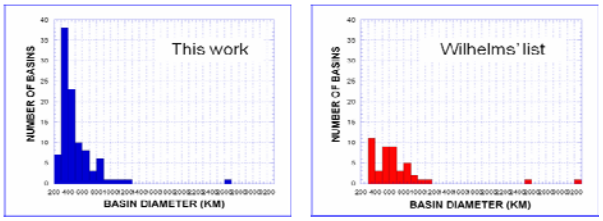

Figure 2. Size distribution of lunar basins > 300 km diameter from Wilhelms [10] (right) and from ULCN topography [6] (left). Note the very large gap between South Pole-Aitken and Imbrium (left).

Likewise it is important to determine, for the Martian basins, if there really are no basins older than those shown in Figures 1 and 2. New crustal thickness data with improved resolution and signal-to-noise quality [23] offers the possibility of finding features not previously recognized, and we are currently searching that data for subtle but unrecognized large basins. Because the present population of basins > 1000 km on Mars [11] has a total area of only 43% of the surface area (not allowing for overlap) and actually occupies less than 35% of the surface area of Mars, it is possible that some subtle signature of even older basins might survive. If so, it will be extremely interesting to determine if such a basin has an N(300) CRA substantially older than 7, and thus might not be part of the apparent spike in CRAs for the basins currently recognized. Note that in the conversion to Hartmann-Neukum model absolute ages, it would require an N(300) > ~15 to have an absolute age > 4.3 BYA (but recall that these model ages are uncertain enough that the peak at 4.10-4.15 could actually be at 3.9 BYA). Such older areas may not exist, however, if the effects of the 20 known very large impacts extend to great distances (e.g., twice the basin diameters), but it is important to search for such very old crust or older basins.

Absolute ages for most Martian and lunar basins will almost certainly require returned samples. In the interim, ages for these basins will come from crater counts. Recent experience indicates that those counts will be substantially higher than we currently have, and that topographic data should be used in conjunction with image data to get closer to the true total cratering on planetary surfaces.

References. [1] Frey, H.V. et al. (1999) *GR.L 26*, 1657. [2] Frey, H.V. et al. (2002) *GRL 29*, 1384, doi:10.1029/2001GL01382. [3] Frey, H.V. (2006*) JGR (Planets) 111*, E08S91,doi:10.1029/2005JE002449. [4] Spudis, P.D. et al. (1994) *Science 266*, 1848-1851. [5] Zuber, M.T., et al. (1994) *Science, 266*, 1839-1843. [6] Frey,. H.V., LPSC 39, abstract # 1344. [7] Neumann, G.A. et al. (2004) *JGR (Planets) 109*, E08002, doi:10.1029/2004JE002262. [8] Edgar, L.A. and H.V. Frey (2008) *GRL 35,* L02201, doi:10.1029/2007GL031466. [9] Archinal, B.A., et al. (2006) USGS Open File Report 2006-1376, Version 1.0. [10] Wilhelms, D.E, (1987) The Geologic History of the Moon, USGS Professional Paper 1348. [11] Frey, H.V. (2008) *GRL 35*, doi:10.1029/2008GL033515. [12] Hartmann, W.K. and G. Neukum (2001) Space Sci. Rev., 96, 165-194. [13] Bottke, W.F. and H.F. Levison (2007) NAC Lunar Workshop, Tempe, AZ. (abstract). [14] Gomes, R. et al. (2005) *Nature 435*, 466-469. [15] Tera, F. D.A. et al. (1974) *Earth Planet. Sci. Lett, 22*, 1-21. [16] Ryder, G. et al. (2000) Origin of the Earth and Moon, (R.N. Canup and K. Righter, eds.), U. AZ Press, 475-492. [17] Lillis et al. (2008) *GRL (in press).* [18] Kuang et al. (2008) *GRL (in press)*. [19] Valley, J.W. et al. (2002) *Geology 30*, 351-354. [20] Neumann, et al. (1996) *JGR 101*, 16,841-16,863. [21] Wieczorek, M. et al. (2006) *Rev. Mineral. Geochim. 60*, 221-364. [22] Smith, D.E. and J.W. Head (2005) GSA Annual Meeting, Paper 154-8. [23] Neumann et al. (2008) LPSC abstract #2167. [24] Zuber et al. (2008) LPSC abstract # 1074.

4.2 BILLION YEAR OLD AGES FROM APOLLO 16, 17, AND THE LUNAR FARSIDE: AGE OF THE SOUTH POLE-AITKEN BASIN? I. Garrick-Bethell[1], V. A. Fernandes[2], B. P. Weiss[1], D. L. Shuster[2], T. A Becker[2]. [1]Massachusetts Institute of Technology, 77 Massachusetts Avenue, Cambridge, MA 02139, iang@mit.edu, [2]Berkeley Geochronology Center, 2455 Ridge Rd, Berkeley, CA 94709.

Introduction: The large number of ~3.9 Ga impact ages in lunar samples has led to several hypotheses regarding the impactor flux at this time: a cataclysmic late heavy bombardment (LHB), a cessation of prolonged bombardment since solar system formation, or an artifact of measuring samples collected from within the limited area of the Apollo landing sites. Testing which, if any, of these hypotheses is correct would have implications for a wide variety of events in the solar system, including the emergence of life on Earth. It is therefore essential to carefully assess the handful of rocks that have impact ages > 4.0 Ga.

Here we present and interpret new ~4.2 Ga Ar-Ar whole-rock ages from Apollo 16 and 17 samples. These rocks are being studied for ancient magnetic remanence, but their old ages are also important in understanding the bombardment history of the Moon. Expanding on our earlier work [1], we will consider the ages in the context of the 4.23-4.24 Ga age of troctolite 76535, whose 40-50 km depth of excavation [2] makes it the oldest known sample from a large lunar basin (> 700 km). The same 4.23 Ga age found in farside meteorites Dhofar 489 [3] and Yamato 86032 [4] suggests that this basin is on the farside. We will consider the possibility that the South Pole-Aitken (SP-A) basin produced these ~4.2 Ga ages.

New and published 4.2 Ga Ar-Ar ages: Table 1 lists new whole-rock high temperature plateau ages for six 2-4 mm light matrix breccias from North Ray crater (63503) [1, 5]. Some plateaus extend from the lowest to the highest temperature steps, indicating that they have been completely reset at ~4.2 Ga and survived the LHB without observable disturbances. Other samples record primary crystallization ages of ~4.45 Ga at high temperatures, and show partial resetting ages of 4.2 Ga at lower temperatures. The mean age for >4.2 Ga 63503 samples is 4.228 ± 13 Ga.

Troctolite 76535: Work by [2] suggests that troctolite 76535 formed at 40-50 km depth. In addition, its isotopic systems were open at the time of its excavation, which was followed by slow (~10,000 year) cooling in a deep ejecta blanket. Because the age of the Serenitatis basin in which 76535 was found is generally believed to be < 4.0 Ga [6], and the isotopic systems in 76535 all closed at 4.23 Ga, it is almost certain that 76535 was excavated by a large basin older than Serenitatis [2]. Its age is 4.238 ± 23 Ga.

Dhofar 489 and Yamato 86032: Dhofar 489 is a spinel-troctolite bearing anorthositic breccia believed to have been excavated from the deep crust on the lunar farside [3]. It has an Ar-Ar high temperature plateau age of 4.23 Ga, which is similar to the 63503 and 76535 ages. An Ar-Ar age of 4.23 Ga is also found for one clast of Yamato 86032, which is also believed to be from the farside.

Other ancient samples: Sample 78155, 78235/6, and 60025 also produce ages that cluster around 4.2 Ga. Sample 78155 has a very well defined plateau age and its consistently lower age of ~4.195 Ga suggests that it may not have been reset by the same impact event that produced the slightly older ~4.23 Ga ages.

Table 1. Ancient lunar ages. Ar-Ar unless indicated.

Sample	Age (Ga, ± Ma)	Ref.
63503,9 (×2)	4.210 ± 18	*
63503,11	4.237 ± 78	*
63503,13	4.230 ± 30	*
63503,15	4.211 ± 45	*
63503,20	4.251 ± 46	*
63503,21	4.237 ± 40	*
63503 Mean	**4.228± 13**	
Dhofar 489[£]	**4.23 ± 34**	[3]
Y-86032,133 Ar-Ar	**4.23 ± 30**[†]	[4]
Y-86032,133 Rb-Sr	4.25 ± 30	[4]
76535, Sm-Nd	4.246 ± 60	[7]
76535, U-Pb	4.236 ± 15	[8]
76535, Pb-Pb	4.226 ± 35	[8]
76535, Ar-Ar	4.230 ± 60[‡]	[9]
76535 Mean	**4.238 ± 22**	
60025	4.26 ± 76	*
60025 (× 2)	4.21 ± 60; 4.17 ± 60	[10]
67955 Sm-Nd	4.20 ± 70	[11]
78155 (× 4)	4.195 ± 74	*
78155	4.22 ± 40	[12]
78155	4.17 ± 30	[13]
78155 Mean	**4.194 ± 18**	
78235,6 (× 2)	4.228 ± 30; 4.188 ± 74	*
78235,6	4.11 ± 20; ≥4.26	[14, 15]
Other A16 breccias	4.04-4.26 Ga	[5, 16, 17]

*This work [5], 2σ errors. £Whole rock. †Feldspathic clast. Lower limit. Rb-Sr age is for plagioclase. ‡ Error estimate from graph.

Source basins for ancient deep-seated samples: Which basin or basins could have excavated troctolite 76535, and reset the ages of Dhofar 489 and 63503? Linking clusters of similar ages to basins or craters has long been a goal of lunar sample analysis. Apart from the geologic applications, such linkages can ultimately

be used to determine impactor size variations as a function of time.

Assuming the depth of excavation is about one tenth the diameter of the basin's transient cavity (see discussion in [18]), the cavity that ejected 76535 must have been at least 400-500 km in diameter. The ratio of the observed rim diameter to transient cavity diameter is not well established in multiring basins, but we can assume a value of ~1.75 for transient cavities >400 km [18], yielding a minimum basin diameter of ~750 km. There are eight known pre-Nectarian basins on the Moon with diameters > 690 km [19]: SP-A, Tranquillitatis, Smythii, Australe, Mutus-Vlacq, Nubium, Tsiolkovskiy-Stark, and Fecunditatis.

South Pole-Aitken: A fair amount of work has gone into estimating the amounts of ejecta contributed to the Cayley Plains from nearby basins. Based on [20], SP-A should contribute ~500 m of ejecta after correcting for spherical geometry [1]. While this is only a rough approximation, the thickness is comparable or higher than the estimated contributions from all other basins using the same model. This is not surprising given the size of SP-A. For comparison, the center of SP-A is about twice as far away from the Apollo 16 site as the center of Imbrium, but SP-A is about twice as large. In addition, several studies suggest that kilometer-deep regolith homogenization should have taken place at Cayley [16, 17, 20-22], implying that multiple ancient basins should be represented in its soil samples.

If troctolite 76535 represents SP-A ejecta, it would mean that it comes from the farside. Elevated abundances of thorium on the nearside makes this element a useful tool for determining if samples originated from the near or far sides. Interestingly, the thorium/FeO ratio for 76535 is almost the same as farside meteorite Y-86032, and falls within the range of feldspathic meteorites (including Dhofar 489) [4].

Tranquillitatis: Tranquillitatis is close to both the Apollo 16 and 17 sites, and would have contributed ~200 m of ejecta to the Cayley Plains [20]. However, the 4.23 Ga age of farside meteorite Dhofar 489 cannot be explained by a Tranquillitatis origin. In addition, the ~700 km diameter of the basin suggests a maximum depth of excavation of ~40 km, from which the amount of material ejected should be volumetrically small, and less likely to be a source for deeply excavated troctolite 76535.

Smythii, Australe, Mutus-Vlacq, Nubium, Tsiolkovskiy-Stark, and Fecunditatis: Ejecta modeling suggests these basins contribute 3-60 m of material at Cayley [20], making their contributions much smaller than Tranquillitatis. Again, the small volumetric contributions from the maximum depth of excavation of these basins (40-50 km) suggests that they are less likely to be the source of 76535.

Nectaris: The age of Nectaris is still debated [11]. Ejecta from Nectaris at Cayley may be as much as 300 m [20], making it a plausible source for the 4.23 Ga ages. However, it is less likely that the basin could explain the 4.23 Ga age of Dhofar 489.

A model for early basin formation: SP-A blanketed much of the Moon with its ejecta at ~4.23 Ga, creating deeply-excavated troctolite 76535, 63503 breccias, and Dhofar 489. These samples survived the putative LHB as hand samples, and one was even ejected to Earth, suggesting far more material with these ages may exist. At Cayley, SP-A ejecta was homogenized with ejecta from later basins and then exposed by North Ray crater, yielding a diverse set of whole-rock ages in its soils from 3.85-4.23 Ga, with an absence of older ages. Basin formation during this entire interval may have been continuous [5, 16, 17], but perhaps less intense than at ~3.9 Ga. If true, this model could make it difficult to determine if there was a gap in basin formation between crust formation and 4.23 Ga, or if the SP-A basin was anomalously large enough to make finding older ejecta less likely. We note that lunar zircon ages of ~4.33 Ga suggest that some event or events older than 4.2 Ga have taken place on the Moon [23]. Unfortunately, the magnitude of these events cannot be determined as easily as with the event that excavated deep-seated 76535.

Conclusion: Just as meteorites from the lunar farside are able to reach the Earth after ejection from comparatively tiny craters, it should be expected that some material from a 2400 km diameter basin on the farside is to be found on the nearside of the Moon. It is obviously difficult to definitively determine if SP-A has an age of ~4.23 Ga, but the hypothesis is viable enough to warrant further consideration in any unified model of lunar chronology and stratigraphy.

References: [1] Garrick-Bethell, I., et al. (2008) *NASA LSIC,* 2131. [2] McCallum, I.S., et al. (2006) *GCA* 70, 6068. [3] Takeda, H., et al. (2006) *EPSL* 247, 171. [4] Nyquist, L.E., et al. (2006) *GCA* 70, 5990. [5] Fernandes, V.A., et al. (2008) *This volume*. [6] Wilhelms, D.E. (1987) *USGS Prof. Paper 1348*. [7] Lugmair, G.W., et al. (1976) *PLSC* 7th, 2009. [8] Premo, W.R. and M. Tatsumoto (1992) *LPSC* 22nd, 381. [9] Huneke, J.C. and G.J. Wasserburg (1975) *LPI* VI, 417. [10] Schaeffer, O.A. and L. Husain (1974) *PLSC* 5th, 1541. [11] Norman, M.D., et al., *LPSC* 38th, 2007, abs. 1991. [12] Turner, G. and P.H. Cadogan (1975) LPSC 6th, 1509. [13] Oberli, F., et al (1979) *LPI* X, 490. [14] Aeschlimann, U., et al. (1982) *LPI* 13, 1-2. [15] Nyquist, L.E., et al. (1982) *PLSC* 12th, 67. [16] Schaeffer, O.A. and L. Husain (1973) *PLSC* 4th, 1847. [17] Maurer, P. and e. al. (1978) *GCA* 42, 1687. [18] Wieczorek, M.A. and R.J. Phillips (1999) *Icarus* 139, 246. [19] Spudis, P.D. (1993) *The Geology of Multi-ring Impact Basins*, Cambridge U. Press. [20] Petro, N.E. and C.M. Pieters (2006) *JGR* 111, E09005. [21] Korotev, R.L. (1997) *M&PS* 32, 447. [22] Morrison, R.H. and V.R. Oberbeck (1975) *PLSC* 6th, 2503. [23] Nemchin, A.A. and R.T. Pidgeon (2008) *LPSC* 39th, abs. 1558.

Review of Cratering Evidence Regarding Early Solar System Bombardment

William K. Hartmann, Planetary Science Institute, Tucson 85719

Pre-Apollo lunar crater count analysis indicated that the cratering rate averaged over pre-mare times was much higher than the present rate [1]. Following the dating of nine landing sites on the moon from Apollo and robotic Luna samples, it became possible to plot crater densities as a function of time, at least during a relatively short interval from ~3.9 to ~3.2 Gy ago. Differential crater densities from older to younger sites showed that the cratering rate was declining rapidly during this period [2,3]. Such work was done by the author in the early 1970s, and again independently, and probably with more precision, by Gerhard Neukum in the mid 1970s and 80s [4,5]. The results were very similar in showing the declining rate.

Most workers have assumed that the cratering rate has been more constant since then (probably with crater-size-dependent spikes associated with asteroid breakup events, especially at smaller crater sizes.) However some authors have suggested a gradual increase, and others, a decrease, since 3.0 Gy ago [cf. 6, 7]. Crater counting with anticipated, high resolution imagining may help clarify this issue, although serious progress requires radiometric dating of some young counting surfaces, such as the interior of Copernicus or Tycho.

A problem has been to affirm whether the decline from ~.9 to ~3.2 Gy ago is (1) simply the tail end of a unique cataclysmic cratering episode centered 3.9 Ga ago, or (2) a time-restricted decline after one of several semi-cataclysmic spikes in cratering, or (3) a decline associated with longer-term sweep-up of interplanetary debris [cf. review in 8].

Comparison of lunar front side impact melts, from Apollo samples, with lunar meteorite impact melts and asteroidal meteorite ages may offer valuable constraints on the nature and time dependence of the intense inner solar system cratering prior to ~3.2 Gy.

References: [1] Hartmann, W. K. 1966, *Icarus* **5,** 406-418. [2] Hartmann, W. K. 1970. *Icarus*, **12**, 131-133. [3] Hartmann, W. K. 1970. *Icarus* **13**, 209-301. [4] Neukum, G., Köngi, B., Storzer, D., and Fechtig, H. 1975 *Prov.6th Lunar Planet. Sci. Conf.* 598 (abstract). [5] Neukum, G. 1983. Habilitation Dissertation for Faculty Membership, Ludwig-Maximilians-University of Munich. 186 pp. [6] Quantin, Cathy; N. Mangold, W. K. Hartmann, P. Allemand 2007 Icarus, **186**, 1-10. [7] Hartmann, W. K., Cathy Quantin, Nicolas Mangold. (2007) Icarus, **186**: 11-23. [8] Hartmann, W. K. 2003. Meteoritics and Planet. Sci. **38,** 579-593.

BOMBARDMENT HISTORY OF THE SATURNIAN SATELLITES. M. R. Kirchoff and P.M. Schenk. Lunar and Planetary Institute, 3600 Bay Area Blvd., Houston, TX 77058 (kirchoff@lpi.usra.edu & schenk@lpi.usra.edu)

Introduction: A few possible hypothesis implicating that dynamic and orbital changes in the outer solar system generated the Late Heavy Bombardment ~3.9 Ga [1-9] have been described in the literature [10-15]. The basic premise of these models is that formation and/or orbital migration of the gas giants triggered scattering of large reservoir(s) of icy planetesimals throughout the solar system. These icy planetesimals, or more likely asteroids also scattered by the perturbations [9], then could have produced the basins associated with the Late Heavy Bombardment on the Moon. These hypotheses might also predict a signature of the Late Heavy Bombardment on the outer solar system satellites produced by the scattered icy planetesimals. Therefore, we will generate impact crater databases through crater counting for relatively older surfaces of Mimas, Dione, Tethys, Rhea and Iapetus to determine the bombardment history of the Saturnian satellites. Once this history is known we can compare it to hypotheses of outer solar system impactor populations including a possible heavy bombardment.

The work here will focus on determining the distribution of the basins and their ages along with comparing the size-frequency distribution between the satellites and different terrains on the satellites. For determining ages of terrain units and basins, we do not have access to samples that we can date by radioactive elements, but we can estimate the age of basins on various satellites using crater counts and estimated impact rates [16]. While dating using crater counts is not as well constrained as radiometric dating, crater counts are all that is available and will give an impression of basin ages and bombardment history.

Data: Most crater counting is performed on controlled global mosaics generated from *Cassini* ISS images with higher resolution *Voyager* images to fill in remaining gaps. The Mimas mosaic ranges from 400 to 1000 m/pxl. Dione and Tethys mosaics are about 500-700 m/pxl. Rhea and Iapetus mosaics are about 1 km/pxl. We also will get data from a selection of high-resolution images for all the satellites except Mimas that range in resolution from 20 to 200 m/pxl.

To determine the crater density within large basins, we will use the highest resolution image available for that basin from either the high-resolution images or global mosaics. Most of the basins are visually determined from the global mosaics, but some of them have been determined through digital elevation maps [17].

Preliminary Results: Fig. 1 shows relative (R) size-frequency distributions of the impact craters for a couple of impact basins and a few different terrains on Mimas, Tethys, Dione and Rhea in raw (A) and averaged (B) data format. These plots allow us to compare the relative densities and pattern (or shape) of the distributions as a function of diameter. We also give the ages of these basins and terrains examined so far in Table 1. Ages are given for both cases A and B in Zahnle et al. [16], where case A is for a small impactor population similar to that seen at Jupiter and case B for a larger small impactor population as seen for Triton's distribution. These preliminary results indicate that the distributions in the oldest terrains on Mimas, Tethys, Dione and Rhea all show a similar distribution both in density and shape. This implies that these oldest terrains on these satellites were impacted by the same impactor population that was likely heliocentric.

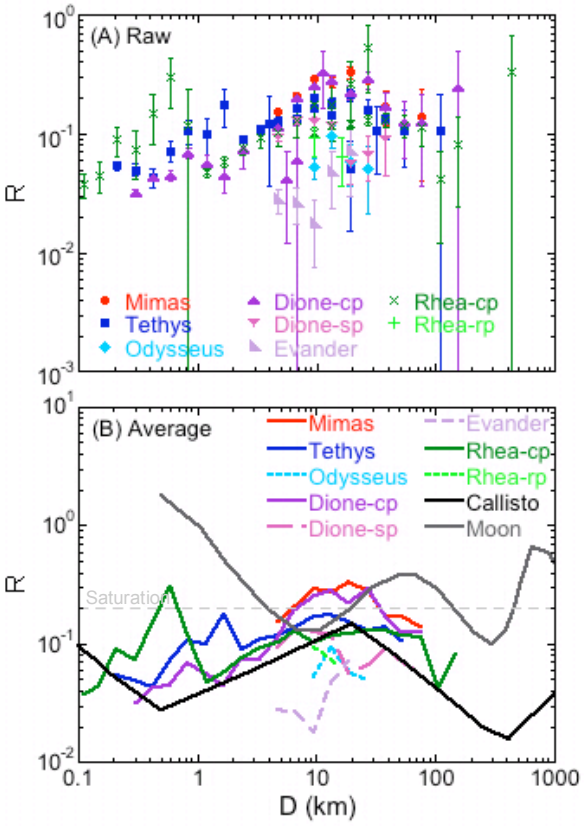

Figure 1. Relative (R) size-frequency distributions. The relative plot (R-plot) shows the ratio of the actual distribution to a distribution with a differential slope of -3. Part (A) shows the raw data for the Saturnian satellites. Counts are shown for Odysseus, a basin on Tethys, and Evander, a basin on Dione. *cp* – cratered plains; *sp* – smooth plains; *rp* – ridged plains. Part (B) shows averaged data for the Saturnian satellites to compare to published data for Callisto [19] and the lunar highlands (Moon) [18].

Also shown in Fig. 1 are the published curves for the lunar highlands [18] and Callisto [19]. When the curves we have derived for the Saturnian satellites are compared to Callisto we find that the shape of the distributions are fairly similar. This further supports the idea that there was one primary, heliocentric impactor population in the outer solar system that bombarded at least the Jovian and Saturnian satellites early in their history. When both Callisto and the Saturn satellite distributions are compared to the lunar highlands, however, the data imply that terrains in the inner and outer solar system were not impacted by the same primary population.

Table 1. Terrain Ages in Gyr

	D ≥ 5 km		D ≥ 10 km	
	A	B	A	B
Mimas	4.39	0.75	4.35	1.33
Tethys	4.56	1.66	4.44	2.10
Odysseus	--	--	3.76	1.06
Dione-cp	4.56	2.60	4.56	3.22
Dione-sp	4.55	1.97	4.43	1.96
Evander	3.62	0.60	3.61	1.00
Rhea-cp	4.56	3.05	4.56	3.67
Rhea-rp	--	--	4.48	2.47

Another important preliminary result of this work is that the impact crater distribution of Dione's smooth plains and, possibly, Rhea's ridged plains, which could be up to ~2 Gyr younger than Dione's and Rhea' cratered plains (Table 1), have a similar shape to the cratered plains (Fig. 1). This implies that the size-frequency distribution of the impactor population striking Dione and Rhea did not change over the time period represented.

Finally, we have computed the ages for two basins in the Saturnian system (Table 1): Odysseus on Tethys and Evander on Dione. Odysseus appears to be 3.8 Gyr or younger and Evander 3.6 Gyr or younger. Given that the error associated the ages is at least 20% (based upon the error for the crater counts), these basins could have been formed around the same time as the Late Heavy Bombardment on the Moon. The caveat is that the small impact population must be similar to that at Jupiter, which our data seems to imply.

Conclusions: The impact crater distribution on the cratered plains of Dione, Rhea, Mimas and Tethys are old surfaces (Table 1) that have likely experienced the same population of impactors according to the similarities of the distributions (Fig. 1). We also conclude that the similarity of the distribution of Dione's smooth plains and, possibly, Rhea's ridged plains to the Dione's and Rhea's cratered plains (Fig. 1) indicates that the impactor population did not change over the first ~2 Gyr (Table 1). When these results are combined with the implication that Saturn's crater distributions appear similar to Callisto's distribution, we can conclude that there possibly was one primary impactor population for the outer solar system that did not change for at least ~2 Gyr. Meanwhile, the distribution for older terrains in the Jupiter and Saturn systems does not appear to be the same as the lunar highlands. The implication, assuming these terrains are representative, is that at least the older terrains of the inner and outer solar systems were bombarded by different impactor populations. The most likely scenario to explain this discrepancy is that the inner solar system cratering record is dominated by asteroids [e.g., 9, 15] and the outer solar system by ecliptic comets from the Kuiper Belt [e.g., 16]. This is an interesting and important conclusion for understanding and comparing bombardment histories of the inner and outer solar systems, and might possibly imply that the signature of the Late Heavy Bombardment in the outer solar system may look different from the one found on the Moon.

The preliminary results for the ages of basins in the Saturnian system have shown that at least two large Saturnian basins could have been formed during the period of Late Heavy Bombardment on the Moon [5-9]. The results here, however, are by no means comprehensive and there are many more basins to explore in the Saturnian system. We will show results for these other basins and discuss implications for recording a late heavy bombardment in the Saturnian system. Other future work will include compiling and comparing Iapetus' impact crater distribution and continuing to generate counts for the relatively younger terrains on Dione, Tethys and Rhea.

References: [1] Turner, G. et al. (1973) *Proc. 4th Lunar Sci. Conf. GCA* **2** Suppl 4, 1889-1914. [2] Tera, F. et al. (1974) *EPSL* **22**, 1- 21. [3] Ryder, G (1990) *Eos* **71**, 313. [4] Dalrymple, G.B. and G. Ryder (1996) *JGR* **101**, 26069-26084. [5] Cohen, B.A. et al. (2000) *Science* **290**, 1754-1756. [6] Cohen, B.A. et al. (2005) *MPS* **40**, 755-777. [8] Cohen, B. (2007) *DPS #39*, abst. #46.03. [9] Kring, D.A. and B.A. Cohen (2002) *JGR* **107**, doi:10.1029/2001JE001529. [10] Liou, J. and R. Malhotra (1997) *Science* **275**, 375-377. [11] Levison, H.F. et al. (2001) *Icarus* **151**, 286-306. [12] Tsiganis, K. et al. (2005) *Nature* **435**, 459-461. [13] Gomes, R. et al. (2005) *Nature* **435**, 466-469. [14] Morbidelli, A. et al. (2005) *Nature* **435**, 462-465. [15] Strom, R.G. et al. (2005) *Science* **309**, 1847-1850. [16] Zahnle, K. et al. (2003) *Icarus* **163**, 263-289. [17] Schenk P.M. and J.M. Moore (2007) *LPSC XXXVIII*, abst. #2305. [18] Ivanov, B.A. et al. (2002) in Asteroids III, pp. 89-101. [19] Schenk, P.M. et al. (2004) in Jupiter: The Planet Satellites and Magnetosphere, pp. 427-456.

CYANIDE PRODUCTION BY CHEMICAL REACTIONS BETWEEN IMPACTOR MATERIAL AND AN AMBIENT ATMOSPHERE AFTER AN OBLIEQUE IMPACT. K. Kurosawa[1], K. Ishibashi[2], Y. Sekine[1], S. Sugita[1], T. Kadono[3], S. Ohno[4], N. Ohkouchi[5], N. O. Ogawa[5], and T. Matsui[1], [1]Dept. of Complexity Sci. & Eng., Univ. of Tokyo (5-1-5, Kashiwanoha, Kashiwa, Chiba 277-8561, JAPAN; kurosawa@impact.k.u-tokyo.ac.jp), [2]Dept. of Earth and Planet. Sci., Univ. of Tokyo (7-3-1, Hongo, Bunkyo-ku, Tokyo, JAPAN), [3]Inst. of Laser Eng., Osaka Univ. (2-6, Yamadaoka, Suita, Osaka, JAPAN), [4]Inst. for Study of the Earth's Interior, Okayama Univ. (827, Yamada, Misasa, Tottori, JAPAN), [5]IFREE, JAMSTEC (2-15, Natsushima, Yokosuka, Kanagawa, JAPAN)

Introduction: Cyanide are considered as one of the most important compounds in the chemical evolution phase of the origin of life [e.g., 1]. However, the production rate of cyanide is estimated to be extremely low if the early Earth atmosphere is redox-neutral (i.e., N_2-CO_2 dominant) [e.g., 2].

Recent studies for the Late Heavy Bombardment suggests that the projectiles during this period contain a large amount of carbons [3, 4]. Such carbon-rich impactor may have played an important role in the origin of life. Hypervelocity impact experiments show that nitrogen from an ambient atmosphere and carbon from fine-grained fragments from obliquely impacted C-rich projectiles react to form CN radicals even when the atmosphere is very oxidizing (N_2-O_2 dominant) [5, 6]. A CN forming region is much more reducing than the ambient atmosphere because this process can supply carbon atoms included in impact fragments into the ambient atmosphere. We call such a reducing gas around fine-grained fragments "ablation vapor". The ablation vapor is likely to subsequently react with the ambient redox-neutral atmosphere. This process may be a much more efficient cyanide production mechanism than that proposed in previous studies because of two reasons. First, CN bond is more stable because the ablation vapor is much more reducing than the ambient atmosphere. Second, this process can use nitrogen from the ambient atmosphere. However, this process has not been investigate experimentally.

In this study, we conduct laser ablation experiments within redox-neutral atmospheres to simulate chemical reactions between impactor material and an ambient atmosphere. We analyze final products from laser-induced ablation vapors using a gas chromatograph-mass spectrometer (GC-MS; Shimadzu Corp. QP2010) and a fourier transform-infrared spectrometer (FT-IR; ParkinElmer, Spectrum 2000) for gas and solid, respectively.

Experiments: We experimentally investigated the effects of the partial pressure of CO_2 on the conversion ratio ϕ from vaporized carbon to HCN molecules and the dependence of atmospheric composition on the relative amount of CN bond in condensates from laser-induced ablation vapors. Here, the total amount of HCN is given by $N_{HCN} = \phi N_C$, where N_C is the total amount of vaporized carbon. Basically, we use the same experimental systems in our previous study [7].

In this study, we used graphite and cast iron (Fe: 94 wt%; C: 3.5 wt%; Si: 2.2 wt%; S: 0.068 wt%) targets were used for gas and solid analysis as analogs of chondrite material, respectively.

Gas-phase analysis: We investigated the total molar amount of vaporized carbon, N_C, the temperature of laser-induced CN, T_{CN}, and the total molar amount of laser-induced HCN, N_{HCN}.

Water vapor, CO_2, N_2, and Ar were introduced into the vacuum chamber after evacuating air. The partial pressures of N_2 and H_2O were fixed at 5.0×10^2 and 30 mbar, respectively. The partial pressure of CO_2, P_{CO2}, was varied from 0.0 to 5.3×10^2 mbar. We use Ar to adjust the total pressure in the chamber to be 1.1×10^3 mbar. The number of laser pulse irradiations was $\sim 3.0 \times 10^2$. The GC-MS was calibrated using standard HCN gas. The detection limit of HCN is about 0.4 nmol/pulse under our experimental conditions.

During the laser irradiation, optical spectroscopic observations of laser-induced ablation vapor were conducted. After laser irradiations, one milliliter of the final product gas was sampled using a syringe and was analyzed with the GC-MS.

Solid-phase analysis: We investigated the conposition of condensates from laser-induced ablation vapors qualitatively.

Gas mixtures of N_2, CO_2, and Ar were used. The total pressure in the chamber was fixed at 13 mbar. We set a CaF_2 disk as a deposition plate on the stage in the chamber. The distance between the laser irradiation spot and the disk is ~5 mm. The number of laser pulse irradiations was $\sim 1.9 \times 10^3$. After laser irradiations, we analyzed condensates on CaF_2 disks by IR absorption spectroscopy with the FT-IR.

The mass and temperature of vapor: To estimate the total amount of vaporized carbon, we assumed that the shape of laser-ablation craters are cylinder and the depth of that are equal to the wavelength of the laser pulse (~1 μm) that is a characteristic scale of energy deposition of laser irradiations. Thus, we estimated that N_C is $\sim 5 \times 10^2$ nmol/pulse.

We carried out band-tail fitting analysis of observed spectra to investigate a temperature of laser-induced

hot CN [8]. The computer software package SPRADIAN (Structured Package for Radiation Analysis) [9] was used to calculate theoretical spectrum.

Experimental results of gas phase: The main result in this study is the conversion ratio ϕ from C to HCN as a function of P_{CO2}.

An observed emission spectrum from laser-induced ablation vapor is shown in Fig. 1. Swan band system of C_2 and Violet band system of CN are mainly observed. Thus, CN radical was formed under our experimental condition. We estimated T_{CN} using Band-tail fitting method. It is nearly constant, ~6500 K, regardless of P_{CO2}. This temperature corresponds to ~8 km/s of impact experiments. This temperature-velocity relation was obtained using a heat balance equation on the fragment surface between energy transfer from the colliding atmosphere and the latent heat of fragments [10].

The HCN yield investigated with the GC-MS decreaces as the P_{CO2} increases. Figure 2 shows ϕ as a function of P_{CO2}. However, it is important that 0.1 – 1 % of HCN was formed in ambient atmospheres contained as much as a few hundred mbar of CO_2.

Experimental results of solid phase: We focused on absorption band around 2200 cm^{-1} in IR spectra. This band corresponds to C≡N, -N=C=N, and C≡C bands [e.g., 11]. Figure 3 shows IR spectra of condensates under three different gas mixtures. These results indicate that the composition of condensates strongly depends on the composition of gas mixtures. Althogh the abundance of CN bond decreases if gas mixture contains CO_2, CN bond is fixed into a condensed phase under redox-neutral atmospheres.

Discussions & Conclusions: An impact-comminuted projectile is broken up further by aerodynamic pressure from the colliding ambient atmosphere. Thus, the size of each ablation vapor around impact fragments may approach to that of laser-induced ablation vapors. Our results are likely to apply to actual oblique impacts if impact fragments are dispersed very efficiently. For expample, a simple model for fragment dispersal dynamics of an obliquely impacted (30° from the horizontal) carbonaceous body 300 m in diameter (i.e., carbon content is ~8 x 10^{11} mol [12]) within 1 bar of redox-neutral atmosphere show that the resulting column density of HCN is ~10 mol/m^2 over ~10^2 km^2 of surface area, where 0.1% of ϕ is used. Since this is a preliminary estimate, its use needs caution. However, this column density is equivalent to HCN production accumulated for ~1 x 10^4 years by lightening within a strongly reducing atmosphere [13]. This is a significant concentration of HCN, although such high HCN concentration is limited in both time and space. Furthermore, this process may supply condensates which contain cyanide compounds into proto ocean and/or lakes. Such a temporally and spatiallyconcentrated supply of cyanide compound may have played an important role in the origin of life.

References: [1] J. P. Ferris & W. J. Hagan (1984), *Tetrahedron*, **40**, 1093-1120. [2] B. Fegley Jr, et al. (1986), *Nature*, **319**, 305-308. [3] R. Gomes et al. (2005), *Nature*, **435**, 166-169. [4] R. G. Strom et al. (2005), *Science*, **309**, 1847-1850. [5] S. Sugita & P. H. Schultz (2000), *LPSC, XXXI*, #2029. [6] S. Sugita & P. H. Schultz (2003), *JGR*, **108** (E6), 5051, doi:10.1029/2002JE 001959. [7] K. Kurosawa et al. (2007), *LPSC, **XXXVIII***, #1629. [8] K. Kurosawa et al., *JTHT*, submitted. [9] K. Fujita & T. Abe (1997), *ISAS Rep.*, **669**. [10] S. Sugita & P. H. Schultz (2003), *JGR*, **108** (E6), 5052, doi:10.1029/2002JE001960. [11] H. Imanaka et al. (2004), *Icarus*, **168**, 344-366. [12] J. T. Wasson & G. W. Kallemeyn (1988), *Phil. Trans. R. Soc. Lond.*, A, **325**, 535-544. [13] R. Stribling & S. L. Miller (1986), *Origins of life*, **17**, 261-273.

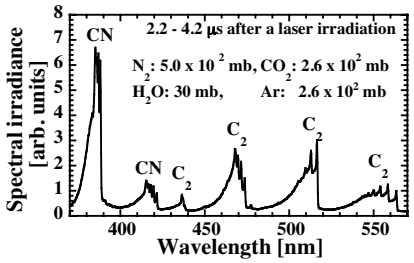

Fig.1 An observed spectrum from laser-induced ablatin vapor.

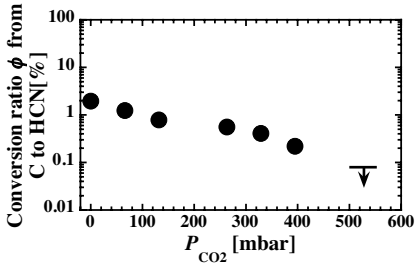

Fig.2 The conversion ratio ϕ from C to HCN as a function of the partial pressure of CO_2.

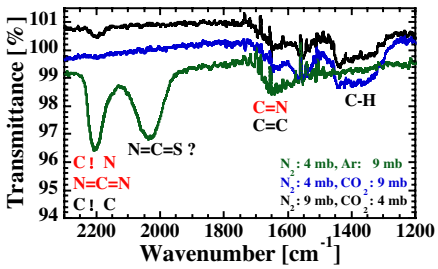

Fig. 3 IR spectra of condensates on deposition plates. The composition of gas mixtures are shown in the figure.

EVIDENCE FOR PLANET MIGRATION IN THE MAIN ASTEROID BELT: IMPLICATIONS FOR THE DURATION OF THE LATE HEAVY BOMBARDMENT D.A. Minton and R. Malhotra, Lunar and Planetary Laboratory, The University of Arizona, 1629 E. University Blvd. Tucson AZ 85721. daminton@lpl.arizona.edu

Introduction We show that the observed distribution of main belt asteroids does not uniformly fill the regions that are dynamically stable over the age of the solar system. The discrepancies indicate an overall trend of depletion that is highest near the inner edge of the asteroid belt and diminishes towards the location of the 2:1 mean motion resonance with Jupiter; in addition, there is excessive depletion of asteroids just outward of the well-known Kirkwood Gaps associated with jovian mean motion resonances. These features are not accounted for by planetary perturbations in the current dynamical structure of the solar system. We show that they are consistent with dynamical ejection of asteroids by the sweeping of mean motion resonances and of the ν_6 secular resonance during the migration of Jupiter and Saturn that has been proposed as the mechanism for initiating the Late Heavy Bombardment (LHB) ~ 4 Ga [1–3]. We will use the observed depletion of the asteroid belt as a constraint on the migration history of Jupiter and Saturn.

The observed craters on Mercury, Mars, and the Moon in the most heavily cratered regions have a common scaled projectile size frequency distribution that is well matched with the size frequency distribution of the main asteroid belt [2]. This implies that some size-independent (i.e. dynamical) depletion event occurred in the main asteroid belt well after the planetary crusts had solidified; its timing has been placed at ~ 3.9 Ga, corresponding to the period of Late Heavy Bombardment (LHB) inferred from lunar geochronology [e.g., 4, 5].

Numerical experiment Is there evidence of the mass depletion event associated with the LHB preserved in the distribution of asteroids in the main belt? In order to answer this question we performed a simple numerical experiment. We compared the distribution of observed asteroids with absolute magnitude $H < 9.7$ (which corresponds to diameters $D \gtrsim 50$ km assuming a visual geometric albedo of 0.09) against a model asteroid belt which is uniformly populated in the dynamically stable zones.

Our model asteroid belt was constructed as follows. The test particle asteroids were given an eccentricity and inclination distribution similar to the observed main belt, but a uniform distribution in semimajor axis. We then did a numerical integration of their orbital evolution under the gravitational influence of the planets, using the public-domain N-body integrator MERCURY [6]. In our simulation, the planets interacted with each other and perturbed the test particles, but the test particles had no effect on the planets. The test particles were considered lost if they passed within 3 Hill radii of a planet or collided with the Sun.

The simulation was ended after 100 My of evolution, and the surviving particles were binned into 0.05 AU proper semimajor axis bins. The proper semimajor axis of a particle was calculated by taking the mean of its semimajor axis for its first 1 My of orbital history. We found that the particle loss history for each bin has two phases, an initial phase when the most unstable particles in the bin are lost, typically lasting 0.1–1 My, and a second phase when the loss rate is relatively slow and is characterized well as linear in $\log t$. A linear regression in $\log t$ was performed on the second phase of the loss history data for each semimajor axis bin, and the number of particles remaining in each bin after 4 Gy was estimated by extrapolation. The estimated number of test particles in each bin was compared with the proper semimajor axis distribution of observed $H < 9.7$ asteroids obtained from the AstDys online information service [7].

Result and discussion The discrepancy between the model asteroid belt and the observed asteroid belt is shown in Fig. 1, where the percent discrepancy is defined as

$$\text{Percent discrepancy} = \frac{N_{sim} - N_{obs}}{N_{sim}} \times 100, \quad (1)$$

where N_{sim} and N_{obs} are the number of asteroids per bin in the simulation and in the observed main belt population, respectively. Overall, we find that the discrepancy is highest at the inner edge of the main belt and decreases to near-zero at the location of the 2:1 jovian mean motion resonance; in addition, there is enhanced discrepancy just exterior to the major Kirkwood gaps.

Any mechanism invoked to explain the discrepancy must account for the features seen in Fig. 1, namely that the discrepancy tends to decrease as a function of semimajor axis from the inner edge of the asteroid belt to the location of the 2:1 mean motion resonance with Jupiter, with enhanced depletion in regions outward of the major Kirkwood gaps.

The observed discrepancy is most consistent with the sweeping of both mean motion and secular resonances during a late migration of Jupiter and Saturn that has

been implicated as the mechanism responsible for the LHB [1–3]. As Jupiter and Saturn migrated, the locations of mean motion and secular resonances swept across the asteroid belt, exciting asteroids into terrestrial planet-crossing orbits [3, 8].

The ν_6 resonance, in particular, may have swept inward through the entire asteroid belt region as Saturn migrated outward from about 8 AU to its present location. The ν_6 resonance removes asteroids from the main asteroid belt by increasing their eccentricity above planet-crossing values so that they either collide with a planet or are perturbed into a new orbit. The efficiency of removal is related to the rate of sweeping: the faster Saturn migrated, the fewer asteroids were removed. The overall trend of depletion in the asteroid belt found in Fig. 1 is consistent with an outward migration of Saturn at a rate that decreased with time.

The size of the regions of enhanced depletion just outward of the Kirkwood gaps associated with the 3:1, 5:2, 7:3, and 2:1 jovian mean motions resonances are explained by an inward migration of Jupiter by ~ 0.2–0.4 AU. This distance is consistent with other estimates of Jupiter's migration distance [9–12]. These regions are highlighted in Fig. 1.

This evidence, together with the evidence that the cratering records of the terrestrial planets associated with the LHB appear to have been dominated by impactors originating in the main asteroid belt [2], lends support to the hypothesis that a late migration of the outer giant planets was responsible for producing the LHB.

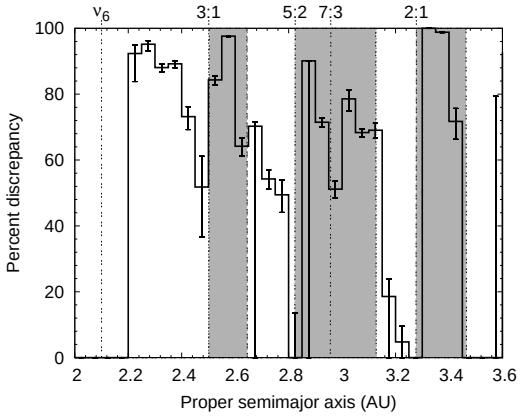

Figure 1: The discrepancy between the observed population of asteroids with $H < 9.7$ and a model asteroid belt. The current positions of the ν_6 secular resonance and the strong jovian mean motion resonances associated with the major Kirkwood gaps are shown. The observed discrepancy may be explained as depletion by orbital sweeping resonances during the migration of Jupiter and Saturn. The shaded regions are the regions where strong jovian mean motion resonances would have swept if Jupiter's initial semimajor axis had been 5.5 AU.

References [1] Levison H.F. et al. (2001) *Icarus*, 151, 286–306. [2] Strom R.G. et al. (2005) *Science*, 309, 1847–1850. [3] Gomes R. et al. (2005) *Nature*, 435, 466–469. [4] Tera F. et al. (1974) *Earth & Planet. Sci. Lett.*, 22, 1–21. [5] Ryder G. (2002) *Journal of Geophysical Research (Planets)*, 107, 6–1–6–13. [6] Chambers J.E. (1999) *MNRAS*, 304, 793–799. [7] Knežević Z. and Milani A. (2003) *Astronomy and Astrophysics*, 403, 1165–1173. [8] Liou J.C. and Malhotra R. (1997) *Science*, 275, 375–377. [9] Fernandez J.A. and Ip W.H. (1984) *Icarus*, 58, 109–120. [10] Malhotra R. (1995) *AJ*, 110, 420–429. [11] Franklin F.A. et al. (2004) *AJ*, 128, 1391–1406. [12] Tsiganis K. et al. (2005) *Nature*, 435, 459–461.

CAN IMPACTORS FROM THE MAIN ASTEROID BELT ERASE A COMETARY CRATERING RECORD ON THE MOON? D. A. Minton, R. G. Strom, and R. Malhotra, Lunar and Planetary Laboratory, The University of Arizona, 1629 E. University Blvd, Tucson AZ (daminton@lpl.arizona.edu)

Introduction The Late Heavy Bombardment (LHB) was a period of intense meteoroid bombardment of the inner solar system that ended approximately 3.8 Ga [e.g., 1–3]. It has been suggested that the LHB was initiated by the migration of Jupiter and Saturn, causing Main belt asteroids (MBAs) to become dynamically unstable [4, 5]. Models for the LHB involving planet migration invoke gravitational interactions between the giant planets and a massive primordial icy planetesimal disk [4, 6–8]. This process inevitably leads to a large number of cometary impacts (from impactors originating from the outer icy disk) onto the inner planets that is comparable to or exceeds the number of asteroidal impacts (from impactors originating from the main asteroid belt) [4]. However, the cratering record on Mercury, the Moon, and Mars suggests that the craters associated with the LHB were caused by impactors originating from the main asteroid belt [9]. Gomes et al. (2005) showed that under the "Nice model" of giant planet migraion, the majority of the cometary impactors struck the Moon prior to the arrival of the asteroidal impactors. It is possible that there were enough asteroidal impacts to erase an earlier cometary cratering record, however this hypothesis has never been tested. Here we use attempt to quantify the amount of asteroidal material needed to erase a preexisting cometary cratering record.

Constructing a comet size frequency distribution The size frequency distribution of KBOs is poorly constrained. Observationally, the visual magnitude distribution of KBOs is reasonable well characterized for visual magnitudes $\lesssim 28$ [10]. Assuming a mean semimajor axis of 42 AU and a geometric visual albedo of 0.04, a visual magnitude $R \lesssim 28$ corresponds to objects diameters $D \gtrsim 30$ km. From Pi-group scaling, a 30 km diameter comet impacting the moon at 50 km s^{-1} would leave a ~ 640 km diameter basin [11]. As there are very few basins of this size on the Moon, the size distribution of objects with sizes much smaller than 30 km will be important in order to distinguish between cometary and asteroidal impactor populations.

In the absence of observational data for $D < 30$ km KBOs, there are other ways in which the KBO size frequency distribution may be estimated. One way is though collisional evolution modeling of the Kuiper belt population, and another is through the cratering record of the icy satellites of the outer solar system. It also may be possible to use the observed size distribution of Jupiter's Trojan asteroids as a proxy for the Kuiper belt size distribution, as it is possible that the Trojans originated in the Kuiper Belt [12].

In a collisionally evolved population, the size distribution will consist of two regimes; a strength-dominated regime where the energy required to disrupt the body decreases as a function of size, and a gravity-dominated regime where the energy required to disrupt the body increases as a function of size [13]. Differences in the resultant steady-state size distributions in the two regimes will cause waves to propagate through the size distribution in the gravity-dominated regime [14]. The waves will oscillate about the gravity-dominated steady-state size distribution, which can be approximated as a power law with an index $-q_g$. The steady-state size distribution strength-dominated regime can be approximated as a power law with an index $-q_s$, which will typically be different than power law index for the gravity-dominated regime. The power law indices, wave amplitudes, wave peak locations, and the transition diameter between the strength and gravity-dominated regime for the population size distribution will depend on several parameters, such as material strength and density, average impact velocity between objects in the population, the population spatial density, and population age [14]. Many of these parameters may be estimated, and a model KBO size distribution can be constructed that can match the observed size distribution for $D \gtrsim 30$ km objects [15].

The cratered surfaces of the icy satellites currently offer the best direct record of the Kuiper belt size frequency distribution for $D \lesssim 30$ km. It is unlikely that asteroids are an important source of impactors in the outer solar system, so outer solar system impactors are likely to be dominated by Kuiper belt objects [17]. However there are several factors that contribute toward complicating the cratering record of the icy satellites. Many of the icy satellites have experienced some amount of surface tectonic activity in their history that has partially or completely erased much of their cratering histories. Of the largest icy satellites, Callisto and Rhea appear to offer the most pristine cratered surfaces relatively free from recent tectonic activity.

Planetocentric debris may be an important component to the icy satellite impactor population, including the formation of "sesquinary" craters (craters produced

on one satellite by ejecta thrown out by an impact on another satellite in the same system) [16]. Planetocentric debris may be an important source of cratering in the saturnian and uranian systems, and possibly also on Europa and Triton and [17, 18]. Planetocentric impactors would presumably have a different size distribution than primary impactors from the Kuiper belt, and so would obscure the signature of KBOs on the cratering record of the icy satellites.

Model Kuiper belt size frequency distributions Due to the uncertainties in Kuiper belt size distribution, we choose two model KBO size distributions to compare with the main asteroid belt size distribution.

Model I is the size frequency distribution given by Pan & Sari (2005) [15], from their Fig. 3. It is based on a collisional model of the Kuiper belt that attempted to fit the KBO observational data of Bernstein et al. (2004) [10].

Model II is a hybrid of two size distributions. For $D < 60$ km it is based on the model Callisto crater size distribution derived from crater counts of Galileo imagery [18]. The craters were converted to projectiles using Pi-group scaling [11] and assuming an impact velocity of $16\ \mathrm{km\ s^{-1}}$, projectile density of $1.5\ \mathrm{gm\ cm^{-3}}$, target density of $1.0\ \mathrm{gm\ cm^{-3}}$, and impact angle of $45°$. For $D > 60$ km model II is identical to model I.

The main belt asteroid (MBA) size distribution is a hybrid of three size distributions. For $D > 10$ km it is based on cataloged main belt asteroids taken the Lowell Observatory Asteroid Orbital Elements Database (ftp://ftp.lowell.edu/pub/elgb/astorb.html). This represents the range of asteroid diameters that are likely to be observationally complete for the main asteroid belt [19]. The catalogued asteroid diameters were used if given, otherwise an albedo of 0.09 was assumed to convert magnitude H into diameter. For $0.25\ \mathrm{km} < D < 10$ km the MBA model is based on the lunar highlands impactor SFD [see 9]. For $D < 0.25$ km the MBA model is based on the strength-dominated regime of a collisional evolution asteroid belt model [20].

The two model KBO size distributions are plotted in the style of an R-plot (normalized by a D^{-3} size distribution) along with the model MBA size distribution in Fig. 1. With these model size distributions and estimates of the impact velocities and projectile densities of the various populations, we will simulate the cratering of the lunar surface first by the equivalent of 5×10^{21} gm of cometary material, then subsequently by an equivalent amount of asteroidal material, consistent with estimates of the impact flux onto the lunar surface under the "Nice model" [4]. The simulation will be performed using a stochastic cratering model which simulates crater production and subsequent erasure due to overlying craters and crater ejecta blanketing [21].

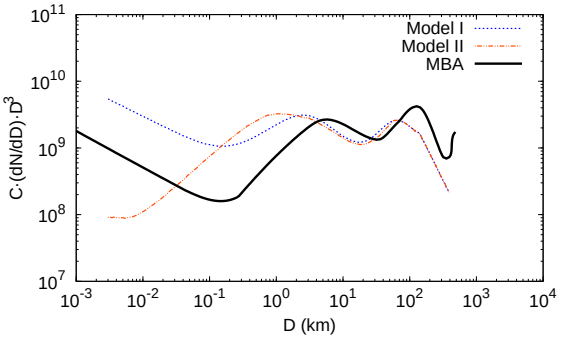

Figure 1: Normalized differential plot of model outer solar system impactor populations compared with a model main belt asteroid population.

References [1] Tera F. et al. (1973) in *LPSC IV*, 723–725. [2] Tera F. et al. (1974) *Earth & Planet. Sci. Lett.*, 22, 1–21. [3] Ryder G. (1990) *EOS Transactions*, 71, 313,322,323. [4] Gomes R. et al. (2005) *Nature*, 435, 466–469. [5] Levison H.F. et al. (2001) *Icarus*, 151, 286–306. [6] Fernandez J.A. and Ip W.H. (1984) *Icarus*, 58, 109–120. [7] Malhotra R. (1995) *AJ*, 110, 420–429. [8] Hahn J.M. and Malhotra R. (1999) *AJ*, 117, 3041–3053. [9] Strom R.G. et al. (2005) *Science*, 309, 1847–1850. [10] Bernstein G.M. et al. (2004) *AJ*, 128, 1364–1390. [11] Melosh H.J. (1989) *Impact cratering: A geologic process*, Research supported by NASA. New York, Oxford University Press (Oxford Monographs on Geology and Geophysics, No. 11), 1989, 253 p. [12] Morbidelli A. et al. (2005) *Nature*, 435, 462–465. [13] Asphaug E. et al. (2002) *Asteroids III*, 463–484. [14] O'Brien D.P. and Greenberg R. (2003) *Icarus*, 164, 334–345. [15] Pan M. and Sari R. (2005) *Icarus*, 173, 342–348. [16] Zahnle K. et al. (2008) *Icarus*, 194, 660–674. [17] Zahnle K. et al. (2003) *Icarus*, 163, 263–289. [18] Schenk P.M. et al. (2004) *Ages and interiors: the cratering record of the Galilean satellites*, 427–456, Jupiter. The Planet, Satellites and Magnetosphere. [19] Jedicke R. et al. (2002) *Asteroids III*, 71–87. [20] Bottke W.F. et al. (2005) *Icarus*, 175, 111–140. [21] Richardson J.E. et al. (2005) *Icarus*, 179, 325–349.

IMPACT ORIGIN OF CHLORINE-BEARING MATERIALS OF SALTY SEA-WATER OF EARLY EARTH, COMPARED WITH THOSE ON MARS AND THE MOON. Y. Miura, Division of Earth Sciences, Graduate School of Science & Engineering, Yamaguchi University, Japan, 753-8512. yasmiura@yamaguchi-u.ac.jp

Introduction: There are few reports on major origin of salty sea water in composition. However sea water contains high amount "chlorine", together with sodium ion. Chlorine element of carbonaceous meteorite is higher than the crust of the Earth [1,2], though there are no chlorine-bearing mineral connected to major supply on the Earth. Recently auther found "chlorine-bearing minerals on fusion crust of meteorites" fallen to the Earth, not only found on with rocks on surface (Kuga, Carancas, and Mihonoseki) but also collected after air explosion by meteoritic shower without any mixing of rocks on the surface (Nio chondrite). If chlorine element is concentrated in meteoritic melting in air from primordial Earth with huge meteoritic impacts, then rain drop from warm atmosphere is considered to be mixing with such chlorine minerals on melted meteorites to produce salty ocean water finally [2], whereas chlorine is remained on Mars and the Moon. The purpose of the present paper is to elucidates chlorine from meteorites finally to produce salty ocean water of the Earth, as well as chlorine-bearing materials on Mars and the Moon .

Samples used in this study: Fusion crusts of four meteorites of the Nio, Kuga, Mihonoseki (in Japan) and Carancas (in Peru) are used in this study, taken by the FE-ASEM (Field-Emission Analytical Scanning Electron Microcopy) in Yamaguchi, Japan operated by author [1,2].

The Nio chondritic meteorite: Meteoritic spherules and fragments formed at explosion of 40km high in atmosphere by the Nio meteoritic shower found at the fallen sites of Niho, Yamaguchi, Japan (without contamination from the ground) reveal sporadic distribution of many Fe rosettes (flake) texture with chlorine, as shown in Fig.1 [1,2].

The Kuga iron meteorite: The Kuga iron meteorite found in Kuga, Iwakuni, Yamaguchi, Japan has "fusion-crust" (with melted layer during passing to atmosphere before impact to the ground) with Fe-Ni-Cl-bearing rosettes (flake) texture formed from meteorite melting in atmosphere, as shown in Fig.2 [1,2].

The Mihonoseki chondritic meteorite: The Mihonoseki chondritic meteorite has been found in the ground after passing through wooden house in Mihonoseki, Shimane, Japan. Minor fragments found in the ground are collected to observe texture by the FE-ASEM in this study. Sporadic distribution of the texture with 1μm in size can be also found in this sample, as shown in Fig.3

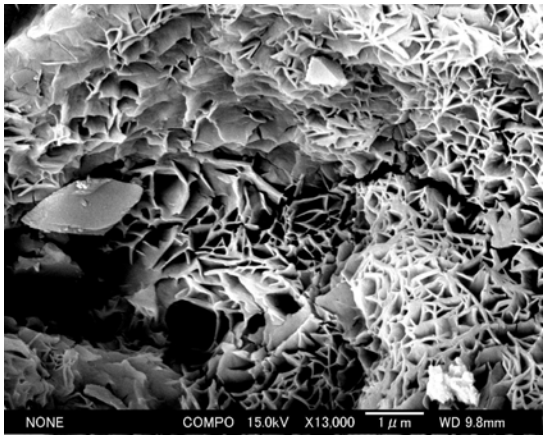

Fig.1. FE-SEM micrograph of Fe-Ni-Cl-rich flake texture of the Nio chondrite fallen in Yamaguchi, Japan.

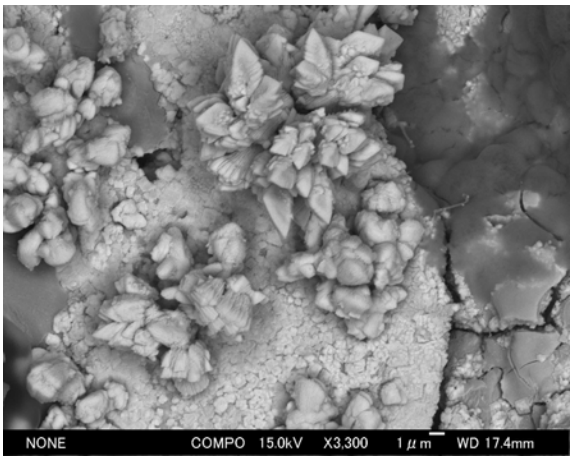

Fig.2. FE-SEM micrograph of Fe-Ni-Cl-rich flake texture of the Kuga iron meteorite found in Kuga, Iwakuni, Yamaguchi, Japan, taken by author [1,2].

Carancas chondrite in Peru: The Carancas chondritic meteorite fallen in Peru recently [1,3] shows Fe-Ni-Cl-bearing flake texture formed at impact reaction at ground) , taken by author.

Formation of rosettes textures with chlorine: The rosettes (flake) texture with meteoritic Fe, Ni, Cl-bearing composition of four meteorites reveals sporadic distribution, where chlorine element can be found during dynamic reaction of impact with melting, which is also proved by artificial experiments of slag melting composition with chlorine element, as listed in Table 3 [1,2].

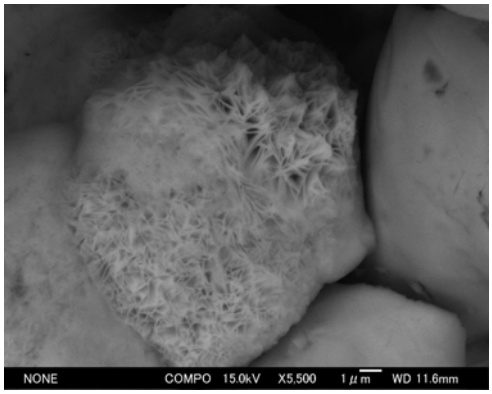

Fig.3. FE-SEM micrograph of Fe-Ni-Cl-rich rosettes (flake) texture of the Mihonoseki chondritic meteorite fallen in Mihonoseki, Shimane, Japan [1,2].

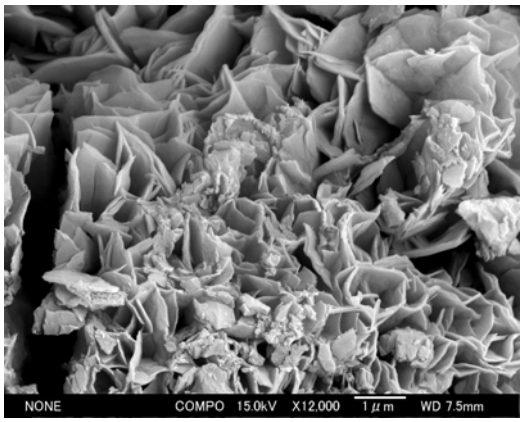

Table 3. Rosettes (flake) textures with Fe, Ni, Cl, O–bearing compositions in the Carancas meteorite in Peru [1,3].

In short, the detailed comparison of chemistry and texture indicates that the rosettes texture with chlorine elements is formed by dynamic impact reaction of meteorite melting to the Earth.

Table 1. Comparison of meteorite with chlorine [1,2].

Sample	Formation
1) Nio chondrite	Explosion as shower in air
2) Kuga iron meteorite	Fusion crust melting in air
3) Mihonoseki chondrite	Melting fragment in air
4) Carancas chondrite	Melting fragments in air
5) Artificial slag melts	Melting glasses

Application of chlorine-bearing materials on the Moon and Mars: On the Apllo 16 samples, mineral akaganeite (β-FeOOH) with chlorine (Cl) is reported [4]. Recent exploration data of Mars include chlorine-bearing minerals on Martian impact materials [5]. Both minerals are not mixed with water to form salty ocean water on the Moon and Mars.

Formation of salty sea water: Chlorine-bearing fusion crusts of meteorites fallen to the surface on primordial Earth are reacted with water from rain-falls to form ocean water finally on the Earth. This meteorite melting process is origin to produce chlorine in sea water in this study as shown in Fig.4 [1,2]:

1) Chlorine (Cl) concentration:
Fusion crusts of Meteorites
(in Air of Earth; craters on Mars,
& meteorite fragments on the Moon)

↓

2) Distribution to the surface:
Huge impacts to collect Cl over surface
(in Air of Earth; craters on Mars)

↓

3) Rain-fall to form salty ocean water:
Rain-fall by cooling from hot vapor, &
Melting to salty ocean water
(mainly on the Earth)

Fig.4. Process to form salty sea-water from meteoritic origin of chlorine element on Earth, Mars and the Moon.

Summary: The present study is summarized as follows [1,2]:

1) Four meteorites of the Nio, Kuga, Mihonoseki and Carancas show rosettes (flake) textures with Fe, Ni and Cl elements to concentrate chlorine elements, which is proved by artificial experiments of slag glass with chlorine reveal Fe-Cl-bearing flake texture at high temperature melting with quenching reaction.

2) Salty ocean water is to form to chlorine concentration of meteorite impact process in air with rain-fall, resulted in ocean water with chlorine on Earth, whereas chlorine elements are found on Mars and the Moon.

Acknowledgements: Author thanks to Drs. T. Kato and T. Tanosaki for discussion of melted glass and analytical data, and to Director Dr. Hemanndo del Prado of INGEMMET (Peru's Geological, Mining and Metallurgical Institute) for exchange of academic information and soils used in this study.

References:

[1] Miura Y.(2008): *LPS XXXVIX*, abstract #2027 *(LPI/ USRS, USA).*

[2] Miura Y. (2008): AGOS Meeting (Busan) , Abstract #ST1-A022.

[3] Macedo F. L. and Macgare J.(2007): Carancas meteorite Report, INGEMMET(Peru) 07092. pp.1-5.

[4] Frondel J.W.(1975):Lunar Mineralogy (John Wiley & Sons), (1975) ,pp.84-87.

[5] Miura Y. (2006): Workshop on Sulfates as Recorders of Atmospheric-Fluid-Rock Interactions, Abstract #7001.

EXPLORING FOR EARLY BOMBARDMENTS ON EARTH FROM PRE-3.83 Ga THERMAL EFFECTS RECORDED IN HADEAN ZIRCONS – A STATUS REPORT. S. J. Mojzsis[1], O. Abramov[1], T.M. Harrison[2], D.A. Kring[3], H.F. Levison[4], D. Trail[5] and E.B. Watson[5], [1]Department of Geological Sciences, University of Colorado, Boulder, Colorado 80309-0399 USA (mojzsis@colorado.edu), [2]Department of Earth and Space Sciences, Institute of Geophysics and Planetary Physics, University of California, Los Angeles, CA 90095-1567 USA, [3]Lunar and Planetary Institute, Houston, TX 77058 USA, [4]Space Sciences Department, Southwest Research Institute, Boulder, CO 80302 USA, [5]Department of Earth and Environmental Sciences, Rensselaer Polytechnic Institute, Troy, NY 12180 USA

Introduction: In the early solar system, Earth was bombarded by comets and asteroids just as the Moon and other solar system objects were. Crustal recycling mechanisms have very nearly erased the geologic record for the first half-billion years (Hadean eon) that would preserve evidence for such cataclysmic events. Presently, there exists no direct means to measure of the influx of extraterrestrial matter to Earth before ~3.85 Ga during the 'late lunar cataclysm' or 'late heavy bombardment' [1,2; LHB]. Several studies have attempted to acquire information on the rate of accumulation and intensity of impacts at the extreme tail end of the LHB from the study of Earth rocks and minerals: Shock features in quartz [3] and zircon [4,5] from ~3.7-3.8 Ga rocks from the Isua supracrustal belt (West Greenland) yielded no optically resolvable shock deformations [6]; no unequivocal chemical evidence from platinum-group elements for the late heavy bombardment was found in paragneisses with minimum ages of ~3.83 Ga [7,8]; W isotope anomalies in ca. 3.7-3.8 Ga paragneisses from West Greenland and Labrador (Canada) were interpreted to be remnants of the LHB in younger materials [9]. However, follow-up studies with platinoid elements, Cr and other isotopic systems [e.g. 10] could find no corroborating evidence for cosmic materials in the Isua rocks [11]. Significantly, the various studies cited above explored rocks with formation times (≤3.85 Ga) that likely did not overlap with the main period of the LHB [e.g. 12].

Hadean zircons: The only vestiges of Earth's crust known to have been present during the LHB are ≤4.38 Ga detrital zircons captured in younger (3.3 Ga) sediments from the Narryer Gneiss complex in Western Australia. These zircons are the oldest known terrestrial solids [13,14]; they record evidence for hydrosphere-lithosphere interactions [15], continental crust formation [16], crustal temperature regimes in the Hadean [17,18], the presence of extinct radionuclides [19], thermal alterations since igneous crystallization [20] and other key planetary processes [21]. Zircons ($Zr(SiO_4)$) are a common constituent of many rocks, and have been found in lunar rocks and in some meteorites [22]. They have the potential to provide robust input parameters to physical models of early impact regimes in the solar system [23]. Zircon is ideally suited for these purposes because they are stable to ~1700°C at 1 bar [24], virtually insoluble in supercritical C-O-H fluids [25], relatively insoluble in most magmas [26], and diffusion is slow for most elements [e.g. 27].

Here we report on our progress with high-resolution ion microprobe U-Th-Pb depth profiles which show that subsequent to their crystallization in melts under typical crustal conditions on Earth, some Hadean zircons record common age domains with unusual chemical and isotopic characteristics consistent with a high-temperature (possibly impact) origin. We have found evidence for later overprints caused by intense thermal alteration between 3.94-3.97 Ga in six of eight studied grains but no evidence for older events. The immediate significance of these findings is that since they crystallized, the Hadean zircons were not destroyed in some wholesale remelting of the entire crust by "Doomsday"-scale impacts at least since 4.38 Ga. Although an admittedly gross constraint, it directly alerts us to two fundamental things we did not know before about the probiotic potential of the Earth in the early solar system: (i) that the LHB epoch did not result in complete destruction of the Earth's crust [e.g. 28] since the Moon-forming event at ca. 4.5 Ga; and (ii) age limits on both sides of the thermally altered 3.94-3.97 Ga zircon domains are very good and so far our data show that no detectable thermal events appear to have affectted the zircons before ~3.97 Ga up to about 4.3 Ga.

Methods: All zircons were analyzed by ion microprobe (ANU SHRIMP II or UCLA Cameca ims 1270) using our conventional U-Th-Pb protocols [29]. Other studies have shown that Hadean and meteoritic zircons can retain secondary overgrowths [e.g. 30-32] developed after primary core crystallization. All previous studies investigated these rims in conventional U-Th-Pb spot mode, and overgrowths smaller than typical ion microprobe spots (10-30 μm) are not resolvable. We employ ion microprobe U-Th-Pb depth profiling which provides continuous sub-micron depth vs. age data for single crystals [e.g. 33]. Selected zircons were removed from their epoxy mounts and recast with an original (unpolished) prism face down with zircon standard AS3 (concordant $^{207}Pb/^{206}Pb$ age of 1099 Ma). Single Hadean zircon mounts are left unpolished, but treated in 1N HCl to remove common Pb contamination prior

to ion microprobe depth profiling, and intermittently repolished during the course of the analysis.

Results and discussion: We find that most profiled zircons retain mid-Archean overgrowths correlatable with documented regional thermal events known to have affected this part of Australia [20]. Thicker overgrowths are present in the ~3.97-3.94 Ga age interval in six of the eight profiled zircons. The ~3.9 Ga overgrowths are typically <20% of the width of a ~25 μm ion beam. Five zircons preserve less defined 3.8–4.0 Ga domains that may be associated with normal crustal metamorphic conditions. In all cases, overgrowths have $[Th/U]_{Zr}$ chemically distinct from core regions, which argues against substantial mixing between mid-Archean rims and core regions.

The favored view to explain lunar isotopic disturbances reported in [1] is shock heating and metamorphism from impacts. Large impacts could cause significant fractionation of Pb relative to U at 3.9 Ga as originally proposed [1]. This is supported by K-Ar data [2] and reinforced by ^{40}Ar-^{39}Ar ages of lunar meteorite impact melts [34]. Before evidence for a terminal cataclysm became available from other planetary bodies (e.g. Mars, Vesta), it was postulated [1] that impact induced terrestrial metamorphism would have been widespread as well. In some LHB scenarios Earth could have intercepted up to four 500 km diameter impactors and experienced 10-30 impacts from 200 km diameter bodies [35]. Over time (but *not* instantaneously), ~40% of the volume of Earth's Hadean crust would have been thermally metamorphosed [23].

To test for discrete Pb disturbances in ca. 3.9 Ga zircon rims, we examined changes in % concordance (i.e. [$^{207}Pb^*/^{206}Pb^*$ age]/[$^{206}Pb^*/^{238}U$ age]) vs. the depth-age relationship of individual crystals. Our analysis assumes that a 100% concordant domain indicates significant Pb loss did not occur within that domain. Of the 6 zircons with defined 3.9 Ga overgrowths, five have domains which are markedly less concordant than surrounding regions. This result is consistent with Pb-loss behavior in lunar rocks [1] ascribed to the LHB.

Conclusions: We have depth profiled eight Hadean zircons by ion microprobe and described well-defined ca. 3.9 Ga overgrowths in six grains contemporaneous with the age ascribed the LHB. We are undertaking $[Ti]_{Zr}$ thermometry [17] on individual growth zones of the zircons to provide temperature data for the zones. Our intention is to further expand the data set of depth profiled zircons by a factor of 5. If we find 4.0 Ga and older overgrowths (such as those associated South Pole-Aitken age events on the Moon [36]?), these data could be used to support (or refute) the exponential decay model [37] or cataclysm model [38] for the 4.3 – 3.85 Ga bombardment flux. Thus far, ~3.9 Ga zircon overgrowths with no (preserved) older events appears to favor the cataclysmic model.

Acknowledgments:
This work is supported by the NASA Exobiology Program.

References: [1] Tera, F. et al. *EPSL* 22: 1-21 (1974). [2] Ryder, G. *J. Geophys. Res.* 107, 6-[1-13] (2002). [3] Koeberl C. and Sharpton V.L. in *Papers presented to the Conference on the Origin of the Earth*, pp. 47-48. LPI (1988). [4] Koeberl et al. In *Origin of the Earth and Moon*, pp. 19-20. LPI Contribution No. 957 (1998). [5] Koeberl C. et al. In *ESF Workshop on Impacts and the Early Earth*, pp. 15-16. Cambridge Univ., Cambridge (1998). [6] Koeberl, C. *Earth Moon Planet.* 92 (1-4): 79-87 (2003). [7] Ryder et al. In *Origin of the Earth and Moon*, pp. 475-492, Univ. of Arizona, Tucson. [8] Anbar, A.D. et al. *J. Geophys. Res. – Planets* 106 (E2): 3219-3236 (2001). [9] Schoenberg, R. et al. *Nature* 418: 403-405 (2002). [10] Frei, R. and Rosing, M.T. *EPSL* 236: 28-40 (2005). [11] Koeberl, C. *Elements* 2: 211-216 (2006). [12] Kring, D. and Cohen, B. *J. Geophys. Res. – Planets* 107 (E2): Art. No. 5009. (2002). [13] Froude, D.O. et al. *Nature* 304 (5927): 616-618. (1983). [14] Compston, W. and Pidgeon, R.T. *Nature* 321 (6072): 766-769. (1986). [15] Mojzsis, S.J. et al. *Nature* 409 (6817): 178-181. (2001). [16] Harrison, T.M. et al. *Science* 310 (5756): 1947-1950 (2005). [17] Watson, E.B. and Harrison, T.M. *Science* 308 (5723): 841-844 (2005). [18] Hopkins, M. et al. (2008) in press. [19] Turner, G. et al. *Science* 306 (5693): 89-91 (2004). [20] Trail, D. et al. 71, 4044-4065 (2007). [21] Trail, D. et al. *G3* 8: doi:10.1029/2006GC001449 (2007). [22] Rubin, A.E. *Met. Planet. Sci.* 32: 231-247 (1997). [23] Abramov, O. and Mojzsis, S.J., this meeting. [24] Speer, F. *Rev. Mineral.* 5: 67-112 (1982). [25] Ayers, J.C. and Watson, E.B. *Phil. Trans. Royal Soc. London – A.* 335 (1638): 365-375 (1991). [26] Watson, E.B. and Harrison, T.M. *Earth Planet. Sci. Lett.* 64 (2): 295-304 (1983). [27] Cherniak, D.J. and Watson, E.B. *Rev. Mineral.* 53: 113-143 (2003). [28] Prichard, M.E. and Stevenson, D.J. In *Origin of the Earth and Moon*, pp. 179-196, Univ. of Arizona, Tucson (2001). [29] Mojzsis, S.J. et al. *J. Geol.* **111**, 407-425. (2003). [30] Maas et al. GCA 56: 1281-1300 (1992). [31] Cavosie, A.J. et al. Precamb. Res. 135: 251-279. (2004). [32] Ireland, T.R. and Wlotzka, F. *EPSL* 109: 1-10 (1992). [33] Mojzsis, S.J. and Harrison, T.M. *EPSL* 202, 563-576 (2002). [34] Cohen, B. A. et al. Science 290, 1754-1756. (2000). [35] Sleep, N.H. and Zahnle, K. JGR. 103: 28529-28544. (1998). [36] Hand, E. Nature 453: 1160-1163 (2008). [37] Hartmann W.K. *Meteor. & Planet. Sci.* 38: 579-593. (2003). [38] Gomes, R. et al. *Nature* 435: 466-469. (2005).

LUNAR BASINS AND BRECCIAS. M. D. Norman[1,2], [1]Lunar and Planetary Institute, Houston TX 77058 USA, [2]Research School of Earth Sciences, Australian National University, Canberra ACT 0200 Australia, marc.morman@anu.edu.au.

Introduction: Absolute ages of lunar basins are critical for assessing the reality of a late cataclysmic bombardment. Two of the younger basins, Imbrium and Serenitatis, are reasonably well dated at 3.85 and 3.89 billion years. Three other basins (Herzsprung, Sikorsky-Rittenhouse, Baily) occur stratigraphically between Serenitatis and Imbrium, and the Schrödinger and Orientale basins are both not much younger than Imbrium based on crater density populations [1], so it is clear that several large (>10 km diameter) impactors did hit the Moon within a relatively narrow interval of time around 3.7-3.9 billion years ago and that similar events have not occurred since then. Absolute ages of older basins are not well established and will be required to resolve an anomalous late spike from the terminal stages of a more continuous impact history.

Significance of Lunar Basins: Most of the surface geology on the Moon is controlled either directly or indirectly by the 50 or so impact basins that have been recognized with varying degrees of confidence from photogeology and orbital geophysical mapping [1,2,3]. These massive events impel punctuated tectonic modification and large-scale resurfacing of the lunar crust on timescales that are brief even by human perceptions. Where these basin-forming impactors came from, why they invaded the inner Solar System long after the initial stages of planetary accretion and differentiation, and their possible influence on the geological evolution of the terrestrial planets are fundamental questions with significant implications for solar system dynamics, crustal architectures of terrestrial planets, and early planetary environments. The lunar impact record provides a uniquely accessible resource for addressing these and related questions [4].

Impact Breccias: Large impact events create major volumes of breccia deposits, and these were natural targets for the Apollo expeditions. Two general classes of lunar impact breccias have been recognised: *fragmental breccias* composed predominantly of clastic rock debris in a finely comminuted, grain-supported matrix of mineral and lithic fragments, and *melt breccias* with crystalline to glassy matrices that formed by cooling of a silicate melt. Based on field studies of terrestrial craters and photogeologic observations of relatively young lunar basins such as Orientale, melt breccias are thought to occur predominantly within and close to the rim of the basin whereas fragmental breccias can be deposited outwards up to several times the radius of the basin.

Of particular interest has been the use of lunar breccias for constraining the timing of large impact events and the provenance of the breccias. Melt breccias are especially useful for geochronology because they stand the best change of having their radioactive clocks completely reset by the impact event, although the presence of relict clasts (Fig. 1) has been a persistent challenge to obtaining reliable ages [5].

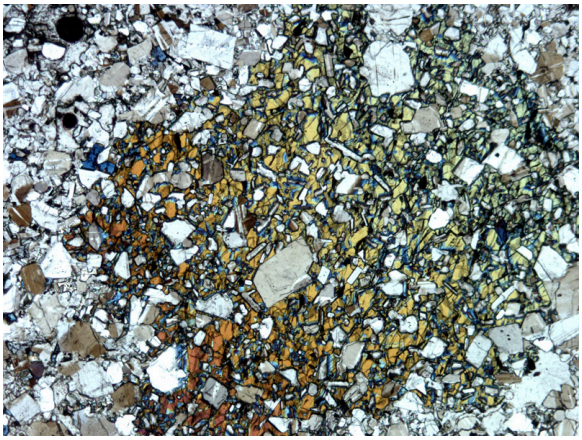

Figure 1. Photomicrograph of aluminous poikilitic impact melt breccia 61569. Field of view is approx. 1 mm wide. Partially x-nicols.

A Late Spike? Crystalline lunar melt breccias ages cluster between 3.75-3.95 Ga. This corresponds with an episode of intense crustal metamorphism defined by U-Pb isotopic compositions of lunar anorthosites, a coincidence that led Tera *et al.* [6] to infer "an event or series of events in a narrow time interval which can be identified with a cataclysmic impacting rate of the Moon at ~3.9 Ga". This discovery produced competing hypotheses for the early impact flux to the Moon and by implication for the early Earth.

In one scenario, the impact flux increased dramatically at ~3.9 Ga, creating perhaps 15 or more lunar basins (>300 km diameter) during a 'Late Heavy Bombardment'. Depending on the relationship between impactor size and basin diameter, this might imply a mass flux to the Moon on the order of about 10^{22} g within 100 million years [7], equivalent to about 0.3% of the current mass of the asteroid belt and an accretion rate 25,000 times higher than the annual impact flux to the Moon over the past 3.6 billion years. Alternatively, the impact flux may have declined more steadily with relatively minor temporal fluctuations since formation of the Moon's crust. In this scenario the apparent clustering of impact breccia ages may be due to de-

struction or burial of older deposits by ejecta from more recent events such as Imbrium and Serenitatis, or a bias due to the relatively small area actually sampled by the Apollo and Luna missions [8, 9].

Influence of Imbrium on the Central Nearside: Despite early evidence for multiple impact events based on ^{39}Ar-^{40}Ar ages [5], analytical and geological uncertainties precluded further resolution of discrete impact events based on either age or chemistry [10]. Recent geochronological studies of Apollo 16 melt breccias have recognized clusters defined by ages and textures that may represent several distinct impact events during the interval 3.75-3.95 Ga [11]. The provenance of these melt breccia groups relative to specific basins or craters is unknown, but most of these groups are equal to or younger than the accepted age of Imbrium (3.85 Ga). The lack of older ages may be due to resurfacing of the central nearside highlands around the Apollo 16 site by the Imbrium event.

The lack of impact-melt breccia crystallization ages older than 4.0 Ga has been cited as strong evidence supporting a late cataclysm [7]. Apollo 16 crystalline rock 67955 (Fig. 2) appears to be one of the few lunar melt breccias with an older age of 4.2 Ga defined by a ^{147}Sm-^{143}Nd mineral isochron [12]. The major and trace element composition of this sample represents a magnesian endmember to the Apollo 16 feldspathic fragmental breccias (FFB) collected around North Ray crater [13], so one interpretation might be that 67955 was delivered to the site as clast within this unit of fragmental breccias. An Imbrium provenance for these breccias is supported by the ^{39}Ar-^{40}Ar ages of anorthositic clasts from these breccias [14], and the KREEPy petrologic and trace element signatures in 67955 and other FFB clasts. This interpretation pulls the pin on the age of Nectaris based on argon ages of clasts eroded from the FFBs [16].

A current controversy concerns the interpretation of 4.1-4.2 Ga ^{39}Ar-^{40}Ar ages commonly obtained from the dark, clast-rich melt breccias contained within and eroded from the A16 FFB's [14, 15]. Maurer et al. [15] and some recent discussions of lunar cratering history [17, 18] have accepted the apparent ages of these clasts as dating a specific impact event. Alternatively these ages may reflect partial resetting of older crustal materials during emplacement of the FFBs [19].

A speculative possibility is that the ~4.2 Ga argon ages obtained from the FFB melt breccia clasts might be inherited either from the same impact event that formed 67955, or from a volume of crust in the Imbrium region that was degassed at that time. Some metamorphosed granulites from the Apollo 17 site also have Ar ages ~4.2 Ga [20], again raising the possibility of one or more large, pre-Imbrium impact events in the northern nearside region of the Moon. Better constraints on megaregolith evolution of the lunar crust between 4.4 and 3.9 Ga are needed to evaluate the significance of an apparent 300-500 Ma gap in impact ages as sampled in the nearside highlands of the Moon.

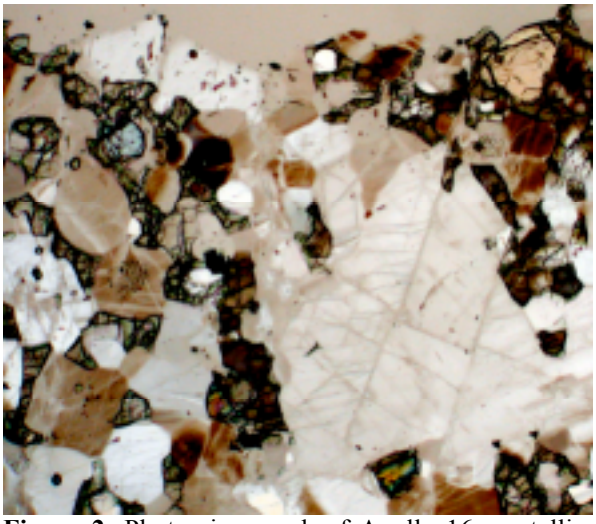

Figure 2. Photomicrograph of Apollo 16 crystalline rock 67955. Field of view approx. 1 mm. Partially crossed-nicols.

References: [1] Wilhelms DE (1987) *USGS Prof. Pap. 1348*, 302pp. [2] Spudis PD (1993) T*he Geology of Multi-Ring Impact Basins*, 263pp. [3] Wood CA (2004) http://www.lpod.org/cwm/DataStuff/Lunar%20Basins.htm. [4] Space Studies Board (2007) Scientific Context for Exploration of the Moon: Final report. 120pp. [5] Jessberger EK, Hueneke JC, Podosek FA, Wasserburg G (1974) *PLSC 5*, 1419-1449 [6] Tera F, Papanastassiou DA, Wasserburg GJ (1974) *EPSL 22*: 1-21. [7] Ryder G (2002) *JGR 107*, 5022, 10.1029/2001JE001583. [8] Hartmann WK (2003) *MAPS 38*, 579-593. [9] Chapman CR, Cohen BA, Grinspoon DH (2007) *Icarus 189*, 233-245. [10] Korotev RL (1994) GCA 58, 3931-3969. [11] Norman MD, Duncan RA, Huard JJ (2006) *GCA 70*, 6032-6049. [12] Norman MD, Shih C-Y, Nyquist LE. Bogard DD, and Taylor LA (2007) *Lunar Planet. Sci., 38*, #1991. [13] Lindstrom MM and Salpas PA (1983) PLPSC 13, A671-A683. [14] Duncan RA and Norman MD (2005) MAPS #5149. [15] Maurer P, Eberhardt P, Geiss J, Grögler N, Stettler A, Brown GM, Peckett A, Krähenbühl U (1978) *GCA 42*, 1687-1720. [16] James OB (1981) *PLPSC 12*, 209-233. [17] Puchtel IS, Walker RJ, James OB, Kring DA (2008) *GCA 72*: 3022-3042. [18] Garrick-Bethell I, Weiss BP, Fernandes VA, Shuster DA, Becker TA (2008) *NLSI Conf.*, #2131. [19] Warren PH, Taylor DJ, de Leuw S, Cosarinsky M, Schmidt BE, Dyl K, and Spengler E (2007) *MAPS, #5313*, A160. [20] Turner G and Cadogan PH (1975) *PLSC 6*, 1509-1538.

CHRONOLOGY AND PROVENANCE OF LUNAR KREEP: A 4.0 OR 4.1 Ga AGE FOR SERENITATIS?

L. E. Nyquist[1] and C-Y. Shih[2], [1]Mail Code KR, NASA Johnson Space Center, Houston, TX 77058, laurence.e.nyquist@nasa.gov, [2]Mail Code JE-23, ESCG/Jacobs Sverdrup, P.O. Box 58477, Houston, TX 77058, chiyu.shih@nasa.gov.

Introduction: Stöffler and Ryder [1] summarized the radiometric ages of lunar samples and lunar surface crater frequencies to derive a chronological standard for the inner solar system. They concluded that the sampled basins formed within the narrow time interval from 3.92±0.03 Ga ago (Nectaris) to 3.85±0.02 Ga ago (Imbrium). We examine the question of basin ages using Rb-Sr isotopic data. Rb-Sr isochrons provide initial $^{87}Sr/^{86}Sr$ values (I_{Sr}) as well as ages (T). I_{Sr} is a tracer for lunar KREEP, which often appears to be associated with lunar basins. A variety of KREEP (or urKREEP) is widely assumed to form a lower crustal layer on the moon. (See [2], Fig. 1, for example.) From these considerations we suggest that the Serentitatis basin may be as old as ~4.1 Ga.

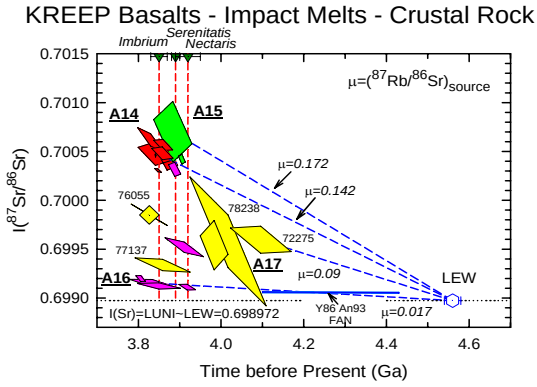

Figure 1. (T,I_{Sr}) values for KREEP basalts and KREEP-enriched impact melts compared to values for crustal rocks. Data from the literature except 78238 norite [9].

(T,I_{Sr}) for KREEP basalts and melt rocks: Fig. 1 summarizes (T,I_{Sr}) values for KREEP basalts and KREEP-rich melt-rocks from Rb-Sr mineral isochrons. A mineral isochron requires the initial existence of a magma which cools slowly enough to allow minerals to nucleate and grow, a requirement satisfied by most indogenously generated basalts, so many of the data plotted in Fig. 1 are for A14 and A15 KREEP basalts and A17 KREEPy basalts. Interpreted in the customary manner, the relatively high I_{Sr} values for these basalts imply that they were produced by partial melting of a portion of the lunar mantle having high source region $(^{87}Rb/^{86}Sr)_{source}$ (μ) values ranging from μ ~ 0.09 for A17 KREEPy basalts to ~0.17 for A15 KREEP basalts.

Distribution of Rb-Sr Ages: Fig. 2 shows a comined probability distribution for the ages shown in Fig. 1. The figure is constructed by expressing the

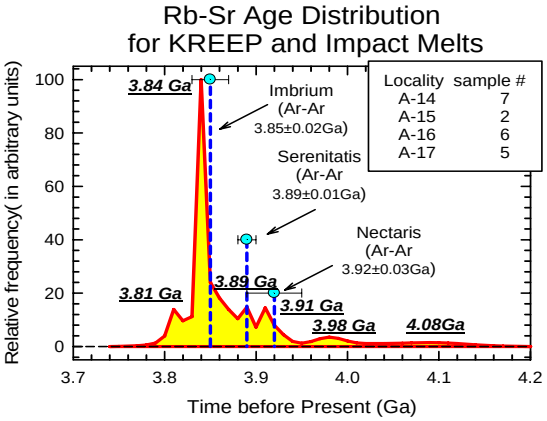

Figure 2. Rb-Sr ages of KREEP basalts and highland melt-rocks.

measured age and error limits as a gaussian distribution in time. Data for several impact-melt rocks are included, including all of the A16 rocks for which (T,I_{Sr}) data are shown in Fig. 1. The oldest Rb-Sr ages of the A16 rocks are in agreement with a 3.92±0.03 Ga age given for the Nectaris basin [1]. Some of the A16 impact melt rocks are younger, consistent with formation via local, smaller-scale, cratering. Alternatively, their ages also are consistent with the 3.85±0.02 Ga age given for the Imbrium event by [1]. This suggests that they may have been ballistically transported to the A16 site by the Imbrium event, but they lack the characteristically high I_{Sr} values of Imbrium ejecta as found at the A14 Fra Mauro site, for example. For that reason, we consider it unlikely that they are Imbriuim ejecta.

^{39}Ar-^{40}Ar ages for A16 melt rocks from [3] also are shown in Fig. 3 in comparison to Rb-Sr ages from the literature [4,5] recalculated with decay constant λ_{87} =

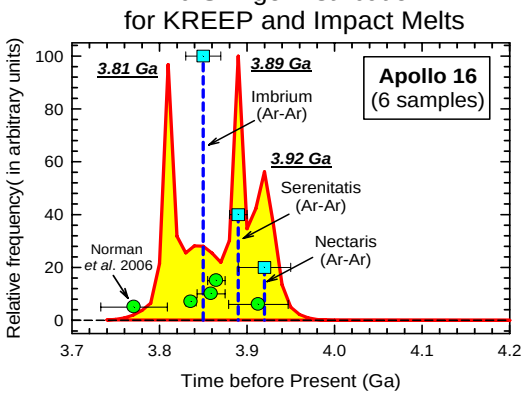

Figure 3. Combined probability distribution for A16 Rb-Sr ages.

0.01402 Ga^{-1}. There is good agreement, even to the existence of four dated events. This observation and close agreement between the Rb-Sr and ^{39}Ar-^{40}Ar ages for Imbrium (Fig.2) demonstrate general concordancy between ages obtained by the two methods.

Fig. 4 shows lack of agreement between the Rb-Sr ages of A17 rocks and the suggested ages of the Serenitatis and Nectaris basins, however. As for the A16 data, the youngest ages are approximately consistent with the ~3.85 Ga age of the Imbrium basin. However the corresponding rocks have lower initial $^{87}Sr/^{86}Sr$ than characteristic of KREEP-rich ejecta from Imbrium. We think it more likely that, like the A16 melt rocks, they represent local cratering events. There is no correspondence between the 3.89±0.01 Ga age suggested for Serentitatis by [1] and any preferred age shown by the Rb-Sr data. In principle, this could be a selection effect caused by the inability to date relevant impact melt samples by Rb-Sr mineral isochron techniques. However, this does not appear to have been a factor for rocks from the other landing sites. A14 and A15 KREEP basalts, for example, appear to record the Imbrium event, perhaps via impact-triggered volcanism. The analogous indogenously generated KREEPy basalts at the A17 site are ~4.1 Ga old. They predate the Serenitatis event if the latter occurred at ~3.89 Ga.

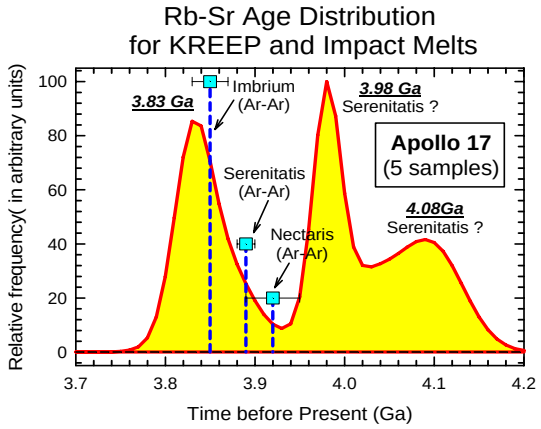

Figure 4. Combined probability distribution for A17 Rb-Sr ages.

Sr isotopic data for KREEP-rich breccias: Fig. 5 may contain some additional clues to interpreting the A17 data. It shows "initial" $^{87}Sr/^{86}Sr$ values calculated from bulk analyses of the matrices of breccias [6,7] that can be reasonably traced to formation of the Imbrium (A14, A15) and Serenitatis basins (A17). These breccia matrices contain multiple components, but their Sr-isotopic compositions are clearly dominated by the KREEP component(s). These data have the geological advantage that the A17 breccia matrices come from boulders that can be traced to the South and North Massifs of the Taurus mountains. Compared to known

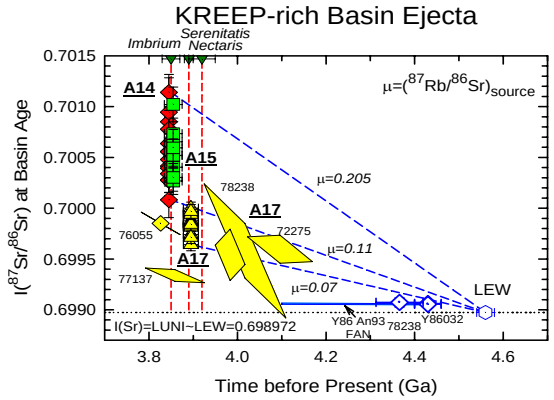

Figure 5. I_{Sr} for KREEP-rich basin ejecta at the basin age.

Imbrium ejecta, they had distinctively lower $^{87}Sr/^{86}Sr$ ratios at ~3.89 Ga ago. Like the impact-melt sample 76055, their $^{87}Sr/^{86}Sr$ ratios are consistent with radiogenic growth in the same "source" with μ ~ 0.09 as for the A17 KREEPy basalt clast in breccia 72275.

Conclusions: By analogy to the apparent linkage via impact-triggered volcanism or impact melting between the ages of A14 and A15 KREEP basalts and the age of the Imbrium basin, there is a significant probability that the Serenitatis basin is as old as ~4.1 Ga. Alternatively, ~4.1 Ga A17 KREEPy basalts may have formed the protolith into which the Serenitatis impact occurred. In this case, the Rb-Sr data suggest a probable age of ~3.98 Ga for the Serentitatis event. The latter age is a particularly good fit to the cratering chronology of [8] (Fig. 6).

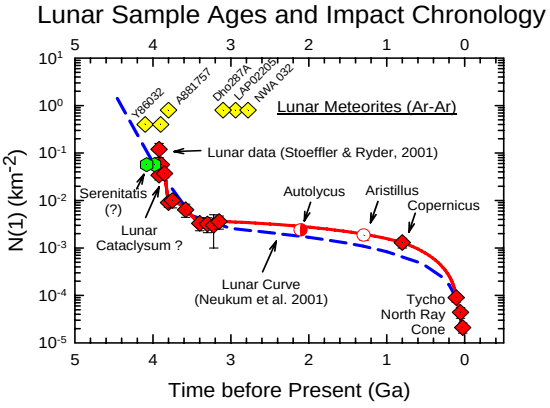

Figure 6. Possible Serenitatis ages compared to the cratering chronologies of Neukum et al. [8] and Stöffler et al. [1].

References: [1] Stöffler D. and Ryder G. (2001) *Space Sci. Rev., 96,* 9-54. [2] Ryder G. and Wood J. (1977) *PLSC8,* 655-668. [3] Norman M. D. et al. (2006) *GCA 70,* 6032-6049. [4] Reimold W.U. et al. (1985) *PLPSC-15th, JGR, 90,* C431-C448. [5] Deutsch A. (1986) *LPS XVII,* 176-177 [6] Nyquist L. E. et al. (1974) *PLSC5* 1515-1539.[7] Nyquist L.E. et al. (1975) PLPSC-6th, 1445-1465. [8] Neukum G. et al. (2001) *Space Sci. Rev., 96,* 55-86. [9] Edmunson J. (2007) Ph. D. thesis.

CONSTRUCTION OF A VOLATILE RICH MARTIAN UPPER CRUST DURING THE IMPACT CATACLYSM. J.A.P. Rodriguez[1](alexis@psi.edu) and J. Kargel[2], [1]Planetary Science Institute, 1700 E. Ft. Lowell Rd., Suite 106, Tucson, AZ, 85719, [2]Dept. of Hydrology & Water Resources, Univ. of Arizona, Tucson, AZ 85721.

Introduction: The early hydrologic history of Mars comprises a longstanding, fundamental mystery regarding the geologic history of the planet. Unresolved issues include *(1)* the timing and mechanisms involved in the formation of a volatile rich upper crust, and *(2)* the nature of the transition from a period of accelerated erosion and sedimentary deposition early in its history, seemingly coeval or overlapping with the late heavy impact bombardment, to a subsequent period dominated by dry and frigid surface conditions.

It has been proposed that the migration of outer planets' orbits may have caused severe depletion of asteroids due to orbital instabilities as strong gravitational resonances swept across the asteroid belt, thereby producing the objects responsible for the late heavy bombardment [1,2,3]. Strom [4] suggested that this period occurred as a cataclysmic bombardment of the Moon and all terrestrial planets and lasted only about 10^7 to 10^8 years between ~4.0 and ~3.85Ga.

The highlands and lowlands of Mars contain large populations of quasi-circular depressions (QCD's), generally interpreted to represent depressions formed due to differential compaction of sediments over buried impact craters [5, 6]. The thickness of the geologic materials that allegedly bury the impact craters has been estimated to range between 1 km and 6 km [7]).

Rodriguez et al. [8,9] characterized the morphology and morphometry of chaotic terrains and zones of plateau subsidence in South Chryse and concluded that buried impact craters may have formed significant regional aquifers and may have promoted long-range groundwater migration through the fractured crust. They proposed that the upper crust of Mars contains extensive sedimentary deposits, in which buried impact craters are likely to have formed aquifers. In their hypothesis, lakes would have frequently formed within impact craters, so that their burial would have led to heterogeneous distribution of volatiles within the upper crust of Mars. The absence of globally distributed chaotic terrains implies that most of these aquifers remain untapped, or that they have lost their volatiles slowly over billions of years.

Concurrent aggradation of the Martian upper crust and heavy bombardment must have taken place during climatic periods that allowed for widespread hydrologic activity on the Martian surface [9]). Kargel et al. [10] proposed that impact crater/basin forming events may have led to the formation of transient atmospheres during the cataclysm, capable of sustaining active hydrologic environments and accelerated water- and ice-driven geomorphic process activity.

Chronology of crustal accretion in southern circum Chryse: The plateau materials of southern circum-Chryse contain dense populations of *(1)* QCD's (interpreted as buried craters), *(2)* impact craters that have been infilled almost to their rims, and (3) degraded and pristine impact craters (Fig. 1). The combined population of pristine, degraded, infilled, and buried craters larger than about 16 km diameter (Fig. 2) is consistent with an overall age of 3.85 ±0.1 Ga, according to the crater density/age calibration model of Hartman [11]; if there had been no crustal aggradation but simply a clean surface produced at 3.85 ±0.1 Ga, that surface would have a crater density equal to this combined crater density. However, looking only at pristine craters > 16 km, the apparent age is ~3.7 Ga; we interpret this to mean that vigorous crustal aggradation occurred simultaneous with heavy impact cratering from 3.85 to 3.7 Ga, and then slowed dramatically. The pronounced rollover of all types of craters, including pristine ones, at diameters smaller than 16 km, especially approaching 4 km diameter, indicates that some significant resurfacing and erosion of many small craters and QCD's occurred, with little crustal aggradation, until at least 3 Ga.

Any such chronology depends on the impact flux history, which is not strictly known, other than for the Moon.
Thus, we propose that between ~3.8 and 3.0Ga, there were three distinct resurfacing stages; *(I)* an oldest stage, 3.85-3.7 Ga, during which the region of the South Chryse Basin accumulated extensive sedimentary deposits, which buried large populations of impact craters formed while the rock record accumulated, *(II)* an intermediate stage, roughly 3.7-3.4 Ga during which large impact craters were infilled but not buried, and *(III)* a subsequent stage during which hydrologic and other surficial activity was significant enough as to degrade crater rims of large craters and wipe out many craters 4 km in diameter, but not significant enough as to lead to extensive burial/ infilling of craters larger than 16 km.

Within the outflow channel and chaos areas, a long-recognized dearth of fresh impact craters (which Figure 1 shows extends to infilled craters and QCD's) indicates that deep-level erosion and disaggregation of the terrain occurred well after late heavy bombardment ended. Within the outflow channel boundaries there are plateau outliers resembling the more heavily cratered terrains indicate, as has been known, that the plateau areas once extended across this whole region. Thus the three-phase history above was followed by, or perhaps stage III above was concurrent with, a prolonged period of intense but strongly localized crustal disintegration to form chaos and outflow channels.

Multi-volatile-driven resurfacing during the cataclysm: The decrease in hydrologic activity presumably occurred in association with a trend in global cooling. Thus, we expect a zonation of volatiles in the upper crust in which volatiles with lower freezing points are preferentially located in areas of colder crust.

Impact-related epochs of globally widespread erosion and deposition of sedimentary rocks would be interspersed with volcanic and impact deposits. Impact crater basins would have accumulated sedimentary deposits and refrozen lake and groundwaters, which would be overlain by, or interlayered, with aeolian, volcanic, and impact ejecta formations.

The impact blitz also would have released other volatiles, besides H_2O, including SO_2, CO_2, CO, H_2SO_4, HCl, elemental sulfur, O_2, alkali metals, and other highly and slightly volatile materials due to impact heating of metal sulfides, sulfate salts and other salts, and silicates. For example, pyrite, upon heating, would yield elemental sulfur liquid (or vapor at low confining pressures); gypsum would dehydrate (yielding H_2O) and, at higher temperatures, give off SO_2 and O_2. In an oxygenic system, sulfuric acid would be produced.

With sudden transient disturbances to the planet's radiative balance and climate caused by atmospheric injection of multiple volatiles, global episodes of acid rain and acid chemical weathering, reformation of sulfates, and oxidation of iron in ferrous silicates would have been widespread. Rapidly evolving climatic excursions would attend drawdown of transient atmospheric species. With each large impact, a transient episode of rainfall, fluvial erosion, and lacustrine deposition (e.g., Segura et al. [12]) would have been followed by an epoch dominated by snowfall and glaciations, and finally increasingly severe periglacial environments.

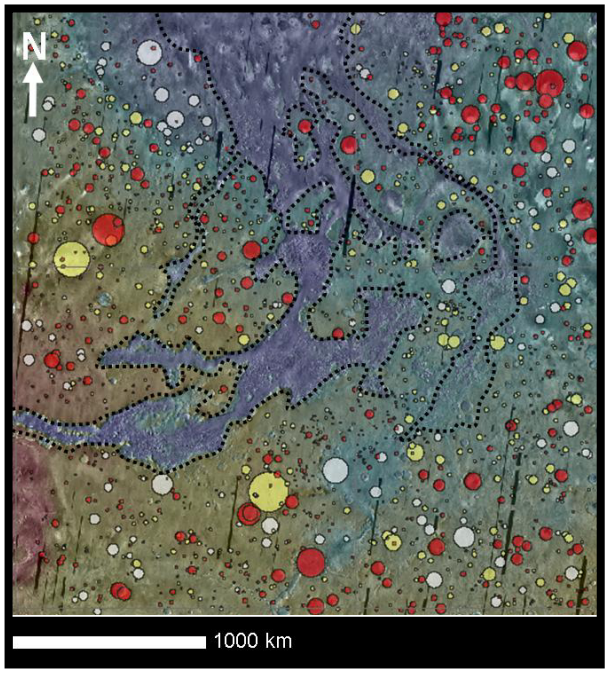

Figure 1. *Color shaded relief view of South Chryse. Shown are the populations of pristine and degraded impact craters (red circles), infilled impact craters (yellow circles), and QCD's (white circles) in the plateau surfaces that form the peripheries of the chasmata, chaotic terrains, and outflow channels (margins outlined by black dots). Composite of MOLA based DEM (128 pixels/degree) and THEMIS IR mosaic (256 pixels/degree).*

The larger and longer lived climatic excursions could have been modulated by obliquity variations and other astronomical forcings as well as by massive volcanism [13], even while trends were toward a geologically rapid drying and cooling of the planet. In sum, the late heavy bombardment also appears to have been a period of cataclysmic crust formation and hydrogeologically driven resurfacing.

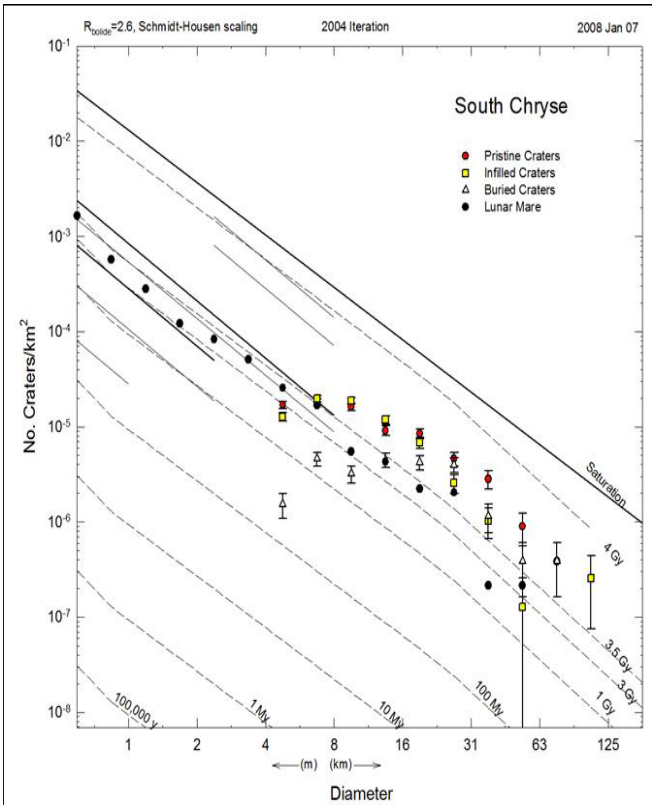

Figure. 2. *Plot showing the relative ages obtained from impact crater populations displayed in Fig. 1 versus impact crater populations in the Lunar Mare.*

References: [1] Gomes et al., (2005) Nature, 435, 466-469. [2]Strom et al., (2005) American Geophysical Union, Fall Meeting 2005, . 309, 1847–1850. [3] Tsiganis et al., (2005) Nature, 435, 459-461. [4] Strom et al., (2005), Science, 309, 1847. [5] Frey, (2004), Proc. Lunar Planet. Sci. Conf., 35th. 1382. [6] Buczkowski et al., (2006) [7] Garvin et al., (2000), Icarus 144, 329-352, Proc. Lunar Planet. Sci. Conf., 37th. 1333. [8] Rodriguez et al., (2005) J. Geophys. Res. 110, E06003. [9] Rodriguez et al., (2005), Icarus, 175, 36-57. [10] Kargel et al., (2006) Proc. Lunar Planet. Sci. Conf., 37th,2052. [11] Hartman (2005), Icarus, 174, 294-320. [12] Segura, et al., (2002), Science,298, 1977 - 1980, DOI: 10.1126/science.1073586.[13] Baker et al., (1991), Nature, v. 352, p. 589-594.

IMPACTOR SURVIVORS AS ADDITIONAL SOURCES FOR THE LATE HEAVY BOMBARDMENT. P. H. Schultz[1] and D. A. Crawford[2], [1]Department of Geological Sciences Brown University, Box 1846, Providence, RI 02912; [2]Sandia National Laboratories, MS 0836, P. O. Box 5800, Albuquerque, NM 87185 (dacrawf@sandia.gov)

Introduction: Before the last major basin-forming events on the Moon and elsewhere, the cratering rate was orders-of-magnitude higher. During this period, crater statistics also document a size distribution of craters different from the last 3.8 Ga, with an excess of craters 1 to 20 km in diameter (for the lunar highlands). Several hypotheses have been proposed to interpret the source of the objects responsible for both the enhanced flux (e.g., [1,2,3]). Significantly, this distribution is recorded on the Orientale ejecta facies. Because Orientale was the last major basin produced on the Moon capable of producing sufficiently large secondaries, returning ballistic ejecta could not be the cause. Here we propose that significant masses of large basin-forming objects survive collisions at modest impact angles (< 40º from the surface tangent) and contribute to the period of heavy bombardment. This suggestion, however, still begs the question as to the origin of the large basin-forming objects.

Background: On flat surfaces, oblique collisions (< 15º) result in large portions of the original impactor (50% of the mass) surviving and re-impacting downrange. This process is well documented in laboratory experiments where the loss of kinetic energy and momentum corresponds to a decrease in the crater size [4], shock coupling [5], and enhanced frictional shear heating [6]. The process has been called "decapitation" and the surviving impactor fragments termed "siblings" [4].

Hypervelocity impact experiments reveal that the energy initially coupled to the projectile results in reduced peak pressures. As the shock reflects off the rear of the projectile, it fails by spallation and shear. The resulting size distribution of surviving siblings departs from expectations for catastrophic failure [4]. Typically, there are 5 to 10 large pieces of nearly equal mass (totaling 50% of the initial projectile mass), in addition to a power-law distribution for smaller fragments similar to results for catastrophic disruption.

Experiments were designed to isolate the siblings before re-impacting the target downrange (Fig. 1). The point of impact was uprange from the edge of the target. The crater formed nominally and the isolated siblings impacted a witness plate downrange, close to the original trajectory. Because the siblings did not re-impact the target, they were larger (the largest approaching 30 to 50% of the initial projectile mass).

A curved surface also prevents the siblings from re-impacting the target and becomes more important as the projectile radius (r) exceeds 10% of that of the target (R). Moreover, the diameter and depth of the resulting crater decreases since a significant fraction of the initial energy/momentum has been decoupled [7]. The impact angle measured by the angle from the tangent plane at first contact progressively resembles a much lower angle collision. For example, the surviving siblings from a 45º impact (the most likely) for a projectile 4R effectively resembles a <15º impact on a planar target. Highly oblique impact craters on the Moon and Mars exhibit remarkably similar patterns, including cases where local slopes (crater walls) acted to isolate the effects of downrange siblings [7]. Consequently, decapitation is a fundamental process, not restricted to laboratory-scale experiments.

The Moon, Mercury, Mars, and Vesta all retain evidence of a collision that approached 0.001% to 0.3% of their gravitational potential energy. Simple geometry reveals that decapitation of basin-forming asteroids yields downrange siblings that cannot re-impact the surface immediately following the event. For shear-controlled failure, a simple geometric relation [7] predicts that one half of the impactor will be decoupled when the impact angle (θ) approaches $\cos(\theta) = R/(r+R)$. As a result, a single mega-impactor (> 700 km) could yield multiple large siblings that will be (by definition) in a planet-crossing orbit initially. In addition to the 5 to 10 largest masses, many more much smaller objects add to the background cratering record. A mega-basin, therefore, may appear much older (based on crater statistics) due to the overprinting by sibling debris arriving over the next 10^2 to 10^8 years.

Computations: In order to test this hypothesis, we used the three-dimensional CTH hydrocode to assess the consequences of undifferentiated dunite bodies of 140-700 km in diameter colliding with the Moon at 20 km/s and angles of 30°, 45°, 60° and 90° (from the impact tangent plane at first contact). This approach kept the energy couple to the Moon approximately the same. The calculations used ANEOS equations-of-state [8] for the dunite, the lunar mantle and the 350 km radius molten iron core with a temperature profile at the time of impact based on theoretical models [9]. The calculations have not fully incorporated fragmentation or shear to the resolution necessary to address the physical state of the siblings (to be addressed in the future). Nevertheless, the results demonstrate the significant decoupling and continued trajectory of the survivors of the collision. The code used an Adaptive

Mesh Refinement (AMR) approach where the resolution of the finest computational zoning was 40 km (cubical zones). The total computational domain was 20,000 km in each direction. The finest resolution (40 km) was reserved for any material with a density greater than 0.1 g/cc, thereby allowing vapor to flow into low-resolution mesh. Consequently, regions of interest (the solid Moon and impactor) could be resolved while not wasting computational resources on the vapor.

Numerical resolution was adequate to capture shock compression, release and tensile fracture (spall) in the bulk of the Moon. For the largest energy events, the impact kinetic energy (KE) represents a significant fraction (up to about 30%) of the total gravitational potential (binding) energy of the Moon. For oblique impacts (30°), however, much of the initial KE (>50%) decouples from the process as the impactor decapitates and continues downrange (Figs. 2 and 3). The subsequent trajectory and speed is modified only slightly (<10° and 10%, respectively).

Implications and Conclusions: At least half of the population of large basins on the inner planets was oblique (<45°). Lower angle collisions (<30°) ensured that a significant portion of the impacting body survived and contributed to subsequent bombardment, whether on the original target planet or on other planets. The Crisium Basin on the Moon illustrates an extremely low-angle impact where the massif-ring was only slightly larger (factors of 3) than the impactor. Downrange siblings from an oblique basin-forming impact would have contributed 20% to 80% of the original impactor. The size distribution of the siblings would not have followed a single power-law distribution because multiple processes control the process (e.g., shear, spallation). Larger masses (or weakly bound masses) would have contributed to subsequent bombardment (later basins), whereas smaller masses would have bombarded the planets or were ejected from the inner solar system. In this scenario, one mega-basin could create its own heavy bombardment. The last oblique basin-forming collision yielded smaller debris with a short dynamical lifetime.

References: [1] Strom, R. G. et al. (2005), *Science* 309, 1847-1850; [2] Ryder, G. (2001), *EOS* 71, 313; [3] Bottke, W. F. et al. (2007), *Icarus* 190, 203-223; [4] Schultz, P.H. and Gault, D.E. (1990), *Geol. Soc. of Amer. Sp. Paper* 247, 239-261; [5] Dahl, J. M. and P. H. Schultz (2001), *Int. Jrnl. Impact Eng.26,* 145-155; [6] Schultz, P. H., et al. (2006), *Int. Jrnl. Impact Eng 33,* 771-780; [7] Schultz, P.H. (1997), *Lunar Planet. Sci. Conf. XXVIII*, LPI, Houston, TX, 1259-1260; [8] McGlaun, J.M., Thompson, S. L., and Elrick, M. G. (1990), *Int. J. Impact Eng.*, 10, 351-360 (1990); [9] Zhong, S., Parmentier, E. M., and Zuber, M. T. (2000), *Earth Planet. Sci. Lett.*, 177, 131–140.

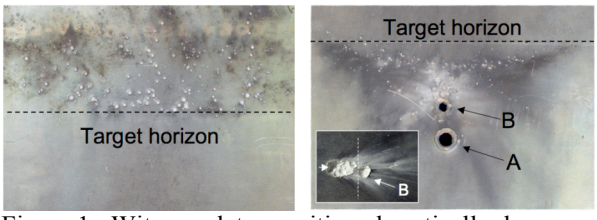

Figure 1. Witness plates positioned vertically downrange for 15° impacts into water (left) and aluminum (right). The source of the downrange pit was isolated by aiming at the edge of the target (line, inset). The decapitated impactor isolated from re-impacting downrange (B), only slightly deflected from the original trajectory (A).

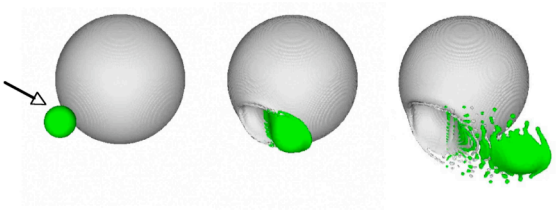

Figure 2: Survival of large impactor (800 km diameter) colliding with the Moon at 10 km/s at an angle of 30° to the surface tangent. Times represent 0, 150 and 300s after impact.

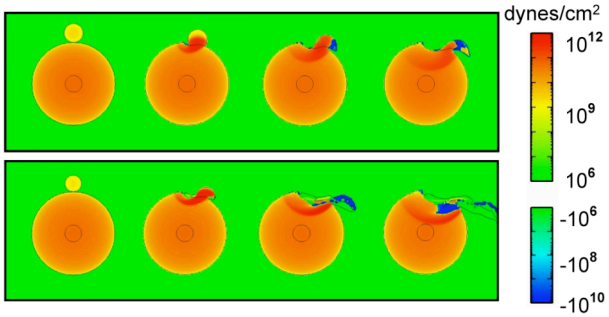

Figure 3: Trajectory and pressure conditions inside the Moon and impacting body impacting at 30° to the surface tangent. Top panel shows an 800 km diameter body at 10 km/s; the bottom panel shows a 700 km diameter body at 20 km/s, both coupling the same energy to the surface. Times represent 0, 50, 150, and 200 s after impact.

AFTER THE DUST HAS SETTLED: HYDROTHERMALLY-DRIVEN CHEMICAL AND MINERALOGICAL CHANGES IN PLANETARY CRUST FOLLOWING IMPACT EVENTS. Susanne P. Schwenzer and David A. Kring, Lunar and Planetary Institute, 3600 Bay Area Blvd., Houston, TX, 77058, USA; schwenzer@lpi.usra.edu.

Introduction: On Earth, evidence for impact-generated hydrothermal systems has been found in more than 60 impact structures [1]. These systems were driven by heat in central melt sheets, impact melt breccias, and uplifted basement material. The amounts of heating and, thus, volumes of the systems scale with crater size and are particularly prevalent in large (>100 km diameter) craters like Chicxulub [2], but can occur in much smaller craters [1]. While crater formation itself happens in seconds to minutes, impact-generated hydrothermal activity can persist for 10^3 to $>10^6$ years [3–5]. Such systems are capable of maintaining temperatures in the range of 100 to 300 °C [3–5], of altering the mineralogy of the target rock [1 and references therein, 6], and of producing hydrothermal brines that can transport ions. We have also argued [7] that these systems may have been important in the origin and early evolution of life.

Impact craters produced during the early evolution of Earth, however, have not survived. The examples cited above are temporal proxies that suggest impact-generated activity was intense during early solar system bombardment, but we do not have a direct measure of that activity on Earth. In addition, the proxies that we have are largely in granitic and/or sediment-rich terrains and do not provide a direct measure of the alteration one might find in more primitive mafic planetary crust.

Ancient cratered terrains on Mars, however, have survived and can provide additional insights about hydrothermal alteration of mafic planetary crust. Thermal models [3,4,8] suggest that impact-generated hydrothermal activity was long-lived and geographically broad. In this paper, we extend those thermal models to investigate the chemical and mineralogical changes induced by those systems and compare them to observations of ancient cratered (Noachian) terrains on Mars.

Hydrothermal modeling and results: Using CHILLER we calculated minerals that precipitate at a variety of P and T, if a rock with the composition of the lherzolithic Martian meteorite LEW 88516 is in contact with an Fe, Mg, Ca bearing fluid [6]. Modeling results can either be read as an evolution with increasing/decreasing water to rock ratio (W/R) or each step can be taken as a reaction of a given fluid with the starting rock plus the precipitates in the system. Here we illustrate the solid and fluid products of hydrothermal reactions with three examples at T=150 °C and P=550 bar: (1) W/R=10000, pH=3.8, fO_2= -42.3 (2) W/R=1000, pH=4.3, fO_2= -43.0 (3) W/R=1, pH=6.2, fO_2= -47.9. The pH and fO_2 are controlled by the mineralogy.

Precipitates. The nature of precipitates changes with fluid composition (especially SiO_2(aq), Ca, and Mg). A rock dominated system (W/R = 1) precipitates an assemblage that chemically resembles the magmatic composition of LEW 88516 (comp. Fig. 1 panel a and b). However, there is one major difference: water is introduced into the assemblage, which dramatically affects the mineralogy. While the magmatic precursor assemblage is made of 95% ortho-, chain- and framework silicates, the alteration assemblage contains 64% sheet silicates. At W/R = 1000, most of the precipitation mass is clay and, specifically, notronite. At higher W/R values (W/R= 1000 to 100000) the system precipitates an assemblage that contains mostly iron: 43% and 90% hematite are precipitated at W/R = 1000 and 100000, respectively (Fig. 1 panel c, d).

Fluids. The amount of dissolved ions varies with the precipitating assemblage controlling it. The elements Na and K largely accumulate in solution. Furthermore, a significant amount of Ca is present. Also, some elements can form molecular complexes (e.g., $Ti(OH)_4$ in one example) and stay in solution.

Collectively, the calculations suggest impact-generated alteration of early Martian mafic to ultramafic crust produced clay-rich assemblages that included smectites (like notronite) and kaolinite. The fluids associated with those alteration assemblages are dominated by those ions that are not preferred by the precipitating assemblage, thus forming an Na, K-rich brine that contains Ca and SiO_2(aq) plus some elements that form molecular complexes.

Discussion. Our model results can be compared and contrasted with two sources of information: spacecraft observations of Mars surface and meteoritic samples of Mars crust.

One Martian meteorite (ALHA 84001) is a crustal sample that crystallized 4.5 Ga and has experienced a complex geologic history, including a thermal metamorphic overprint at ~4.0 Ga and the formation of carbonates about 400000 years thereafter [9]. Several mechanisms for the formation of carbonates [see 10 and references therein] have been proposed, amongst which are carbonic fluids forming carbonates at the

expense of maskelynite [11, 12] or by precipitation from solution [10]. Hydrothermal modeling [13] and the incorporation of fractionated Martian atmosphere [14 and references therein] support the reasoning of a carbonic (atmosphere derived) fluid interacting with a host rock at elevated temperatures.

Spacecraft observations of the Martian crust also indicate water was available for many geologic processes in the Noachian, including the formation of valley networks [15], rampart craters [16] and clay minerals [17,18]. Recent and ongoing orbiter missions reveal several indications of impact-generated hydrothermal systems, amongst which the strongest are hydrous signatures in crater rims and central peaks [19,20].

The number of craters on Noachian surfaces of Mars approach the saturation limit [21] and the old highlands "should have been gardened to a depth of a kilometer or so" [21]. Given the fact that hydrothermal systems reach even deeper [3,4], Mars crust can be deeply affected by gardening, fracturing and subsequent hydrothermal alteration. The latter thereby will change the rock properties from a solid magmatic rock that does not contain water to a hydrothermally altered rock (comp. Fig. 1) that

- contains structurally bound water in sheet silicates,
- contains exchangeable water in interlayer positions,
- contains exchangeable ions in some of the clay mineral assemblages,
- has a different chemistry, thus liberating ions that are available for transport and deposition elsewhere,
- has different physical properties such as density and strength.

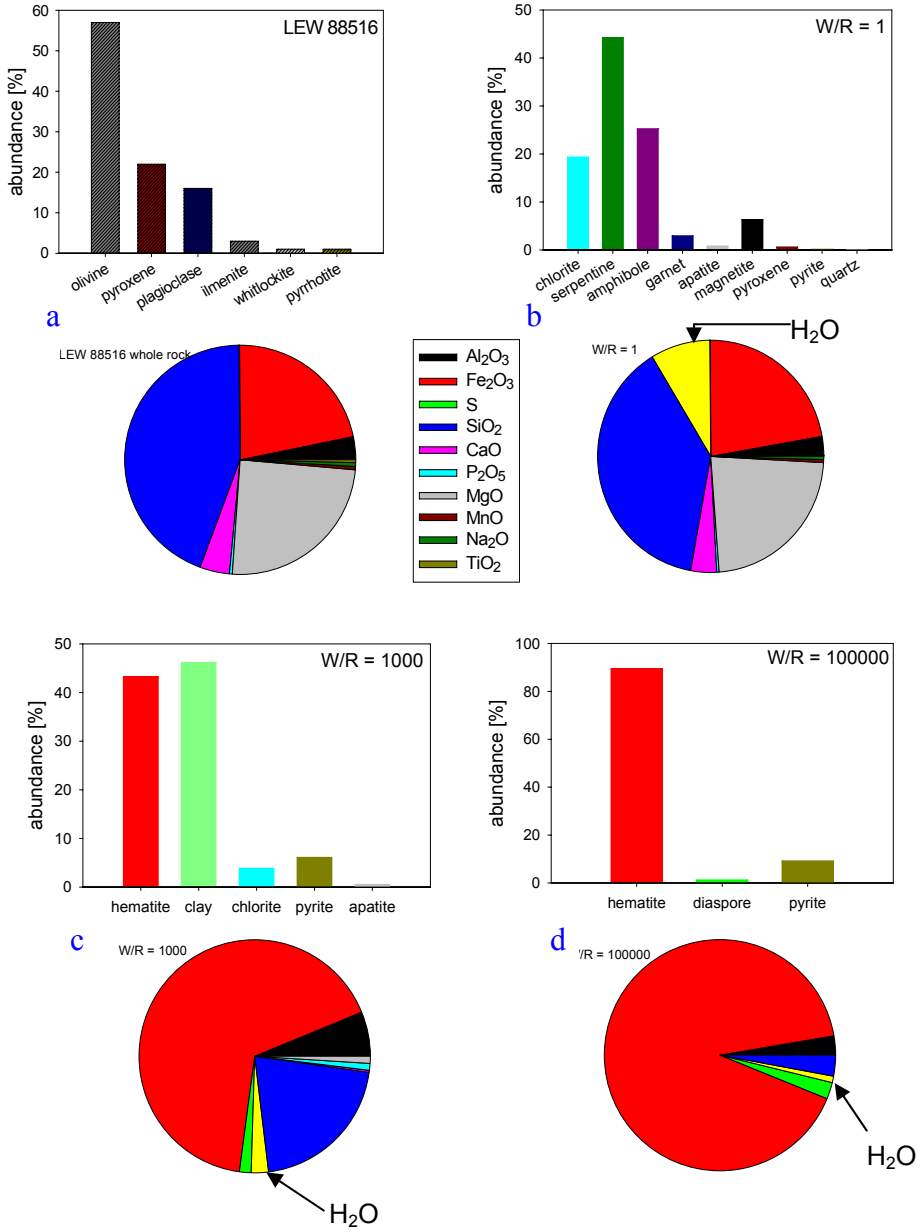

Fig. 1. Results of model calculations of LEW 88516 chemistry with an ion containing fluid: starting rock mineralogy and composition(a), W/R = 1 (b), W/R = 1000 (c), and W/R = 100000 (d). Details on the modeling see [6].

References: [1] Naumov, M.V. (2005) *Geofluids, 5*, 165–184. [2] Zurcher, L. and Kring, D.A. (2004) *MAPS, 39*, 1199–1221. [3] Abramov, O. and Kring, D. A. (2004) *JGR, 109,* E10007, doi: 10.1029/2003JE002213. [4] Abramov, O. and Kring, D.A. (2007) *MAPS, 42,* 93–112. [5] Sanford, W. E. (2005) *Geofluids, 5*, 185–201. [6] Schwenzer, S.P. and Kring, D.A. (2008) *LPSC, XXXIX*, abstr. #1817. [7] Kring, D. A. (2000) *GSA today*, 10(8), 1–7. [8] Rathbun, J. A. and Squyres, S. W. (2002) *Icarus, 157*, 362–372. [9] Treiman, A. H. (1998) *Meteoritics, 33*, 753–764. [10] Golden, D. C. et al. (2001) *American Mineralogist, 86*, 370–375. [11] Gleason, J. D. et al. (1997) *GCA, 61*, 3503–3512. [12] Kring, D. A. et al. (1998) *GCA, 62*, 2155–2166. [13] Griffith, L. L. and Shock, E. L. (1995) *Nature, 377*, 406–408. [14] Schwenzer, S. P. and Ott, U. (2006) *LPSC, XXXVII,* Abstr. # 1614. [15] Fassett, C. I. and Head III, J. W. (2008) *Icarus, 195*, 61–89. [16] Reiss, D. et al. (2006) *MAPS, 41*, 1437–1452. [17] Bibring, J.-P.et al. (2005) *Science, 307*, 1576–1581. [18] Poul et, F. et al. (2007) *JGR, 112*, : E08S02, doi: 10.1029/2006JE002840. [19] Ehlmann, B. L. et al. (2008) *LPSC, XXXIX*: #2326. [20] Loizeau, D. et al. (2007) *JGR, 112*, E08S08, doi: 10.1029/2006JE2877. [21] Hartmann, W. K. and Neukum, G. (2001) *Space Sci. Rev., 96,* 165–194.

CHRONOLOGICAL EVIDENCE FOR THE LATE HEAVY BOMBARDMENT IN ORDINARY CHONRITE METEORITES. T. D. Swindle[1] and D. A. Kring[2], [1]Lunar and Planetary Laboratory, University of Arizona, Tucson AZ 85721-0092 (tswindle@u.arizona.edu), [2]Lunar and Planetary Institute, 3600 Bay Area Boulevard, Houston TX 77058 (dkring@lpi.usra.edu).

Introduction: The first evidence of the Late Heavy Bombardment ("LHB"), or Lunar Cataclysm, came from Ar-Ar and Pb-Pb analyses of lunar samples [1, 2]. But was this restricted to the Moon?

In his classic review, Bogard [3] suggested that there was some evidence in Ar-Ar ages of HED meteorites, and perhaps a hint in ordinary chondrites. Meanwhile, Wasson and Wang [4], in compiling U,Th-He ages based on measured ^{4}He contents and average actinide compositions for the various chemical classes, found that few chondrites had ages older than 4.0 Ga, although many had ages 3.5-4.0 Ga. In the last 10-15 years, several laboratories, including ours, have investigated a variety of shocked ordinary chondrites, as well as lunar impact glasses [5-7] and lunar meteorite impact melts [8, 9]. In addition, LHB-aged (3.5-4.1 Ga) samples of HED meteorites [10] and silicate inclusions within IIE irons [11] have also been reported.

In this abstract, we report on the growing chronological evidence for an LHB event in ordinary chondrites. As it turns out, ages between 3.5 and 4.0 Ga (LHB) are not uncommon, nor are ages >4.4 Ga (presumably from the accretionary era of the Solar System). On the other hand, ages between 2.0 and 3.5 Ga are virtually non-existent, as of yet, and ages between 4.0 and 4.4 Ga are rare, except in shocked LL chondrites, where they are common.

"LHB" Ages of Ordinary Chondrites: It is impossible to tell from a petrographic examination of a shocked chondrite what its age is. Hence, the chronological data base tends to grow slowly, with some events coming into focus long before others. Following is a summary of the current status of ages of ordinary chondrites, with a focus on ages older than 3 Ga.

H Chondrites. The impact record in H chondrites (Fig. 1) includes six meteorites with impact ages of 3600-4000 Ma [12-16], and another, Yangzhuang (melt) at 4090±40 Ma [14]. Besides three that have ages consistent with the accretionary era (4360±120, 4480±20 and >4420, respectively) [16-18], no others are >1400.

This strongly suggests that the impact history of the H chondrite parent body included, after early impacts associated with accretion, a decrease in impact flux until ~4 Ga, followed by an increase for a few hundred Ma, then a decrease. Although it has been pointed out that the near absence of pre-4.0 Ga impact ages in the lunar record could be the result of complete destruction

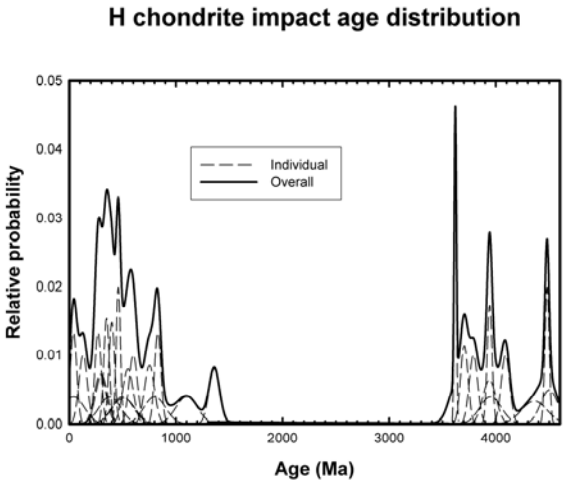

Figure 1: Ideogram of impact ages of H chondrites [16]. Each age is represented by a Gaussian distribution of unit area, so precisely determined ages appear as tall spikes, poorly determined ones as low, broad humps. References for ages >1.4 Ga given in text.

of impact melts during the last stages of the LHB [19],the same argument cannot be made for the H chondrites – since impact melts of ~4.5 and 3.9 Ga survived, why wouldn't those of 4.2 Ga? The much greater abundance of ages in the last ~1 Ga than in the 2 Ga before that suggests that there is a typical lifetime for melts produced in the current environment, which would mean that the number of 3.6-4.0 ages reflects a considerable increase in impacts at that time. So the lack of ages between 4.4 and 4.1 Ga, while representing a period of relative quiescence, does not necessarily represent an impact flux lower than the present, just one lower than before (during accretion) or after (during LHB) it.

L Chondrites. The most common shocked ordinary chondrites are shocked L chondrites. It has been recognized since the 1960s that this represents an impact event ~500 Ma ago [20]. More recently, studies of fossil meteorites in Swedish quarries [21-23], including cosmic ray exposure studies [24] and more accurate Ar-Ar dating [25], has tied the abundant shocked L chondrites to a single asteroid collision 470 Ma ago.

Ironically, although most shocked ordinary chondrites are L chondrites, the 470-Ma event is so dominant among the L chondrites that there are far fewer L

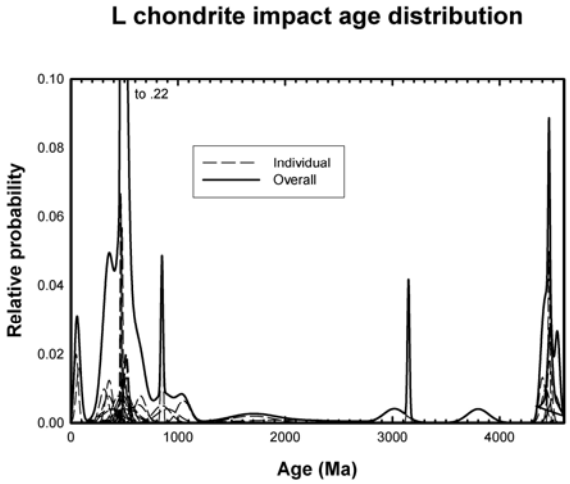

Figure 2: Ideogram of impact ages from L chondrites (see Fig. 1 for explanation).

chondrites with old impact ages than there are H's or LL's (Fig. 2). The total roll call of L chondrites with impact ages >1700 Ma includes two with ages of 3.0-3.2 Ga [14, 26], one with an age of ~3.8 Ga [27], and at least six with ages >4.4 Ga [28-31]. There are no ages between 4.0 and 4.4 Ga or between 1.6 Ma and 3.0 Ma.

LL Chondrites. The LL chondrites (Fig. 3) are dominated by ages of ~4.2-4.3 Ga [32-34], the only place where that age has been seen. Interestingly, several of those 4.2-4.3 Ga ages come from [32], who were not trying to analyze shocked meteorites, but frequently got that age anyway. There are two ~3.9 Ga ages among the 15 LL chondrite impact ages, Appley Bridge [35] and DOM 85505 [32], and two more with minimum apparent ages of 3.6-4.0 Ga, GRO 95658 and Savtschenskoje [32]. There are no others >1.3 Ga.

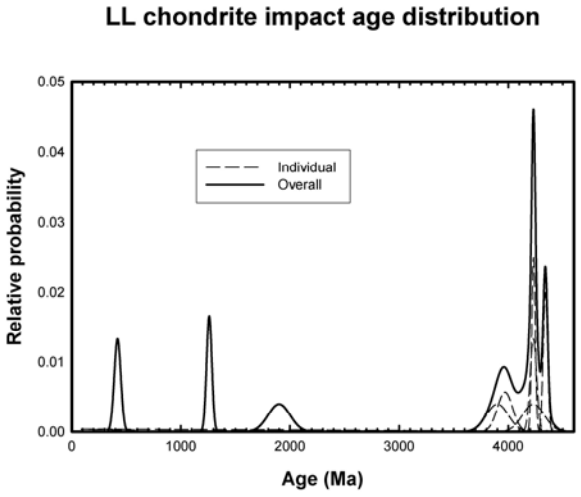

Figure 3: Ideogram of impact ages from L chondrites (see Fig. 1 for explanation).

Summary:

There is definitely an "LHB" (3.6-4.0 Ga) peak among H chondrites, and at least one meteorite in that range in both the L and LL.

There is definitely not a 3.9-4.0 Ma spike among the ordinary chondrites, although we cannot rule out the possibility of a spike becoming apparent as more data comes in.

There is a 4.2-4.3 Ma event in the LL's, not apparent in L or H, where there is a total of one meteorite (at 4.09±0.04) between 4.0 and 4.4 Ga.

"Accretionary" impacts (>=4.4 Ga) are apparent among L and H chondrites (though not LL), so impact melt can survive.

Including the long "tail" of ages later than 3.9 Ga, the ordinary chondrite data are consistent with HEDs, lunar glasses, lunar meteorite clasts, but not with Apollo melt rocks or Apollo Pb data.

References:

[1] Turner G. et al. (1973) *Proc. Lunar Sci. Conf.*, 4th, 1889-1914; [2] Tera F. et al. (1974) *EPSL*, *22*, 1-21; [3] Bogard D. D. (1995) *Meteoritics*, *30*, 244-268; [4] Wasson J. T. and Wang S. (1991) *Meteoritics*, *26*, 161-167; [5] Culler T. S. et al. (2000) *Science*, *287*, 1785-1788; [6] Levine J. et al. (2005) *GRL*, *32(15)*, doi:10.1029/2005GL022874; [7] Delano J. W. et al. (2007) *MAPS*, *42*, 993-1004; [8] Cohen B. A. et al. (2000) *Science*, *290*, 1754-1756; [9] Cohen B. A. et al. (2005) *MAPS*, *40*, 755-777; [10] Bogard D. D. and Garrison D. H. (2003) *MAPS*, *38*, 669-710; [11] Bogard D. D. et al. (2000) *GCA*, *64*, 2133-2154; [12] Keil K. et al. (1980) *EPSL*, *51*, 235-247; [13] Müller N. et al. (1983) *Meteoritics*, *18*, 359; [14] Kunz J. et al. (1997) *MAPS*, *32*, 647-670; [15] Folco L. et al. (2004) *GCA*, *68*, 2379-2397; [16] Swindle T. D. et al. (2008) *MAPS*, *43*, A150; [17] Garrison D. H. and Bogard D. D. (2001) *LPSC*, *XXXII*, Abstract #1137; [18] Swindle T. D. and Kimura M. (2008) *MAPS*, *43*, A150; [19] Chapman C. R. et al. (2007) *Icarus*, *189*, 233-245; [20] Heymann D. (1967) *Icarus*, *6*, 189-221; [21] Schmitz B. et al. (2003) *Science*, *300*, 961-964; [22] Schmitz B. et al. (1996) *EPSL*, *145*, 31-48; [23] Schmitz B. et al. (2001) *EPSL*, *194*, 1-15; [24] Heck P. R. et al. (2004) *Nature*, *430*, 323-325; [25] Korotchantseva E. V. et al. (2007) *MAPS*, *42*, 113-130; [26] Stephan T. and Jessberger E. K. (1988) *Meteoritics*, *23*, 373-377; [27] Bogard D. D. et al. (1987) *GCA*, *51*, *2035-2054*; [28] Turner G. et al. (1978) *Proc. Lunar Sci. Conf.*, *9th*, 989-1025; [29] Benedix G. K. et al. (2008) *GCA*, *72*, 2417-2428; [30] Weirich J. R. et al. (2008) *LPS*, *XXXIX*, Abstract #1665; [31] Ozawa S. et al. (2008) *MAPS*, *43*, Submitted; [32] Dixon E. T. et al. (2004) *GCA*, *68*, 3779-3790; [33] Trieloff M. et al. (1989) *Meteoritics*, *24*, 332; [34] Trieloff M. et al. (1994) *Meteoritics*, *29*, 541-542; [35] Turner G. and Cadogan P. H. (1973) *Meteoritics*, *8*, 447-448.

HIGHLY SIDEROPHILE ELEMENTS IN THE EARTH, MOON, AND MARS: UPDATE AND IMPLICATIONS FOR PLANETARY ACCRETION AND DIFFERENTIATION. R.J. Walker[1] , I.S. Puchtel[1], J.D. Day[1], A.D. Brandon[2], O.B. James[3] and L. Loudin[4]. [1]Department of Geology, University of Maryland, College Park, MD 20742 (rjwalker@geol.umd.edu), [2]NASA, JSC, Houston, TX 77058, USA, [3]U.S. Geological Survey, 926A National Center, Reston, VA 20192, [4]Keene State College, Keene, NH 03431

Introduction. The highly siderophile elements (HSE) include Re, Os, Ir, Ru, Pt and Pd. These elements are initially nearly-quantitatively stripped to some extent from planetary silicate mantles during core segregation. They then may be re-enriched in mantles via continued accretion upon cessation of further core segregation. Processes that include metal-silicate segregation at high P and T the base of a magma ocean [1], and late accretion have been touted as the dominant controls on HSE abundances in planetary mantles [2]. Thus, depnending on the dominant process, this suite of elements and its included long-lived radiogenic isotopes systems ($^{187}Re \rightarrow {}^{187}Os$; $^{190}Pt \rightarrow {}^{186}Os$) might either be used to constrain the depth of metal-silicate segregation, or to "fingerprint" the characteristics of late accreted materials. If the latter, the fingerprints may ultimately be useful to constrain the prior nebular history of late accreted materials, and to compare the proportion and genesis of late accretionary materials added to the inner planets.

The past ten years have seen considerable accumulation of isotopic and compositional data for HSE present in the Earth's mantle, the lunar mantle and lunar impact melt breccias, as well as martian meteorites. Here we review some of these data and consider the broader implications of the compiled data.

Earth. Studies of the Os isotopic compositions of terrestrial peridotities that have been long isolated from convection in the upper mantle (e.g. ancient subcontinental lithospheric mantle) have led to the conclusion that the inferred $^{187}Os/^{188}Os$ of Earth's Primitive Upper Mantle (PUM) matches that of enstatite/ordinary chondrites, not the more volatile rich carbonaceous chondrites [3].

Recent attempts to constrain the absolute and relative HSE budget of the PUM have led to recognition that there are some discrepancies between the relative abundances of these elements in the PUM and chondrites. For various suites of peridotites (including continental mantle, orogenic lherzolites and abyssal peridotites), HSE were correlated with melt depletion/enrichment indicators and extrapolated to an estimate of the PUM [4]. For most HSE, abundances in PUM are similar to earlier estimates. However, estimates of Ru/Ir and Pd/Ir derived from most suites indicates modestly suprachondritic compositions for average PUM. This has been observed by other groups as well [5-6], although the effects of melt depletion can now be discounted. Thus, although HSE in the terrestrial PUM can be placed in a broad "chondritic" family, it is not a perfect match to any one chondrite group that exists in our collections. This can be interpreted in one of several ways. First, if the HSE were established by late accretion, the dominant late accreted materials may have had a somewhat different nebular history compared to the chondrites in our collections. This would not be surprising. Nebular, and perhaps subsequent processing on parent bodies has been shown to result in considerable fractionation of HSE. Second, the deviation from chondritic ratios could be an indication that processes other than, or in addition to late accretion controlled HSE abundances in the mantle. For example, many workers have experimentally explored the possibility that the comparatively high abundances of HSE in the mantle are a result of relatively low metal-silicate bulk partitioning at the base of a deep magma ocean. Recent studies have demonstrated that Re, Pd, Pt and Au may have sufficiently low D values at magma ocean conditions to explain their mantle abundances [7-9]. This is an unlikely explanation for Re and Os, given the close adherence of $^{187}Os/^{188}Os$ and $^{186}Os/^{188}Os$ to chondritic (which allows us to constrain Re/Os and Pt/Os in the PUM better than any other HSE ratios). Retention of precisely chondritic Pt/Re/Os is an unlikely result of metal-silicate partitioning. Nonetheless, this possibility begs future experimental consideration. Retention of excess Ru and Pd in the silicate Earth following metal segregation, relative to other HSE, could result in suprachondritic ratios involving these elements, allowing the possibility of a hybrid model for generating HSE abundances. Finally, it may be that mantle processes (melt removal & refertilization, crustal recycling) have complicated the HSE budget of the mantle beyond our current capability to deconvolute them and obtain an accurate estimate of the PUM.

Moon. There are currently no known samples of the lunar mantle in our collections, so HSE abundances in the lunar mantle must be estimated from derivative melts. This is non trivial. Most prior studies of HSE in lunar volcanic rocks have reported relatively low concentrations of HSE, such as Ir, in lunar basalts and picritic glasses [10-12]. Relative to terrestrial rocks with comparable MgO contents, the lunar mantle sources of these rocks appear to be depleted in the HSE by at least a factor of 20 (**Fig. 1**). This observation may indicate that the lunar mantle did not receive a late accretionary component like that suggested to

explain the HSE budget of Earth's mantle. The "missing" HSE could reside in a late-formed lunar core. However, because metal segregation would likely lead to strong fractionation of Re from Os in the silicate mantle, the approximately chondritic initial $^{187}Os/^{188}Os$ ratios of lunar basalts weighs against this possibility [11-12]. Alternately, the low abundances could indicate that either late accretion was not the dominant process controlling HSE in the terrestrial mantle (and so, the Moon), or that late accretion preceeded formation of the Moon. The chondritic Re/Os of the PUM is problematic for the former interpretation, yet the latter possibility is also difficult to envision, given the likelihood HSE stripping of the mantle during the putative giant impact that created the Moon.

Potentially direct information regarding the chemical nature of late accreted materials to the Earth-Moon system can be obtained by examining the HSE contained in lunar impact-melt rocks. Our work on lunar impact melt rocks indicates that at least some of the impactors that created the lunar basins had relative abundances of the HSE outside of the range of chondrites currently sampled by Earth [13] (**Fig. 2**). This may mean that the supra chondritic Ru/Ir and Pd/Ir of the PUM can be accommodated by a late accretion model that is dominated by materials with HSE characteristics slightly outside of the range of known chondrite groups.

Mars. Re-Os studies of SNC meteorites indicate that the martian mantle evolved with a dominantly chondritic Re/Os [14]. HSE measurements for SNC meteorites are broadly consistent with derivation from mantle sources bearing HSE concentrations similar to those present in the terrestrial upper mantle (**Fig. 1**). The HSE abundances and chondritic Re/Os of SNC meteorites suggest that, if established by late accretion, the martian mantle received a proportionally similar mass of late accreted materials as was added to Earth. This would be somewhat surprising given that final core segregation may have occurred 10s of Ma apart for the two planets. Consequently, a similar bombardment flux would have to be either coincidence, or the result of dominantly later stage events that may have substantially postdated final core segregation. If instead the HSE abundances in both the terrestrial and martian mantle were established primarily by lowered D values under magma ocean conditions, D values were remarkably similar for both planets.

References. [1] Murthy (1991) *Science* **253**, 303. [2] Chou (1978) *Proc. 9th Lunar Planet. Sci. Conf.*, 219. [3] Meisel et al. (2001) *Geochim. Cosmochim Acta* **65**, 1311. [4] Becker et al. (2006) *Geochim. Cosmochim Acta* **70**, 4528. [5] Pattou et al. (1996) *Nature* **379**, 712. [6] Schmidt (2004) *Met. Planet. Sci.* **39**, 1995. [7] Righter & Drake (1997) *Earth Planet. Sci. Lett.* **146**, 541 [8] Cottrell & Walker (2006) *Geochim. Cosmochim Acta* **70**, 1565. [9] Righter et al. (2008) Nature Geosci. doi:10.1038/ngeo180 [10] Warren et al. (1989) *Earth Planet. Sci. Lett.* **91**, 245 [11] Walker et al. (2004) *EPSL* **224**, 399 [12] Day et al. (2007) Science 315, 270 [13] Puchtel et al (2008) *Geochim. Cosmochim Acta* **72**, 3002 [14] Brandon et al. (2000) *Geochim. Cosmochim Acta* **64**, 4083 [15] Walker et al. (1999) *Geochim. Cosmochim Acta* **63**, 713.

Acknowledgements. This work was supported by NASA grants NNG04GJ49A and NNX07AM29G.

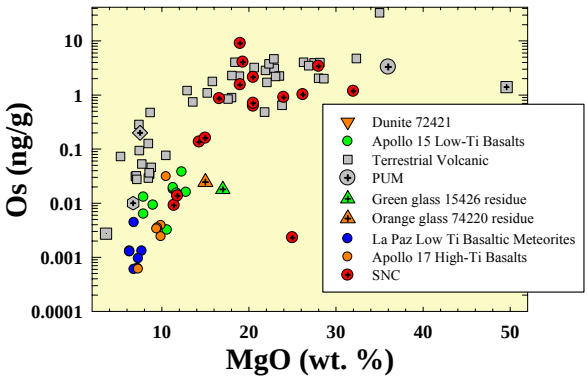

Fig. 1. Plot of Os concentrations (ng/g) versus MgO for lunar, SNC and terrestrial volcanic rocks. Most lunar data are offset significantly below the terrestrial array, suggesting that abundances of the highly siderophile elements in the lunar mantle are substantially lower than in the terrestrial mantle. Terestrial data are from the literature but are mostly from the Caribbean Large Igneous Province [15]. Lunar data are from [11-12]. Data for most SNC [14] are similar to terrestrial.

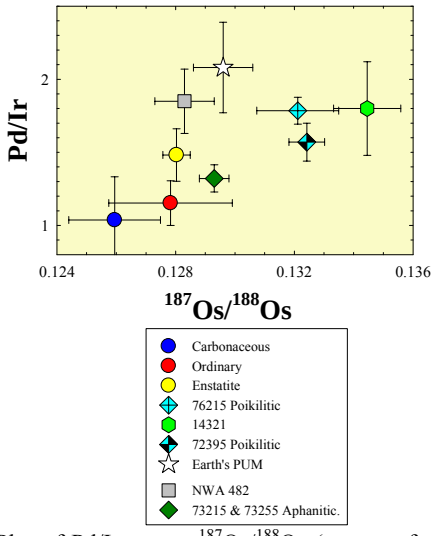

Fig. 2. Plot of Pd/Ir versus $^{187}Os/^{188}Os$ (a proxy for Re/Os) for lunar impact melt rocks. Shown for comparison are the range of compositions for chondritic meteorites, and estimates of Earth's primitive upper mantle. Data are from [3,13].

USMI – ULTRAVIOLET SPECTRAL MAPPING INSTRUMENT FOR THE GERMAN LUNAR EXPLORATION ORBITER (LEO). K. Werner[1], J. Barnstedt[1], N. Kappelmann[1], W. Kley[1], H. Tomczyk[1], H. Wende[1], H. U. Keller[2], U. Mall[2], H. Becker-Roß[3], S. Florek[3], H. Hoffmann[4], S. Mottola[4], D. Kampf[5], G. Staton[5]

[1]Universität Tübingen, Institut für Astronomie und Astrophysik, [2]Max-Planck-Institut für Sonnensystemforschung, Katlenburg-Lindau, [3]Institute for Analytical Sciences, Berlin, [4]Deutsches Zentrum für Luft- und Raumfahrt (DLR), [5]Kayser-Threde GmbH, München; Germany; werner@astro.uni-tuebingen.de

Introduction: The German initiative for the Lunar Exploration Orbiter is aimed at providing a globally covered, highly resolved, integrated, geological, geochemical, and geophysical database of the Moon [1]. LEO is planned to be launched in 2012 and shall orbit the Moon for about four years at low altitude (<50 km) in order to map the Moon geomorphologically, geochemically, and geophysically with resolutions down to less than 1 m globally. Among the future planned missions to the Moon, LEO will be unique, because it will globally explore the Moon in unprecedented spatial and spectral resolution: <1 m in stereo, <10m spectrally (0.2-14µm), 2 m subsurface resolution, 0.2 mGal for lunar gravity at 50 km resolution.

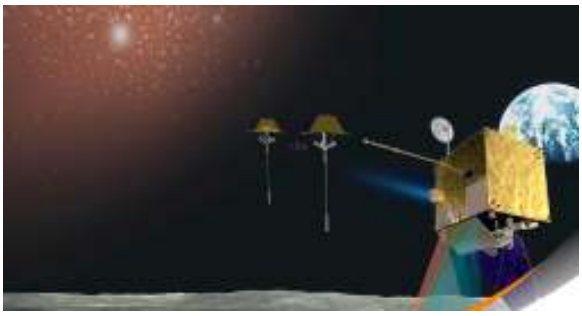

LEO is currently in phase A. The mission scenario foresees a launch in 2012, a five-day lunar transfer, a two-month commissioning phase, and a four-year mapping phase.

Scientific approach: Why UV mapping of the Moon? The reflection characteristics of solid surfaces in the UV spectral range can be used to constrain the mineralogical, petrologic, and chemical composition of geologic material or, in combination with observations in the visual and IR, to determine it in greater detail. Laboratory research of lunar material and other minerals shows that in this wavelength range characteristic features exist for many minerals relevant for planetary geological science.

The spectral dependence of the reflectivity of solid surfaces is determined by many factors (weathering, grain size, crystallisation sequence, material composition) whose de-convolution can often be achieved only by observation over the entire spectral range from the UV to the IR with adequate spectral resolution.

Lunar material was analysed in the laboratory in the nineteen-seventies and -eighties. Lunar rock like KREEP (mainly pyroxene and plagioclase) or basalt with low or high titanium content as well as others often show a steep characteristic absorption edge in the range 250 to 400 nm (Figure 1). For lunar soil these absorption edges are less pronounced (Figure 2). Just by combination with observations at longer wavelengths (VIS and IR) the potential for identification can be significantly enhanced.

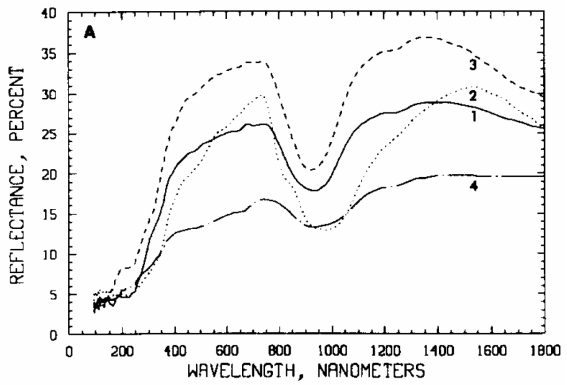

Figure 1. Spectra of powdered samples of lunar rocks. 1,2,3,4: Apollo samples 14310, 15555, 65015, 70017, respectively. From [2].

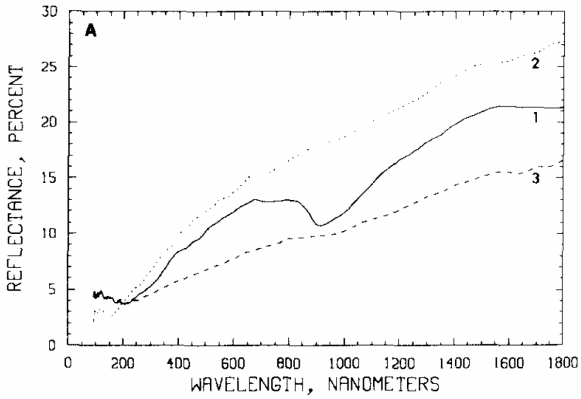

Figure 2. Spectra of lunar soils. 1,2,3: Apollo samples 15601, 68501, 70011, respectively. From [2].

Recent laboratory research in the UV range reveals relations of the spectral shape with the minerals. One example is feldspar (Figure 3). Another example is ilmenite that, in contrast to other minerals, shows a characteristic absorption minimum between 400 and 500 nm and, hence, can be distinguished from other lunar minerals in the UV. In titanium-rich basalts titanium is mainly stored in ilmenite, so that in this case the UV-to-VIS ratio is hardly affected by other minerals. On the other hand, in titanium-poor soil one has to consider that the effect of some titanium-poor or even titanium-free minerals (chromite or ulvöspinel) on the reflection spectrum is very similar to that of ilmenite and, thus, can severely corrupt estimates of the ilmenite content if the spectral resolution is too low.

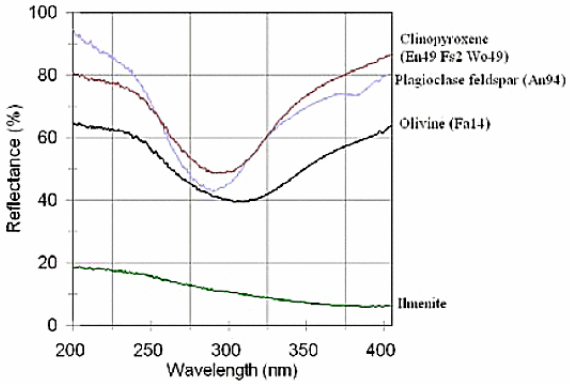

Figure 3. Representative 200-400 nm sample spectra (clinopyroxene, plagioclase feldspar, olivine, ilmenite). From [3].

Space weathering on the lunar surface by influences of the Sun (solar wind and UV radiation) and by cosmic particle radiation acts to make the spectra redder in the IR as well as to make them bluer in the UV. It is possible to distinguish surface material from crushed lunar rock. The increased blue colouring is strongest in the range 300 to 400 nm, because here the above mentioned absorption edge is being degraded. Therefore, quantitative observations in the UV can also be used for a relative age determination of the material on the lunar surface.

A UV spectrometer to characterise the mineral composition and to determine the degree of weathering in the wavelength range 200 to 400 nm does not need to have a high spectral resolution because all phenomena cover broad bands over several 10 nm. A resolution of $\lambda/10$ is sufficient.

The Ultraviolet Spectral Mapping Instrument (USMI): USMI has been selected as one of the instruments to be flown aboard LEO. It will globally map the Moon in the wavelength range from 200 to 400 nm in 10 bands with a resolution of 10 m per pixel.

USMI will provide UV data which will be complementary to those of other LEO instruments that shall perform observations from the visual to the thermal infrared. Combined with the geological and morphological mapping by the high-resolution camera HRSC-L in the visual, and the mineralogical measurements of the VIS-NIR instrument in the near infrared, and the SERTIS instrument in the medium infrared, USMI will enable to determine, spatially highly resolved, the distribution of the principal minerals on the lunar surface by a broad, up to now never achieved coverage of the electromagnetic spectrum. The strived resolution of about 10 m on the lunar surface represents a quantum leap in the multi-spectral mapping of the lunar surface (up to now about 100 to 400 m) and will yield significant progress in detection of the surface mineralogy, because the spatial smearing of spectral signatures will be strongly reduced.

A particular technical challenge for the USMI design is the low surface brightness of the Moon in the 200-250 nm range caused by both the low lunar surface albedo and the strongly reduced solar flux in this spectral range. This is clearly demonstrated by Figure 4 which shows a ultraviolet spectrum of the Moon in the range from 180 to 320 nm, that was observed by the astronomical International Ultraviolet Explorer (IUE) observatory.

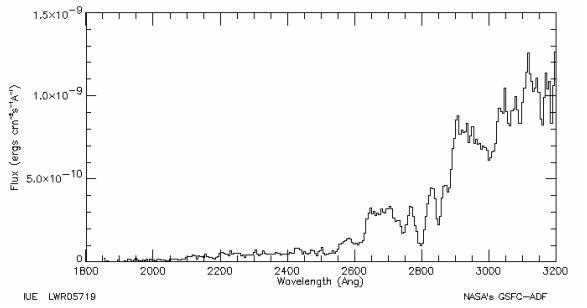

Figure 4. Ultraviolet spectrum of the Moon, recorded in 1979 by the IUE satellite observatory (image number lwr05719 Large Aperture). Retrieved from the NASA Multimission Archive (MAST) at the Space Telescope Science Institute.

References: [1] Jaumann R., et al. (2008) *LPS XXXIX,* Abstract #1391. [2] Wagner J. K., Hapke B. W., Wells E. N. (1987) Icarus, 69, 14. [3] McCormack K., et al. (2006) *LPS XXXVIII,* Abstract #2158.

Impacts in the Earth-Moon System as Told by Lunar Impact Glasses N.E.B. Zellner[1], J.W. Delano[2], T.D. Swindle[3], and D.C.B. Whittet[4] [1]Department of Physics, Albion College, Albion, MI 49224, nzellner@albion.edu, [2]Department of Earth and Atmospheric Sciences, University at Albany (SUNY), Albany, NY 12222, [3]University of Arizona, Lunar and Planetary Laboratory, Tucson, AZ 85721, [4]Department of Physics, Applied Physics and Astronomy, Rensselaer Polytechnic Institute, Troy, NY 12180.

Introduction: Impact events have played important roles in the evolution of planets and small bodies in the Solar System. Over 500 impact glasses from four Apollo regolith samples have been geochemically analyzed and a subset has been dated by the $^{40}Ar/^{39}Ar$ method.

These 65 dated glasses show interesting trends in the bombardment history in the Earth-Moon system that do not necessarily correlate with the history shown by lunar meteorites and other lunar samples individually. Using Apollo 14 glass spherules, [1] argued that over the past ~3.5 Ga, the cratering rate decreased by a factor of 2-3, while [2] found that impact melt clasts show no ages more than 1σ older than 4.0 Ga. Similarly, the work of [3] showed that very few Apollo 12 impact glass spherules have old (>3200 Ma) ages. The ages of our impact glasses, which are comprised of spherules and fragments, from wide-ranging Apollo landing sites, are as old as ~4000 Ma and represent multiple old impact events into geochemically similar and different terrains. Understanding all of these samples together provides important information about the geology of the impacted body and the age of the impacting episodes. Specifically, impact glasses provide another set of data to address the question of whether or not there was a lunar cataclysm and to shed light on its details if it did happen.

Lunar Impact Glasses: Lunar impact glasses possess the refractory element ratios of the original fused target materials at the site of impact [4] and offer the potential for providing information about local and regional units and terrains. Orbital data [e.g. 5] has been used to show that impact glass composition(s) most often represent regolith composition(s), and old ages represented in our impact glasses and in some of the glasses of [1] show that old glasses are not necessarily destroyed. The compositions of lunar impact glasses indicate their original geology, often several hundreds of kilometers away from the site where they were collected by the Apollo astronauts [e.g. 6]. In this way, "exotic" and "local" regolith compostions can be determined [5, 6] in an effort to distinguish among impact events.

Sample Analysis: Glasses from Apollo 14 regolith 14259,624, Apollo 16 regoliths 64501,225 and 66041,127, and Apollo 17 regolith 71501,262 were analyzed for Si, Ti, Al, Cr, Fe, Mn, Mg, Ca, Na, and K using a JEOL 733 electron microprobe in the Department of Earth and Environmental Sciences at Rensselaer in the manner described by [5]. Uncertainties in the measurements were usually < 3% of the amount present. These compositions can be seen in Figure 1.

Impact glasses were subsequently irradiated and analyzed in order to determine their $^{40}Ar/^{39}Ar$ ages. Laser step-heating on these samples was carried out in the University of Arizona noble gas lab, in the manner described by [6]. Finally, several spherules of Apollo 15 volcanic green glass, which has a well-defined ^{40}Ar-^{39}Ar age, were used as isotopic working standards in order to verify that the data reduction procedure resulted in expected ages within uncertainties.

Results: Lunar impact glasses show ages that range from ~20 Ma to ~4000 Ma, spanning most of lunar history (Figure 2). Uncertainties in these ages depend on the amount of K in the sample and the amount of Ar detected by the mass spectrometer, but when considering geochemistry together with chronology, certain events become distinct. For example, [6] showed that at a 2σ level, four glasses represent one distinct impact event at ~3730 Ma into the same compositional terrain most similar to the basaltic andesitic (BA) glasses found by [7]. This integrated approach thus rules out that these four impact glasses were formed during four separate events. Similarly, a suite of 12 impact glasses from the Apollo 14, 16, and 17 regoliths shows formation ages of ~800 Ma [8], as seen in Apollo 12 samples [3, 9], all with different geochemical compositions, implying some sort of global lunar impact event that has not yet been seen in most meteorites or in terrestrial samples.

Finally, of the samples analysed so far, there is no indication of an increase in recent impact events, as reported by [1, 3] and modeled by [10], nor is there evidence of impacts on the Moon during the time interval of 400 – 500 Ma ago, when the meteorites record the break-up of the L chondrite parent body in the Asteroid Belt [11]. Perhaps debris did not hit the Moon; perhaps this is solely an artifact of sampling.

From Figure 2, it can be seen that, ages >4000 Ma are rare or absent, as is true for Apollo impact rocks [11], impact melts from lunar meteorites [2], and other lunar impact glass data sets [1,3]. However, like the lunar meteorite impact melts and ordinary chondrites, but unlike the Apollo samples, ages ~3500-4000 Ma

are common in our data set. These ages are not evident in the Apollo 12 impact glasses, which [3] attributes to the soil sample having come from the bottom of an ejecta deposit of recently inverted stratigraphy, and the trend is hard to determine in [1]. While the histogram in [1] does show spikes in this time interval, the data set may unfortunately be confounded by the possibility of volcanic glasses composing a significant fraction of the "impacts", as described in [6].

Conclusions: When age data from all lunar samples are analyzed collectively, we can begin to understand when impact events occurred and how widespread they were. Specifically, by integrating geochemistry and age [6], multiple impact samples formed at the same time in the same terrain can be eliminated from the data set. The challenge comes in trying to distinguish among the impact events, including determining which samples (impact glasses, melt rock, meteorites) were formed during the same impact event and which were not, so that the impact flux is not artificially inflated.

References: [1] Culler *et al.* (2000) *Science*, **287**, 1785. [2] Cohen *et al.* (2005) *MAPS*, **40**, 755. [3] Levine, J. *et al.* (2005), *GRL*, **32**, L15201. [4] Delano, J.W. (1991) *GCA*, **55**, 3019-3029. [5] Zellner, N.E.B. *et al*. (2002) *JGR*, **107(E11)**, 5102, doi:10.1029/2001JE001800. [6] Delano, J.W. *et al.* (2007) *MAPS*, **42**, 6, 993-1004. [7] Zeigler, R.A. *et al.* (2006) *GCA*, **70(24)**, 6050. [8] Zellner, N.E.B *et al.* (2006), *LPSC 37th*, 1745.pdf. [9] Barra, F. et al. (2006) *GCA*, **70**, 6016. [10] Bottke *et al.* (2007) *Nature*, **449**, 48. [11] Bogard, D. (1995) *Meteoritics*, **30**, 244-268.

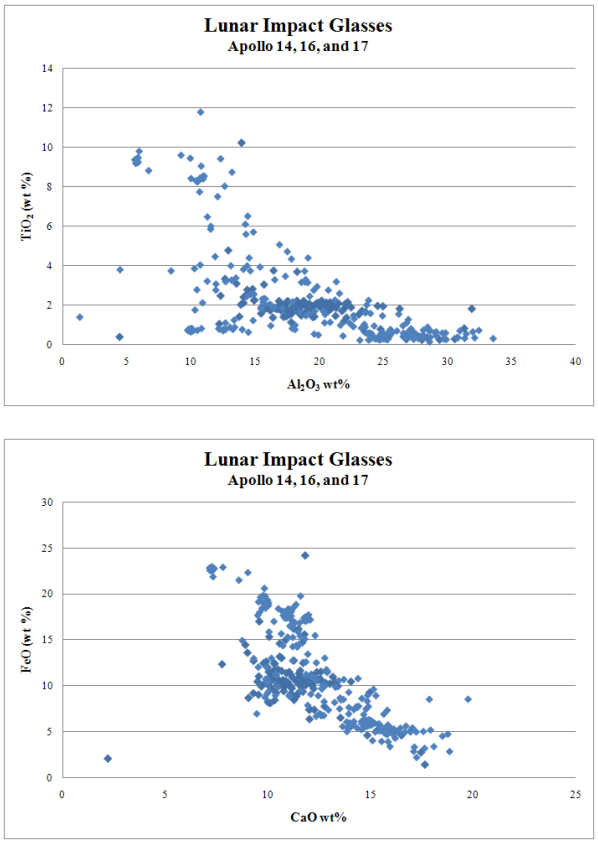

Figure 1. Compositions of over 500 lunar impact glasses.

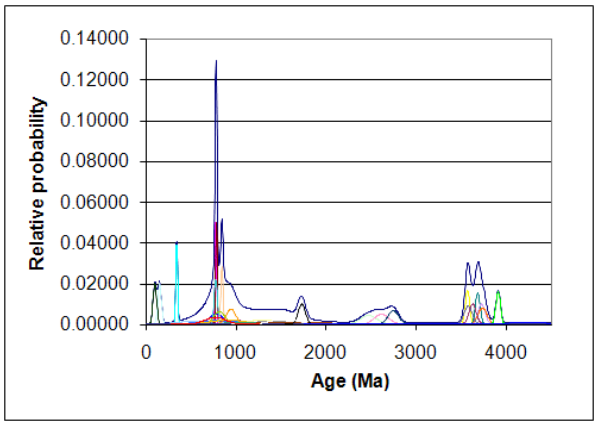

Figure 2. Ideogram of ages from 35 lunar impact glasses whose ages have so far been determined, with 2σ uncertainty. An ideogram of the entire data set will be presented at the workshop. The event described in [6] at ~3730 Ma is shown as one event and not four.

NOTES

NOTES